

AGSE 2018

Franz-Josef Behr, Christine Brönnert, Miguel Orti, Kaleb
Negussie (Editors)

Namibia University of Science and Technology,
Windhoek, Namibia

Stuttgart University of Applied Sciences
Stuttgart Active Alumni Group

Geoscience for Crisis Management

Applied Geoinformatics for Society and Environment

Geoscience for Crisis Management

Applied Geoinformatics for Society and Environment

AGSE 2018

Franz-Josef Behr, Christine Brönnner, Miguel Orti, Kaleb Negussie (Editors)

AGSE Publishing

08 – 16 November 2018, Namibia University of Science and Technology

ISBN 978-3-943321-17-3

Editors

Prof. Dr. Franz-Josef Behr
Stuttgart University of Applied Sciences
Email: franz-josef.behr@hft-stuttgart.de

Christine Bröner
Geoinformation Management and Interoperability Expert (Germany)
Email: broenner@whenmapsmatter.com

Miguel Orti
Namibia University of Science and Technology
Email: morti@nust.na

Kaleb Negussie
Namibia University of Science and Technology
Email: knegussie@nust.na

Conference Web Site. <http://applied-geoinformatics.org/>

Photo on cover page: Edith Behr

Authors retain copyright over their work, while allowing the conference to place their unpublished work under a Creative Commons Attribution License, which allows others to freely access, use, and share the work, with an acknowledgement of the work's authorship and its initial presentation at this conference.

Authors have the solely responsibility concerning all material included in their contribution.

The use of general descriptive names, registered names, trademarks, etc. in this publication does not imply, even in the absence of a specific statement, that such names are exempt from the relevant protective laws and regulations and therefore free for general use.

Table of Contents

Letter of Welcome	1
Preface	2
Concept and Implementation of an Architecture for the Immediate Provision of Geodata in Disaster Management.....	3
F.-J. Behr, S. Fleischhauer	
The application development for 3D city model using game engine and its utilization to facilitate the disaster management.....	14
Shafiq H. M. A, Volker Coors	
Development Of An Integrated GIS-Based Emergency Response System	24
Moses Murimi Ngigi	
Geospatial support in the context of internal displacement caused by natural disasters.....	31
Christine Broenner	
Deriving Vegetation Health Index in Hong Kong and Colombian Amazon by using Sentinel 2 and Landsat 8 in Google Earth Engine.....	37
Andres Felipe Ramirez, Yuk Kit Chang and Michael Hahn	
Geodatabase of Base Map for Structure Plan of Adama City, Ethiopia	48
Yonas Asefa Fufa	
Assessing the use SEPAL cloud based system to perform remote sensing tasks for REDD+ Projects	56
Gillie Cheelo	
Assessment of Fire Induced Forest Degradation in Heterogeneous Forest Type of Nepal using Remote Sensing data with Google Earth Engine	67
Raja Ram Aryal and Nishanta Khanal	
Concept for High-resolution Aerosol Monitoring using Satellite Imagery and Sensor Networks in Stuttgart City80	
J. Gitahi, M. Hahn	
Food insecurity, Fortunate Index and Refuse Removal as Indicators for Resilience to Disasters	90
PMU Schmitz	
Digital Elevation Model Generation From CARTOSAT-1 Using LEICA Photogrammetry Suite.....	102
Karuppasamy S.	
Flood Vulnerable Zone Identification In Tamirabarani River Using CARTOSAT-1, Tirunelveli, Tamilnadu, India	103
Karuppasamy S.	
Geo-statistical Analysis and Modelling of Malaria Distribution in Namibia.....	104
Heita Anditanga M. M.	
Open Source as inner Habit and the Impact of the OSGeo Foundation	105
Franz-Josef Behr	
Early stage detection of Bark Beetle infestation using UAV (Unmanned Air Vehicle) based Hyperspectral and Thermal image	106
Rajan Paudyal, Peter Hofmann, Martin Hais, et al.	

Risk Sensitive Land Use Planning (RSLUP).....	107
Umesh Kunwar	
The use of Map-server and Geo-server in the Geographic Information Technology world	108
Kevin A.J Geingob	
Food insecurity, Fortunate Index and income as possible indicators for vulnerability (Workshop).....	109
Peter Schmitz ^{a, b}	
Interoperability issues in disaster contexts - with an Internally Displaced People worked example	110
Christine Broenner	

Letter of Welcome

Disasters cause massive disruption to societies and overburden economic systems. Many people are killed, thousands lose their livelihoods and in many occasions thousands and thousands are displaced from their homes every year by drought, storms, floods, volcanic eruptions and earthquakes. Vital resources are destroyed, infrastructure is damaged, and transport and communications are jeopardized

Even more critical is the gradual but clear upward trend, which is likely to continue into the future due to the impacts of climate change and population growth in areas exposed to natural hazards and landslides.

Such losses of lives and properties can be minimized by better risk analysis, prevention, earlier alerts triggered by sensor networks, and support for relief work. In all these phases of hazard prevention, handling and relief as well reconstruction after the disaster stroke, geo-information is needed and can contribute significantly.

We like to personally welcome each of you to the 9th International Conference Applied Geoinformatics for Society and Environment where we will be dealing with different approaches for such contributions of Geoinformatics, Remote Sensing, and Planning to preparation, response, recovery, and mitigation of disasters. The concept includes invited talks by international experts in combination with presentations by participants in the mornings and workshops in the afternoons on current topics. Personally we like this participative approach a lot: We all learn if we share what we know!

AGSE 2018 is incorporated into the DAAD supported alumni work of the University of Applied Sciences Stuttgart. Therefore, participants from different countries worldwide contribute with experiences from their home countries.

It's an exciting time for us and the geospatial community as we continue to recognize the importance of geospatial data and technologies in so many fields.

We may have a vision, the knowledge, and the experience to have a momentum for further developments. We ask you to stay engaged, proactive and engaged to shape the future. Our personal respect and thanks goes out to all of you.

We wish this event a successful exchange of knowledge crossing borders and disciplines.

Prof Tjama Tjivikua

Prof. Dr. Franz-Josef Behr

Preface

Applied Geoinformatics for Society and Environment (AGSE) series of conferences and summer workshops started in 2008 in Trivandrum, initiated by the initiatives of Dr. Pradeepkumar (University of Kerala) and of the Alumni Representative of Stuttgart University of Applied Sciences, Dr. Franz-Josef Behr. After the successful follow-up conferences in Stuttgart (2009), Arequipa (2010), Nairobi (2011), Asia (Johor Bahru, Malaysia (2012), Ahmedabad, India (2013), Stuttgart (2014), in 2017, Kish Island, Iran (2017). This year, 2018, the conference is being held at Namibia University of Science and Technology (NUST) in Windhoek, Namibia.

With the focus on "Crisis and Disaster Management" the conference aims at contributions of Geoinformatics, Remote Sensing, and Planning to preparation, response, recovery, and mitigation of disasters. The school concept includes invited talks by international experts in combination with presentations by participants in the mornings and workshops in the afternoons on topics like the technological breakthroughs of Unmanned Aerial Systems (UAS) for emergency response.

AGSE 2018 is incorporated into the DAAD supported alumni work of the University of Applied Sciences Stuttgart. Therefore, participants from many countries worldwide contribute with experiences from their home countries.

The conference aims also at the integration of outcomes of the events into eLearning modules. All interested participants are called to contribute and benefit from eLearning materials such as

- white papers,
- lecturing materials or
- videos,

For example, on the worldwide regulations and the developments of UAS and the experiences on autonomous flights, access to hard-to-reach areas and data-gathering tasks that are otherwise unsafe or impossible for humans.

The objective of the conference is to 'take the benefits of geographic information technologies to a wide canvas of applicable areas, particularly in the realms of crisis and disaster management'. Since 2008 we – scientists, practitioners, students and alumni – continue this path to empower one another in a participative way.

We wish this event a successful exchange of knowledge crossing borders and disciplines.

Acknowledgements

The conference would not have been possible without the collaboration and support of different people and organizations. The members of the organizing committee would like to express their gratitude to "German Academic Exchange Service (DAAD)" for the support of the alumni conference provided by the German Federal Ministry for Economic Cooperation and Development (BMZ).

The support of Deutsche Gesellschaft für Internationale Zusammenarbeit (GIZ), Namib Geomatics Technologies, esri Southern Africa, Geocata Namibia, Namibia Statistics Agency and Knoedler-Decker-Foundation is greatly acknowledged.

The authors wish to thank Namibia University of Science and Technology and Stuttgart University of Applied Sciences.

Concept and Implementation of an Architecture for the Immediate Provision of Geodata in Disaster Management

F.-J. Behr, S. Fleischhauer

Stuttgart University of Applied Sciences, Germany – franz-josef.behr@hft-stuttgart.de, steven9490@gmail.com

KEY WORDS: *Disaster management, rapid mapping, geodata, OpenStreetMap, remote sensing, free software, free data*

ABSTRACT:

Statistics prove that the number of disasters, especially weather-related, increased during the last decades. This leads to high demands on participants in disaster management processes where the information base is an essential part in these processes. Geodata, as a part of this information base, play a key role.

This report shows an approach using geodata to support decision makers and helpers in disaster situations. In a preliminary theoretical consideration the potential of geodata in disaster management is explained by the results of the VALID study. The economic value is illustrated by the estimated cost savings within a case study. Evaluations by participants in disaster management illustrate the strategic and operational benefits for the use of significant geodata products. This background research delivers as well the requirement specification for geodata provision and related products. These requirements are based on the use of general information structures in disaster scenarios. Specific aspects for the application of geospatial information are accentuated. To illustrate the state of the art this work gives an overview of existing concepts using geodata. The rapid mapping approach with remote sensing data illustrates the coordinated mapping process in consequence of a disaster event. The focus lies on the collaborative data acquisition based on the International Charter "Space and Major Disasters". Flood risk maps are an exemplary approach that shows the possible area-wide realization of a precautionary measure. The attention is focused on the mapping process and the position of politics as a driving force behind this realization.

As an alternative, this work introduces a new concept of immediate geodata provision for disaster management based on the usage of free data and free software components. The data storage is partitioned into a file-based system and a database system. The functionality of every single system component and the process of implementation are explained. The two data sources, remote sensing data from the United States Geological Survey (USGS) and vector data from the OpenStreetMap (OSM) project, are examined in detail regarding data structure and the form of data provision. In the examination of the remote sensing data there is a comparison between USGS's offers and the Copernicus Programme of the European Union in relation to the data provision.

In the implementation of the system takes batch script controls every software component and data flow. During this workflow the user specifies interactively the OpenStreetMap data for this area are downloaded using regional data extracts or automatically using the Extended OpenStreetMap Application Programming Interface. Osm2pgsql stores this data as geospatial objects in a PostGIS database. By processing incremental update information the vector data of the disaster area are kept up-to-date. The satellite images are converted by the Sentinel Applications Platform to a RGB raster image. A sub-programme of the Geospatial Data Abstraction Library (GDAL) re-projects this raster image to the consistent target spatial reference system World Geodetic System 84/Pseudo Mercator.

The render software Mapnik uses both data sources to create mapping tiles of the affected area. The style sheet is optimized for visualization of disaster related information. The image tiles are suited for immediate use by end-users in disaster management and can be provided on a web-server.

After the first implementation under Windows OS the port of the solution to Linux was undertaken using the Python programming language as a framework for the integration of the different tools.

The presented system makes it possible to provide geodata for disaster management purposes within minutes.

1 Introduction

Disasters are an omnipresent phenomenon. Statistics of the Munich Re (Munich Re, 2015) and of the United Nations Office for Disaster Risk Reduction (UNISDR, 2012) show an increasing number of disaster situations during the last three decades. The devastating effects are evidenced by the total extent of damage. From 2000 to 2012 material damages in the amount of US\$ 1.7 trillion and a loss of 1.2 million human lives worldwide were recorded (UNISDR, 2013).

These numbers show the importance of efficient disaster management. One fundamental element in the disaster management process is the basis of information and in particular geospatial information, as the Spatial Data Infrastructure Germany (GDI-DE) committee, an initiative of public authorities in Germany, states (Ostrau et al., 2013): „The Management [...] of disasters require static geodata (for certain areas) as well dynamic geodata (i.e. flooded areas).“ The general benefits of the use of geoinformation in disaster scenarios are discussed in the VALID study by the United Nations. Its results regarding the economic and strategic value of geodata are presented in the following section.

From a variety of solutions using geoinformation to support the disaster management this work will present some existing concepts to point out the state of the art.

A requirements specification will show criteria taken into consideration during the conception phase of the approach presented here.

Some definitions will be helpful for the further sections. IFRC (2011) describes a disaster as “a serious disruption of the functioning of society, which poses a significant, widespread threat to human life, health, property, infrastructure or the environment, whether arising from accident, nature or human activity, whether developing suddenly or as the result of long-term processes, but excluding armed conflict.”

According to the Copernicus website (European Commission, 2017) rapid mapping “consists of the [...] provision (within hours or days) of geospatial information in support of emergency management activities immediately following an emergency event. The products are standardized.” *Reference Maps* show the boundaries, names and unique identifiers of standard geographic areas, as well as major cultural and physical features, such as roads, railroads, coastlines, rivers and lakes, i.e. topography, *delineation maps* the extents of the area affected by the disaster and *grading maps* present the assessment of the damage grade and its spatial distribution.

The main part of this paper describes an alternative concept of a geoinformation system (GIS) for disaster management support. The description of the process and its architecture depicts the functionality of the system with all its components. We will show that a mapping solution can provide reference maps and delineation maps rapidly within minutes or a few hours. The reference map will be created based on the worldwide data coverage of the OpenStreetMap database, complemented by remote sensing imagery. Assessment of the damage grade could be done additionally afterwards based on remote sensing products.

2 Theoretical Consideration

Before going into details regarding the technical implementations of geoinformation systems in disaster scenarios it has to be determined which status geoinformation has in the field of disaster management. These theoretical considerations provide the basis for subsequent sections.

2.1 Benefit assessment of geodata in disaster management

One basic question is to what amount users benefit from the usage of geoinformation in disaster situations. The United Nations Platform for Space-based Information for Disaster Management and Emergency Response (UNSPIDER) in cooperation with the Joint Board of Geospatial Information Societies (JB GIS) and scientists from the University of Amsterdam created the VALID study to evaluate the economic value and the strategic and operational benefits (Altan et al., 2013)

The 2009 flood catastrophe in Namibia served as case study for the monetary evaluation. Stakeholders had to estimate the potential cost savings for the use of a flood early warning system in this scenario, yielding a final result of 40% of cost savings.

The strategic and operational benefits were determined by two online surveys. In the first survey participants had to choose the most important geoinformation items for disaster management. Out of the responses the ten most frequently mentioned (regarding floods, earthquakes and drought) were used again in a second survey (Altan et al., 2013:23). The participants had to estimate the strategic and operational benefits of these ten geoinformation products. The responses showed appreciation for risk and vulnerability maps. For all strategic and operational aspects of every single product the benefits were valued medium to high. Benefits for preventions measures, economic loss reduction and for the usage in both disaster prevention and management were estimated high.

2.2 Requirements specification

In the conception of geoinformation processing systems it is important to incorporate the conditions and requirements of the field of application, i.e., disaster management. The Open Geospatial Consortium (OGC) has published a discussion paper with theoretical aspects for the conception of information structures in disaster management (Penman et al., 2015). Out of these considerations the following points can be adapted for the conception and usage of geospatial information structures for rapid mapping:

- Reliable data basis,
- Data of different sources,
- Predefined formats and interfaces,
- Possibility to integrate optional new data sources,
- Application of data under supervision of experts,
- Access control by user authentication,
- Comprehension and transparency of information,
- Predefined symbology.

Other aspects mentioned by Penman et al. (2015), like alert messages and independent network, are not part of the solution presented here. Further design considerations however were:

- Rapid provision of geodata,
- Availability for everyone instead of a limited group of people, especially for local actors (IFRC, 2011:9), and accordingly,
- Usage of free/respectively open source software and data.

3 State of the Art

After the evaluation of the benefits of geodata and the delineation of the requirements some existing approaches in the field of disaster mapping are described.

3.1 Collaborative remote sensing data acquisition

In 2000 the International Charter "Space and Major Disasters" was created to allow an immediate data acquisition for disaster situations. The approx. 16 members of this charter include *inter alia* the French and the European Space Agency, the National Oceanic and Atmospheric Administration (NOAA) and the Indian Space Research Organization (ISRO) (<https://www.disasterscharter.org/web/guest/about-the-charter>). To activate the charter an access point is established. Authorized institutions can start a data acquisition cycle in case of a disaster situation through request to this access point. Under the administration of a project manager appropriate satellite data from a wide range of sensors are requested from archives as well as active satellites are programmed to record new images of the disaster area. The acquired data can be processed in the affected country to create maps via interpretation algorithms and analysis. For example radar images are suitable for the identification of flood areas whereas optical images are appropriate for fire disasters or visual damage mapping after earthquakes (Danzeglocke, 2014).

As charter member the DLR Center for Satellite Based Crisis Information (ZKI) provides a permanent service for the rapid provision, processing and analysis of satellite imagery (Voigt, 2013). The focus of this approach is the current provision of processed imagery and its analysis and interpretation, not of reference maps. However, as DLR (2017) points out, the “Charter has committed resources to support [only] some specified authorised users such as relief organisations as well as civil protection and defence organisations with free of charge satellite data in order to help mitigating the effects of disasters”.

3.2 Volunteered Geographic Information (VGI)

If a disaster strikes often the OSM community like the Humanitarian OpenStreetMap Team (HOT, <http://hotosm.org/>) is activated to collect additional data for the affected area. Following the crowd sourced approach of OpenStreetMap the data are contributed on a voluntary basis. The contribution for the mitigation of the Haiti earthquake disaster is one of most prominent examples (Neis et al., 2010, Neis & Zielstra, 2014).

According to the Annual report there were five activations of HOT in 2015 due to disaster situations. In the course of the earthquake in Nepal in April 2015 over 8000 people contributed more than 13 million edits (HOT, 2015).

3.3 Flood hazard maps

Altan et al. (2013) have shown that flood related geoinformation items have a high impact in disaster management. *Flood hazard maps* visualize information about potential flood hazards from a relatively common to an extreme scenario and probability (Müller et al., 2009). Like *flood risk maps* they are defined in the EU Floods Directive 2007/60/EG. This policy instructed the member countries of the European Union to create both type of maps for significantly vulnerable areas until 22 December 2013. According to article 10 of the policy these maps have to be available for the public. German states provide them web-based by administrative authorities.

Based on a risk analysis for every area in accordance with the determinations in article 5 of the EU Floods Directive 2007/60/EG data has been collected by terrestrial surveying. The flood hazard maps can be derived from this data blended with a digital terrain model and hydraulic models. Starting 22 December 2019 the update frequency will be six years.

3.4 SARONTAR

The system SARONTAR results from a cooperation between the University of Technology Graz, the alpine police and the telecommunications company TeleConsult Austria. In two implementation phases they created an operation control system for accidents and disasters in the Alpine region. The system architecture consists of mobile terminals, a mission control centre and a central server component (Prüller et al., 2015). The purpose of this approach is to coordinate the rescue forces on site to supply affected people efficiently. The rescue workers navigate with the mobile terminals in the destination area via satellite-based DGPS (Hofmann-Wellenhof, 2010). On these mobile devices runs the SARONTAR application that visualizes the current position on a map and allow communication with the operation control centre. On the other side the movement of the rescue teams can be monitored and corrected through instructions if necessary. The used maps are official topographic maps provided through a map service. In a pilot stage in 2015 the system was tested under real conditions (Prüller et al, 2015). The core aspects of this approach are real-time communication and positioning in dynamically changing rescue missions.

4 Concept

This work provides an alternative concept of a geoinformation system for the use in disaster scenarios. The main task is to provide geodata in separate data storage and visualize it as reference map delineating the extents of the affected area. The concept is extends the work of Hellal (2012). It is based on the usage of free software and free data combined in a multi-tier architecture as depicted in Fig. 1 comprising

- Data import tier

- Data tier
- Application and styling tier
- Web tier for presentation and export

The user defines the extent of the disaster area. This area is used as a region of interest for data acquisition in the data import segment. OpenStreetMap (OSM) data can be exported in different ways using the Extended OSM API or regional extracts. The export results are imported into a PostgreSQL database with *osm2pgsql*. Afterwards the user chooses a suitable satellite image based on the defined polygon. The system uses the Sentinel Application Platform (SNAP) to convert the remote sensing product into a geocoded RGB raster image. *Gdalwarp*, part of the *Geospatial Data Abstraction Library* (GDAL), serves to re-project the converted satellite image to a uniform target spatial reference system World Geodetic System 84/Pseudo Mercator. The stored data in the data tier can be visualized with the render software *Mapnik* in the application tier. The result of the concept is a map, which can be used in to support the disaster management tasks. There is also an option to update the OSM data in the database. With Osmosis replication files can be exported from OSM and the changes within the affected area imported into the existing database using *osm2pgsql*.

5 Workflow

5.1 Preparation

The conceptualized system was labelled “*disasterGIS*” and implemented as a first version for Windows 10 due to the potentially wider range of users¹, according to the experience of the authors especially in public authorities. A central batch script controls the several system components and the data stream during the mapping process. Therefore the interaction with the user primarily takes place in the windows console. In 2018 the port of the solution to the Linux was undertaken using the Python programming language as a framework for the integration of the different tools.

The final version requires PostgreSQL with PostGIS extension, Python 2.7, the Sentinel Application Platform and an executable version of GDAL as prerequisites. In addition the user has to set environment variables for the main executables of these tools. Other system components are directly integrated in the folder structure of the *disasterGIS* provided as a portable zip archive

¹ See Desktop Operating System Market Share Worldwide <http://gs.statcounter.com/os-market-share/desktop/worldwide/>

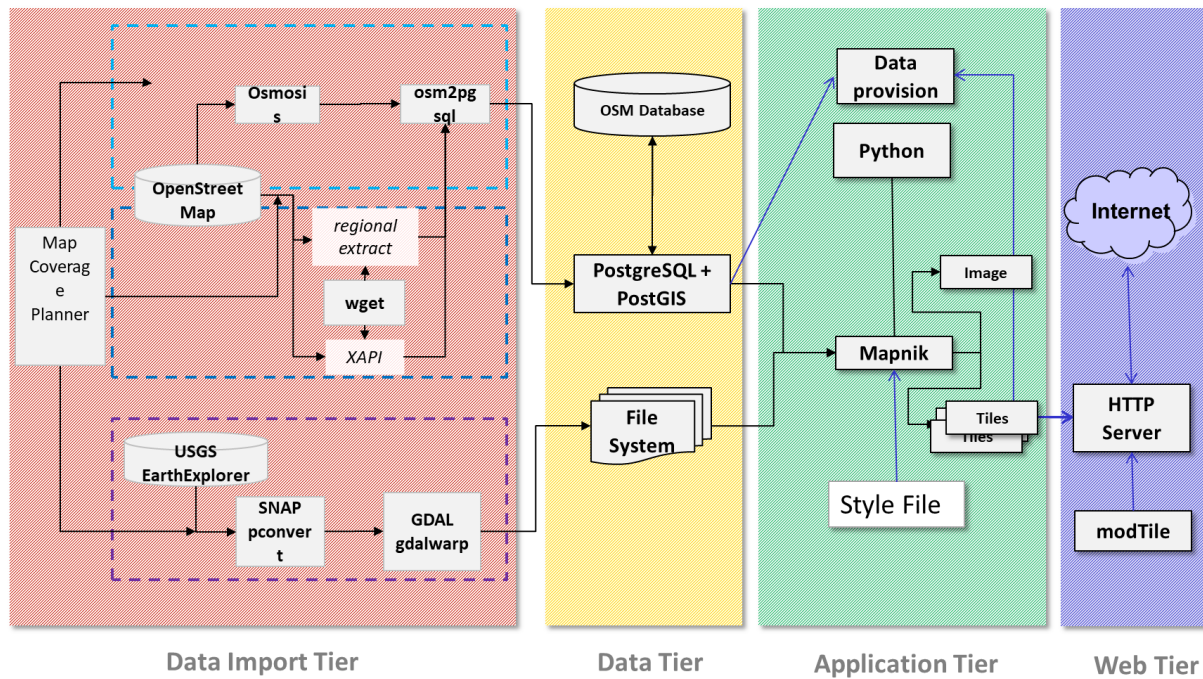


Figure 1. System architecture and components

The archive contains a README file that provides the necessary instructions for the setup of the system.

During the mapping workflow the user is guided by instructions in the console window. Export results are stored inside a separate project folder in disasterGIS.

As first step the script creates a new local PostgreSQL database with PostGIS and hstore extension. For each database operation the user has to authenticate himself by user id and password.

After the preparation of the database a local web browser opens a HTML document referencing the OpenLayers library. In the appearing map window the user navigates to the affected area and delineates its extents. When closing the map window the coordinates of this rectangle (in WGS 84) are transferred to the clipboard. The user can paste the coordinates to the console window to continue the mapping process. After confirming the coordinate input the script creates a KML file used for the satellite image acquisition in later steps of the workflow.

5.2 Import of OpenStreetMap vector data

There are two options implemented to obtain OSM data for the reference map. On the one hand the disasterGIS processes regional extracts based on administrative boundaries (see https://wiki.openstreetmap.org/wiki/Processed_data_providers and https://wiki.openstreetmap.org/wiki/Planet.osm#Regional_extract_sources). The user is redirected to the website of Geofabrik GmbH, a provider of regional OSM extracts on a daily basis². It is necessary to manually choose a suitable PBF-encoded file and paste the URL in the console window. After confirmation the batch script retrieves the file using *wget* and saves it to a predefined folder.

On the other hand the *OSM Extended API* (XAPI, <http://wiki.openstreetmap.org/wiki/Xapi>) is supported as second option. Based on the disaster extent a bounding box is submitted. Main advantage is the automatic retrieval of OSM data in uncompressed OSM XML format, using again *wget*.

The standard OSM API was not used because of its limitations in the amount of data; however the *Overpass API* (<http://overpass-api.de/>) could be additionally integrated.

The script now parametrizes *osm2pgsql* to import the downloaded data into the PostGIS database.

² <http://www.geofabrik.de/en/data/download.html>

As an alternative *Osmosis* (<http://wiki.openstreetmap.org/wiki/Osmosis>) was tested. This command line based tool uses database schemas similar to the original OSM data structure. A disadvantage is the lacking support of areal features. Even the manual creation of areal features using SQL queries cannot compete with *osm2pgsql*'s result. Therefore *osm2pgsql* is the preferred database import tool, but *Osmosis* is used to synchronize the data with updates of the central OSM server (see section 5.5).

5.3 Import of remote sensing data

Remotely sensed data from satellite-borne or airborne sensors are widely used in disaster mapping (Theilen-Willige & Wenzel, 2011; NASA, 2015; FSD, 2017). In the approach described here satellite-borne remote sensing data are incorporated. The United States Geological Survey (USGS) *Earth Explorer* (<https://earthexplorer.usgs.gov/>) serves as basis for satellite images. The web portal provides for example Landsat-8 and Sentinel-2 mission images as free data. The data offered by EU's Copernicus platform (<https://scihub.copernicus.eu/>) could not be integrated into this study due to technical limitations in November 2016.

The rectangular extent of the disaster area is used to create a KML file which is used in Earth Explorer as region of interest. The user still has to download manually suitable datasets completely covering the affected area without cloud coverage.

The Sentinel Application Platform's sub-programme *pconvert* (SNAP, <http://step.esa.int/main/toolboxes/snap/>), converts each file to GeoTIFF, a format supported by the rendering components. Because of the identical index of the spectral bands for Landsat-8 and Sentinel-2 mission products only these two types of satellite images are allowed in the disasterGIS.

The link between the downloaded satellite image and the batch script is a metadata file in the extracted dataset. Its file path has to be inserted in the console window to continue the conversion process with *pconvert*. After this CPU- and time-intensive process the satellite image is saved. Because the geocoding refers to WGS 84 the image still has to be re-projected by GDAL's *gdalwarp* tool to the uniform target spatial reference system WGS 84/Pseudo Mercator.

5.4 The rendering process

Vector and raster data are now available in the platform's data tier. *Mapnik* (<http://mapnik.org/>), a well-known render tool for various OSM maps, is used to generate a map image using the Python bindings (with Python 2.7 as additional prerequisite).

The main batch script creates now an additional project-specific script which starts the rendering process after the termination of the main script. Currently rendering is based on a former OSM XML style with some modifications to reduce the density of information and to emphasize the transport infrastructure to support navigation and logistics. Raster tiles and/or a raster image of the affected area are created.

5.5 Updating the local database

To synchronize the local database with the central OSM database, i.e. to retrieve collaboratively collected data from the OSM community, an update mechanism has been implemented. Replication files, also known as replication diffs, contain changes within a specific period of time. In the main batch script the user chooses the period from the options minutely, hourly and daily (see <http://wiki.openstreetmap.org/wiki/Planet.osm/diffs>). At first the command line based programme *Osmosis* initializes a working directory while the main batch script creates a configuration file that determines the update rhythm with the chosen option. The main script also generates a project-specific update script similar to the render batch script. After this step the disasterGIS project is completed and ready to be visualized or updated.

Updating the project data is done by *Osmosis*. With the period of time from the configuration file *Osmosis* compares the timestamp of the local state file with the timestamp of the state file on the OSM servers. If the time difference is greater than the defined time period *Osmosis* requests all OSM data changes in *osmChange format* up to the last point of update. To transfer the data changes into the database *osm2pgsql* is used again,

however in append mode. Thereby the new data are appended to the existing data instead of overwriting it. By using a bounding box only the relevant information for the disaster area will be stored in the database.



Figure 2. Exported image file of a disasterGIS project

5.6 Results

The final products of the mapping process in disasterGIS are tiles or images of the affected area. A printout of an image (see Figure 2) for example can be used as an overview map and be distributed among the auxiliary staff. In case of the collapse of communication infrastructures in the disaster area these printed maps can provide a current overview.

In comparison to the raster image the tiles have to be provided via webserver. Figure 3 shows a mapping client accessing the disasterGIS server.



Figure 3. Tile-based visualization of flooded areas (flood event in India, 2016, data © OpenStreetMap-Contributors, USGS)

The tile-based map presentation can be retrieved via stationary and mobile devices with internet access.

6 Summary and Conclusions

6.1 Outcomes

Geodata are a key resource in successfully handling disaster situations. The results of the VALID study prove the positive effects of the application of geospatial information in disaster management in both economic and operational regards. Cost savings around 40% illustrate the monetary potential for a specific case study. Experts in disaster management also acknowledge a medium to high additional value in the use of geoinformation in all strategic and operational aspects.

The disasterGIS provides an alternative approach for a geoinformation-based solution of free software components using freely available data to create reference maps for disaster management. In the crisis management cycle, the response phase is the one where immediate access to information and different resources is needed. DisasterGIS can provide geospatial information very rapidly within minutes or a few hours.

Regarding the requirements specification (see chapter 2.2) most of the mentioned criteria are implemented. DisasterGIS provides an automated, rapid workflow to create a reference map. Even if the architecture is quite complex the system is easy to deploy/to install, for small and large public agencies and NGOs, for any nations.

“Domestic actors have the primary role” (IFRC 2011) – the approach enables local actors to collect and provide geospatial information.

Another particular aspect regarding the relevance of geoinformation is its actuality. The data sources used provide a medium to high topicality: Landsat-8 and Sentinel-2 have a repetition cycle of 10 to 16 days, OSM data can be up-to-the-minute. DisasterGIS can take the advantage of data updates in disaster areas due to crowd mapping events (see chapter 3.2). It offers a continuous synchronisation with the central OpenStreetMap database to retrieve collaboratively collected data from the communities like HOT. This approach enables also local actors to collect and provide geospatial information.

The cartographic presentation is controlled by a style file. Modification can be applied to support local map styles, even using with toponyms in different languages.

The disasterGIS approach distinguishes itself from the approaches mentioned in chapter 3:

Compared to the “Collaborative remote sensing data acquisition” approach the disasterGIS is available for everybody, not only for a limited group of organisations. In addition the mapping process takes less time. A disadvantage however is the smaller number of available satellite missions and the lack of further analysis of the data.

The volunteered geographic information of the OSM community (see chapter 3.2) is essential part of the disasterGIS as OpenStreetMap is a main data source.

Flood hazard maps, as shown for the EU member states, provide full areal coverage of reference data with consistent quality and high reliability whereas the coverage of OSM data in the proposed reference map differs between urban and rural regions and different regions/countries. Both approaches address however different phases of the disaster management cycle (prevention vs. response phase). The flood hazard maps are characterized by long update intervals compared to the reference maps created by disasterGIS.

Regarding the SARONTAR system disasterGIS can be an addition instead of an alternative. It is conceivable that the map tiles generated with disasterGIS can be used as map background for the interactive map services like SARONTAR.

6.2 Limitations and potential extensions

In general there are areas of improvement in disaster management. The lack of interoperability is one aspect. Bartels (2015) cites security and privacy concerns as well as the competitive situation as possible reasons for obstacles to data sharing. Developing interoperable systems for disaster management bears financial risks and the needs-based conception is a precarious point. National and international infrastructures for spatial information, e.g. the European Spatial Data Infrastructure (INSPIRE), can play a decisive role. With disasterGIS the geodata collected in the data tier can be made available using standardized OGC web services (e.g., WMS and WFS).

The current version of disasterGIS is executable under Windows 64 bit because some components are not available as 32 bit versions. Although disasterGIS is currently implemented under Windows it is possible to implement the system architecture under a Linux distribution too. The port to Linux is planned as a next step. The mapping products of disasterGIS – geodata, map images and tiles – can be used however independent of the operating system.

Currently two data sources are integrated in disasterGIS. Due to the plugin architecture of Mapnik to a variety of formats additional data sources could be supported.

Concerning the accuracy both type of data are sufficient for orientation and navigation in disaster management. The ground resolution of the satellite images amounts to minimum 10 m. OSM's data positional accuracy, usually captured with civil GNSS accuracy, is also around 10 m. However as another potential resource for disaster management UAV-based imagery could be integrated after processing and rectification. The immediate operational readiness and better ground solutions have advantages compared to satellite imagery. In conjunction with the rapid data provision presented here this would be an interesting contribution to the generation of near real-time ground information.

7 References

- Altan O., Backhaus R., Boccardo P., Tonolo F. G., Trinder J., van Manen N., Zlatanova S. (eds.), 2013. *The Value of Geoinformation for Disaster and Risk Management (VALID) Benefit Analysis and Stakeholder Assessment*. <http://www.un-spider.org/sites/default/files/VALIDPublication.pdf> [2017-05-22]
- Bartels, M., 2015. Warum scheitern interorganisationale Katastrophenmanagementsysteme bisher? In : *Akteure verbinden, Lösungen finden - Katastrophenvorsorge im Dialog zwischen Wissenschaft und Praxis*. 14. Forum Katastrophenvorsorge. Bonn, Leipzig: Dt. Komitee Katastrophenvorsorge (DKKV-Publikationsreihe), pp. 24–25. http://www.dkkv.org/fileadmin/user_upload/Veroeffentlichungen/Publikationen/DKKV_54_14._Forum_Katastrophenvorsorge.pdf [2017-05-22]
- Danzeglocke, J., 2014. Hochwasserkatastrophen – Unterstützung aus dem All. In: *Zeitschrift für Vermessungswesen* 139 (1/2014), pp. 50–53
- DLR, 2017. International Charter 'Space and Major Disasters'. <https://www.zki.dlr.de/services/charter> [2017-05-24]
- European Commission, 2017. Service Overview. <http://emergency.copernicus.eu/mapping/ems/service-overview> [2017-05-22]
- FSD – Swiss Foundation for Mine Action, 2017: Drones in Humanitarian Action – A guide to the use of airborne systems in humanitarian crises. <http://drones.fsd.ch/wp-content/uploads/2016/11/Drones-in-Humanitarian-Action.pdf> [2017-05-26]
- Hellal, K., 2012. Rapid Mapping to Support Disaster Management based on Open Sources. Unpublished Master's Thesis, Stuttgart University of Applied Sciences, Germany
- Hofmann-Wellenhof, B., 2010: Der Alpenraum und seine Herausforderungen - manchmal ein Wettlauf mit der Zeit. Graz. http://www.tzs.at/fileadmin/TZS/Intra-net/PDF/Hofmann-Wellenhof_geschuetzt_Gmunden_24-11-2010.pdf [2017-01-03].
- Humanitarian OpenStreetMap Team (HOT), 2015. 2015 Annual Report - Mapping Our World Together. https://www.hotosm.org/sites/default/files/HOT_2015_Annual_Report.pdf [2017-05-25].
- International Federation of Red Cross and Red Crescent Societies (IFRC), 2011. IDRL Guidelines Guidelines for the domestic facilitation and regulation of international disaster relief and initial recovery assistance. [http://www.ifrc.org/PageFiles/41203/1205600-IDRL%20Guidelines-EN-LR%20\(2\).pdf](http://www.ifrc.org/PageFiles/41203/1205600-IDRL%20Guidelines-EN-LR%20(2).pdf) [2017-05-22]
- Müller, M.; Panczak-Geörg, M.; Mattes, E.; Ellmenreich, B.; Schillinger, W.; Moser, M. et al. (2009): GIS-Einsatz zur Web-basierten Darstellung von Hochwassergefahrenkarten in Baden-Württemberg. In *zfv* 134 (6/2009), pp. 333–339

- Munich Re, 2015. Loss events worldwide 1980 – 2014. http://www.preventionweb.net/files/44281_19802014paketworldusde4zu3.pdf [2017-05-22]
- NASA, 2015. Landsat 8 Reveals Extent of Quake Disaster in Nepal's Langtang Valley. <https://www.nasa.gov/jpl/landsat-8-reveals-extent-of-quake-disaster-in-nepal-s-langtang-valley> [2017-05-22]
- Neis, P., Singler, P., Zipf, A., 2010. Collaborative Mapping and Emergency Routing for Disaster Logistics—Case Studies from the Haiti Earthquake and the UN Portal for Afrika. In *Proceedings of the Geoinformatics Forum*, Salzburg, Austria, 6–9 July <http://koenigstuhl.geog.uni-heidelberg.de/publications/2010/Neis/un-osm-emergency-routing-gi-forum2010.full.pdf> [2017-05-26]
- Neis, P., Zielstra, D., 2014. Recent developments and future trends in volunteered geographic information research: The case of OpenStreetMap. *Future Internet*, 6(1), 76-106 2010 <http://www.mdpi.com/1999-5903/6/1/76/htm> [2017-05-26]
- Ostrau, S. et al., 2013. Einsatz von Geoinformationen in den Kommunen. Ergebnisse der Umfrage, Good Practice Beispiele, Handlungsempfehlungen. http://www.geoportal.de/SharedDocs/Downloads/DE/GDI-DE/KoKoStudie_Einsatz_Geoinfo_Kommunen.pdf?__blob=publicationFile [2017-05-22]
- Penman, J.; Knudson, J.; Luraschi, G. (2015): OGC 15-095 *Emergency and Disaster Management Information Framework*. Version 0.0.2. Open Geospatial Consortium. https://portal.opengeospatial.org/files/?artifact_id=66868 [2017-05-22]
- Prüller, R., Fösleitner, C., Sommer, C., 2015. SARONTAR – ein Einsatzleitsystem für Notfälle in alpinen Regionen. In: Josef Strobl (Hg.): *AGIT 1-2015*. Journal für Angewandte Geoinformatik. Berlin: Wichmann, S. 252–257. http://gispoint.de/fileadmin/user_upload/paper_gis_open/AGIT_2015/537557036.pdf [2017-05-22]
- Theilen-Willige. B., Wenzel. H., 2011. Remote Sensing And GIS Contribution to Earthquake Disaster Preparedness in Hungary. Geoinformation for Disaster Management Gi4DM, 03/05/2011 - 08/05/2011, Antalya, Turkey. <http://www.isprs.org/proceedings/XXXVIII/Gi4DM/CDDATA/sessions.html> [2017-05-25]
- UNISDR, 2012. Number of Climate-related Disasters Around the World (1980-2011). www.preventionweb.net/files/20120613_ClimateDisaster1980-2011.pdf [2017-05-22]
- UNISDR, 2013. DISASTER IMPACTS / 20002012. https://www.preventionweb.net/files/31737_20130312disaster20002012copy.pdf [2019-12-15]
- Voigt, S., 2013. DLR Center for Satellite Based Crisis Information. In: Altan O., Backhaus R., Boccardo P., Tonolo F. G., Trinder J., van Manen N., Zlatanova S. (eds.), 2013. *The Value of Geoinformation for Disaster and Risk Management (VALID) Benefit Analysis and Stakeholder Assessment* . <http://www.unspider.org/sites/default/files/VALIDPublication.pdf> [2017-05-22]

The application development for 3D city model using game engine and its utilization to facilitate the disaster management

Shafiq H. M. A^a, Volker Coors^b

^a Department of Space Science, University of the Punjab, Quide-e-Azam Campus, Canal Bank Rd
54590 Lahore, Pakistan- anas.4gs@gmail.com

^b Department of Geomatics, Computer Science and Mathematics, University of Applied Sciences Stuttgart
Schellingstraße 24, D-70174 Stuttgart (Germany), - volker.coors@hft-stuttgart.de

KEY WORDS: *Visualization, 3D-Model, CityGML, Game Engine, Data Integration, Application Development, Disaster Management, Emergency Response*

ABSTRACT:

3D visualization of spatial data is gaining popularity, particularly for the 3D city models. It enhances the level of detail, improves accuracy of the data, establish an environment to give users a sense of reality. A quick render able nice and realistic appearance of a 3D building model would be very helpful to yield more to support disaster management. For example, comparison of a 3D city model before and after the destruction (flood, earthquake etc.), 3D building model for a fire fighter responding fire or to rescue the people stuck in it, 3D model of an airport or hospital or supermarket for management and security purposes are some of the examples through which we can facilitate disaster management using 3D GIS. This paper explains the work, results and the experience based on using game engine's state of the art technologies to visualize 3D city model to support disaster management. Since the game engines are not designed to support the GIS data formats, a process-pipeline has been developed to import GIS data of different formats in the Unity, the game engine.

1 Introduction

It is a reality that the population, especially in urban areas, growing very fast. People from remote or undeveloped areas are constantly moving towards cities for a better lifestyle. This the urban encroachment is happening across the world and causing several issues especially in developed cities. These issues are related to facility management, traffic, energy and disaster management. For a city like Stuttgart, the local governing bodies are now more concerned to make better and effective decisions to handle the issues for over a longer period of time. For this, they are required to have more information about the issues and their forecasting. Visualization is one of the most important elements to present the information. It has been greatly enhanced by the quality and speed of rendering in the past decade by using improved CAD system. 3D visualization of a data or the city model made it possible for us to increase the level and quality of information and the data accuracy. Thus it raises more expectations and possibilities to deal with GIS data in a more user friendly and interactive way. 3D visualization is "a shift from 2D to 3D analysis, which opens up a whole range of possible new applications" (Engel and Döllner, 2009). Due to its effectiveness, the 3D visualization is encroaching very fast in the field of GIS. GIS specialists are looking forward to discover new ideas and approaches to find the ways of representing the Geo spatial information through a different aspect. In the mid of 90s with a quote from Autodesk themselves. "Autodesk today took its first step into the fast-growing geographic information systems (GIS) market, as the company began shipping its first dedicated mapping and GIS product, AutoCAD® Map" (Map 3D and Murphs Law, 2010). Now there are many software that serves the Geo data using modern technologies. Game engines, in this case, will be explored in this research.

In recent decades, due to more advance graphic and processing hardware, the gaming industry flourish rapidly. Game engines are the combination of many reusable software components and physics related abilities that require to create most of the games. "Game Engine (or 3D Engine) is a complex system, responsible for the

visualization and sound of the game that handles the user input and provides resource management, animation, physics and more" (Valient, 2001). Likewise, game engines provide support for real time rendering, data compression, programming language, artificial intelligence and Physics-effects. For the high quality 3D GIS data visualization, Geo data should also assist by the modern game engine. There is a need of a 3D application that require less hardware or software, but give a realistic appearance of the city model to facilitate the end user like urban planners and architects. Unity, the game engine, comes with a huge library of tools and objects. It also supports third party assets and algorithms in C#, JavaScript and Boo language.

In this research the motivation was to use a 3D city model of Stuttgart and produce a virtual scene using the game engine and analyze the ways that it could support disaster management. The reason of using game engine was due to the fact that they are quite efficient and powerful to create 3D scenes. Game engines provide more graphical, navigational, animation and rendering tool which greatly enhance the overall appearance of the scene. Hence, combining the capabilities of the game engine with geo data will facilities more to the end user. A conversion mechanism needs to be developed so that the geo data or CityGML data in this case can be used in Unity. Using the gaming environment, a scene of 3D city model will be created in which the end user could experience the gaming spectacle while using some GIS functionalities and additional text-based information from the 3D models, on demand. The structured 3D city model scene should also be capable to give the results of line-of-sight either from a fixed location or by moving object in real time, i.e. viewshed analysis. 3D data optimization for fast data rendering has to be taken into account due to the large size of the Stuttgart city model. Finally, it was also aimed to create multiplatform applications that could be accessed by the user easily according to their hardware or software requirement

1.1 Related Work

Manyoky et al. (2014) worked on a GIS Based Visual-Acoustic 3D Simulation model for Wind Farm assessment for renewable energy installation. It was done by using the game engine named 'CryENGINE'. The research was conducted to evaluate and analyze the effect of the sound on the neighboring residents produced by the rotating windmill blades. Their motivation was to create such a visual and acoustic models from which the people can anticipate the effect of these turbines on their daily routine. In this way, it will become easy for the 'planners' to figure out the location that would be acceptable for people living around.

Agugiario et al. (2012) described their project work which was based on the creation of a web based prototype tool. The tool, named "Query Arch3D" developed for 3D visualization and especially to meet the needs of workers at cultural heritage site. The heritage which was actually sited at Copan, Honduras represented by multi resolution 3D visual and was able to make queries on. The site was surveyed and modeled (non-textured) by the CAD system. The design principles for the semantic and geometric data was made similar to CityGML modeling principles. The final implantation of the Copan site model was taken from the Unity game engine. To choose Unity, they reasoned that it was due to its fast processing time.

2 Methodology

2.1 Stuttgart CityGML Model

The main data for this research work is the textured 3D city model of Stuttgart in CityGML format provided by Stuttgart municipality. It covers an area of about 1.77 km². The data contain building objects, terrain and solitary vegetation objects. The building models constructed by using Lidar survey data and by using Google Sketchup. The process started with the conversion of CityGML model (without loss of information) to make it able to use in the Unity game engine. Although Unity supports different 3D formats, but FBX (FilmBox) format appeared the most suitable format since it supports the multimedia format and all 3D features that converted from CityGML city model, including polygon-ids, mesh, texture and texture-coordinates.

2.2 Data Optimization

Due to the size, extent, features and large number of files of the Stuttgart 3D model, it appeared vital to take many steps to make the model easily handle able and fast process able. The model in FBX format was 276MB

of size without textures and 885 including textures which Unity was unable to load even after many hours. So another way of importing the entire data was required.

Data Division: The data divided into three classes Building, Vegetation and Terrain. The 'Building Data' exported into FBX format and then subdivided into 25 parts. The building data division was done 'spatially' and randomly without distorting the geometry where terrain and solitary vegetation object data exported as 2 separate files.

Textures Compression: The number of textures and their total size had a great impact to slow down the import, loading and processing of the city model. Decreasing the number of texture files means removing the textures of the buildings. On the other hand using JPEG compression, the overall size of textures can be reduced. So a compression has been made which decreased the size of 8571 texture files from 609MBs to 189MBs, a total of 68.97%. The compression set to balance between size and the image quality (Figure 1).



Figure 1: Texture compression. Before (Left). After (Right)

2.3 Constituents of 3D City Model

In this section, the main constituents of the 3D city model of Stuttgart are described.

Buildings: Once Unity load all building polygons, the material for each polygon created automatically by Unity if both 'polyid' and 'textureid' available in CityGML data. Furthermore, each material looks for the texture that referenced to it in CityGML and merge with it if available. While inserting building data from the Stuttgart 3D model inside Unity, each polygon of the building created its own material entity because of the 'Polyid' that defined in the CityGML data for each polygon. For 'raycast feature' only the polygonal mesh of each building was not enough since it is opaque to the object that does not have a collider where collider is an imaginary object in Unity used to implement the behavior of physics for collision effects. For example, when it is required to collide the RayCast with buildings for viewshed analysis, it is necessary to assign a mesh collider so that

- The RayCast collide the building exactly according to the shape of the building
- The RayCast collision represents the collision with entire building rather than the collision with many polygons of the building

So for viewshed analysis, the mesh of each polygon of each building joined and welded together. In this way each building gets a 'single' mesh for it. In this way the entire mesh does not behave in several parts, but as one single entity, required for viewshed analysis.

Terrain: To create the terrain of Stuttgart model in Unity, high resolution image from 'Google Earth Pro' has been used. Using image processing traffic vehicles was removed to enhance visuals of the roads in the scene. Five strips of images from 'Google Earth' were extracted and stitched into one (of resolution 27800x40400 covers the entire 3D building model). A collider of the same size created and merged with terrain in Unity for collision effects.

Streetlight: To add the streetlights into the scene, first their spatial locations (contain streetlights and power-lines) in Stuttgart integrated as points in Autodesk DXF (. dxf) format into the model the then the street light model copied and placed into these locations. For design, only three different designs (close to reality) was modeled using CAD. All streetlight 3D models (73 in total) exported in FBX format for Unity. Each design, then customized in Unity for real look (according to the ground truth). To add the real time light (139 in total)

effects, Unity's spot light and bulb-flare in pale-yellow color was installed to each light for realistic visual effect. The angle, intensity and the range of the spotlight was set accordingly (Figure 2).

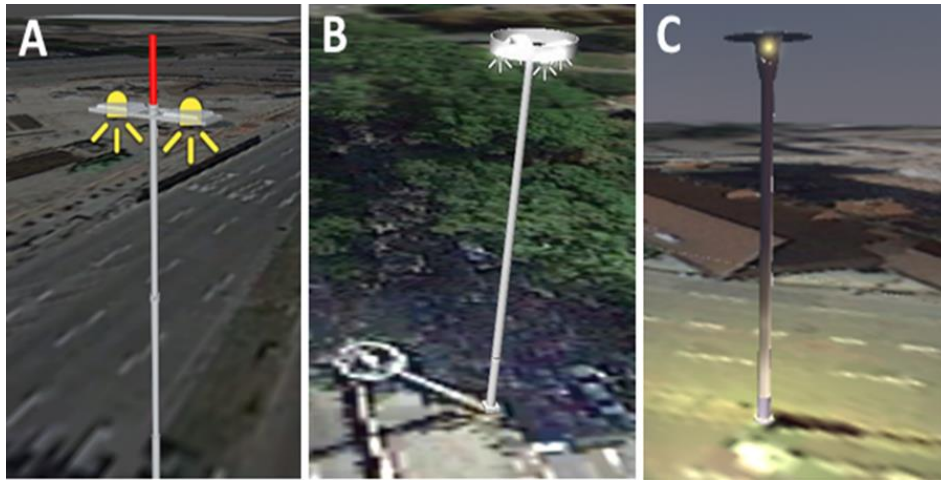


Figure 2: 3D models of street-light in the 3D city model

3D Trees: To add 3D trees that fit into the scene closer to the reality, trees of different sizes (representing age) and shapes (representing types) integrated. Since these trees constructed via 'procedural mesh geometry' hence can be edited using the model diagram. The spatial location of trees (according to Stuttgart) extracted from the CityGML model of Stuttgart (Figure 3). Second, in Google image of terrain, it was easier to identify the location of the tree directly. The final placement of the trees (107 in total) has been the combination of both visual analysis as well as exact spatial location.

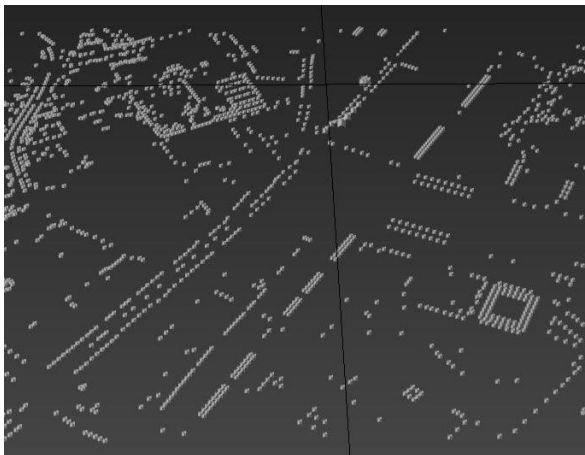


Figure 3: Vegetation location data, extracted from CityGML

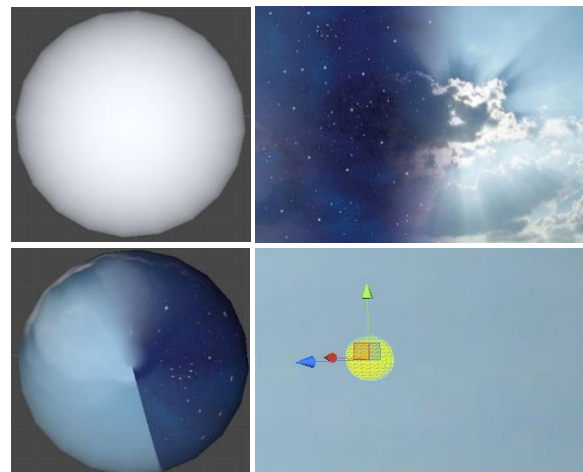


Figure 4: 3D Sky globe, day/night image and the Sun at bottom right

3D Sky System: The surrounding environment, especially in a 3D scene plays an important role in the overall realistic appearance of the scene. For this, a so called 'sky system' has been developed in Unity (Figure 4). It comprised of components, including sky-globe (sphere), the sun (sphere), the moon (sphere), day/night RGB image (contains gradient day and night appearance), cloud (cloud image with irregular 3D mesh constructed

using CAD) and three directional lights for the sun (yellowish colored), the moon (white colored) and one for overall luminance (to make a balance especially during the day/night transition). That globe being the base component of the sky system set to rotate in the scene with a suitable rotational speed of 10 minutes for a day by developing a short algorithm. It also attached with day/night RGB image using material object. Since in Unity the properties of parent element transferred to each child object, so other components the sun/the moon with their respective lights and the clouds attached to that globe at their suitable locations (Sun and Moon opposite to each other, clouds spread at random). This system is also responsible for the shadows and variation of light intensity according to day/night.

Lights, Shaders and Shadows: Three directional lights have been used one is for the illumination of the overall scene, directed towards the terrain and is static. Where the other two has been attached to the Sun and the Moon rotates due to the rotation of the sky system. Since the Sun and the Moon are placed opposite to each other, only two directional lights will take part at-a-time for the illumination of the visible content. The directional-light attached to the Sun is set more intense than it is attached to the Moon. As a result, during the daytime, the overall illumination of the scene was high as it should be in the daytime and the shadows are also more intense than due to the moonlight. On the other hand the night scene is relatively dark and the streetlights become prominent. Two self-illuminating diffuse-shader has been used to glow the Sun and the Moon. The strength or density of the shadow defined by the intensity of the directional light. Since the Sun, the Moon and their directional light rotate with sky-globe at the same speed the shadow of the objects i.e. buildings, streetlights, trees also change accordingly (Figure 5).

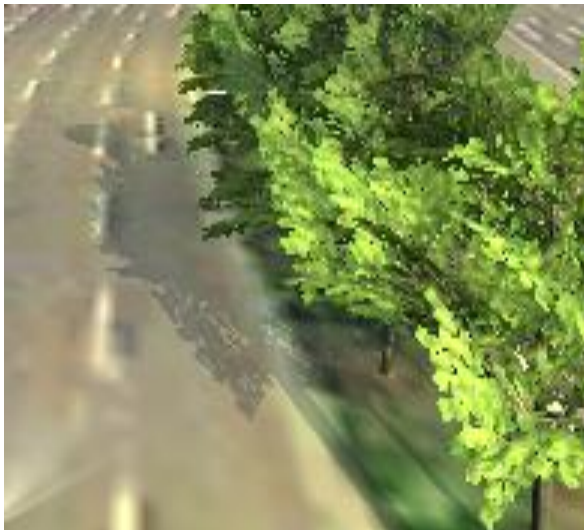


Figure 3: Shadows from 3D objects in the developed application

Camera: A 3D scene enriched with data, functions, operation that even render in high quality graphics, but if the camera is not set to an appropriate position, FOV and range the entire development could be at risk for visualization. So for a suitable location of the camera for the visualization in developed applications following key points were taken into account

- The camera should neither too close nor too far from the terrain that it looks fuzzy or goes out of range
- To avoid cover on data, the camera should not close enough to the navigating objects
- To avoid system overload, FOV and range of the camera should not be too wide or long respectively

It has been inspected that when the user moves the camera-view to a 3D-asset-crowded view, the lag could happen. Where the intensity of lag mainly depends on the system capabilities.

Raycast: Raycast is a feature of using a ray for different purposes that originates from a point in 2D or 3D. To use the function of Raycast in Unity, an algorithm has been developed to do the viewshed analysis using the Raycast by customizing it in Unity (Figure 6). When the algorithm run, it initializes the Raycast function from the

physical location that defined in Unity scene. Once Ray-Cast initializes, it extend towards the defined direction and extends to the length, defined for the extension. The quality of the mesh created by rays has also implemented using simple multiplication factor. So, for example, if the angle of FOV is 90 and the quality factor is 20 then the total number of rays in the mesh will be 1800. Once the direction of the rays, FOV angle, length and the quality factor has been defined the mesh created and visualized in Unity's game-mode and to make it

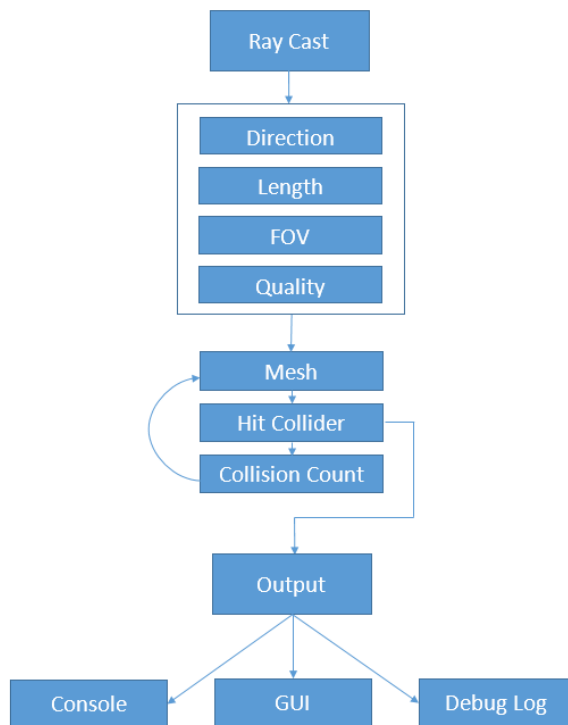


Figure 6: Algorithm for viewshed and range trigger

effective and responsive the algorithm was extended with collider and collision-count variables. Collider is a narrative variable of RaycastHit in Unity. Its value will be 'null' if raycast does not hit or collide with any object. So the RaycastHit function was inserted for the collision detection because for the viewshed the ray-mesh has to collide with objects like buildings, trees etc. The length of the rays restrict to the point of collision. In this way user presume that each colliding object casting its shadow to incoming rays. The shape or structure of the shadow depends on the part of the object facing the rays. To prevent ray-mesh for being one single entity, collision by each ray has to be accounted separately. Colliding rays for each object has to be evaluated by their hit-count to make the collision response accurate. In this way the ray mesh become able to detect each object in one instance. With a hit-count, if more than one object appear in the FOV of ray's mesh, the algorithm respond for each object separately.

2.4 Results and Analysis

2.4.1 Game Engine

The Unity game engine has shown the potential to support GIS data that was in CityGML format. Unity was

used for the visualization of 3D city model and to integrate different object classes i.e. terrain, streetlights, trees and sky system together.

Support to GIS data: Unity does not support to CityGML format directly. It fully supports the CityGML data that has been converted to other 3D formats. It not only support the geometry of the object, but also the textures and the location data of vegetation objects.

Support to Algorithms: The Unity game engine fully supported the algorithms developed in C#. Unity's MonoDevelop IDE synchronize with Unity and support as a code-editor and compiler. The algorithms that developed using MonoDevelop were integrated into the city model. MonoDevelop IDE supported to edit the integrated algorithms on-the-fly where Unity's game-mode, in parallel, display the change due to the change in the algorithm, in real-time.

Data Rendering: There were the large size and a huge number of files of the 3D assets that has been used in the developed application. To visualize the results and to evaluate the overall working performance of the developed application, test-run of each application has been made. It has been observed that when the user navigate to a place where the assets are crowded and scene become denser, the data rendering performance fall down and user face low FPS rate for data rendering. This effect is highly depending on the application platform and the operating system's specification. The major cause of this issue is the memory of the system's graphic display card. Other considerable problems were low RAM, low processing speed or too many software that run in the system's background. In case of online hosted web application, depending on both the system and the internet-bandwidth the user could face either one or both the lag and latency issue.

2.4.2 Results of the Constituents of 3D Scene

Building Data: Building data retrieved from CityGML was the key component and has been the largest part (including textures) of the 3D scene that used in the developed applications. For fast processing, about 35% of

the total 3D buildings has been visualized in the applications. The 3D building data transformed to local coordinate system of Unity. Each building attached with a mesh-collider of the exact geometry of it. The buildings in the developed applications have the following features

- All buildings are visible according to their defined geometry in CityGML
- They have colliding property as in real scenario
- All solid objects casting the shadow in real-time according to the angle of directional light
- All buildings displaying their textual information (stored), on-demand
- All buildings are capable to respond to the viewshed analysis

Terrain: Textures and terrain images are the major constituent of the total size of developed applications. The



Figure 7: Terrain view in the application

terrain created from real imagery has some visual issues as well. (Figure 7) the terrain has visible road marks. These marks which define the lanes on the road are distorted. This distortion is inversely proportional to the distance between the road lane-mark and the origin of the camera. Moreover, in (Figure 7) the shadow of two different strengths or intensity can be observed on the terrain. One is from the car, on the right side of it due to the directional light in real-time, whereas the other one is from the building on the left hand side of the building due to the shadow that cast because of the real sun, when the imagery was taken in the real world.

2.4.3 Applications Development

Using the 3D city model of Stuttgart in CityGML with Unity game engine, four different applications have been developed successfully while it was the aim to develop lightweight applications that could be run easily with average processing and graphic hardware. These applications developed for three different platforms, including web, windows and Android. To create a balanced comparison to evaluate the applications for each different platform, each application initially created with the same size of 3D data and rendering quality settings (Table 1). For the final application of this research, varying amount of data has been used according to requirement. According to results, the developed application for windows has the larger size (342.3MBs) than where web (176.9) and Android (169.5) applications has nearly the same size to each other. Since PCs come with high hardware system capacities so for windows application development Unity's built-in compression-algorithm does not set much to reduce quality to it. For the web-application the high compression applied as it is aimed to host or publish the web application online, where the large size web application will make latency rate problem for the end user. As it can be seen in Table 1 the size of the Android application is quite large and not suitable for Android device with an average hardware specification. Furthermore, it also crosses the limit of 'Google Play Store' (if intended to publish commercially) which is 50MB. The application tested on an Android Device (Sony Xperia Z). The application still exhibits low latency rate issues, to some extent.

Table 1: Statistics of developed applications.

	Windows	Web	Web	Android
Access	-	3dstuttgart.tk	3dstuttgartvs.tk	-
Total Size (MB)	342.3	96.4	16.2	86.8
Texture's Size from Total	81%	84%	82%	91%
Textured Buildings	Yes	Yes	No	Yes
Shadows	Yes	Yes	No	No
3D Data Usage (from the total building data)	~ 35%	~25%	~30%	~25%
User Interaction	Navigation, Text information (Auto/Manual)	Navigation, Text information (Auto/Manual)	Navigation, Viewshed, Text information (Manual only)	Navigation, Text information (Auto/Manual)

2.4.4 Viewshed

In GIS, viewshed is an important feature to analyze the line of sight of a viewing objects from any particular position. The viewshed analysis could have different aspects and reasons. The visibility of sign boards of advertisements and number of visible buildings or shops from any point are some of the examples of the viewshed analysis. For this, the inherited feature of 'Ray Cast' of Unity game engine has been used. A web application has been developed for the purpose of viewshed or line-of-sight from a dynamic location (mobile location). This application was successfully published online as well, so that it can be accessed online anywhere in the world (3dstuttgart.tk). As the textures were not so important for this intent, to increase the processing, the building data represented without textures (Figure 8). Due to the un-textured buildings, the size of the application greatly reduced. A pedestrian cartoon character has been used to walk through. While the



Figure 8: Viewshed in 360° FOV from a point source

viewshed or line of sight has been set to function 360° of the FOV at 1m height (from the terrain) around the cartoon. Whereas the range or distance of the line of sight is 100meter from the center. The end user can control the pedestrian and move it like a normal walk/run and analyze the line of sight in real-time.

2.4.5 Application for Disaster Management and Emergency Response

The developed-application suggest various possibilities to support emergency response.

Damage Cost Evaluation: The results of viewshed analysis application propose that its application can help in a disaster to analyze the damage of a building/s. For example, when a severe disaster like earth quake or a flood cause damage somewhere, especially in urban areas, the destruction to the buildings greatly change their structure, depending on the impact. This change in structure can be detected and evaluate using raycast of the Unity game engine. The difference of the shadows of a building due to raycast before and after the destruction of that building will tell the intensity of the disaster and will help to evaluate the damage cost.

VVIP Movement: The movement of high risk personnel, for example head of state, politicians, celebrities, international delegations or prisoners etc. is always very crucial when it comes to travel through public traffic routes, especially in non-peaceful cities or countries. Spatial analysis of routes using 3D city model can help to optimize the route, to simulate the effect of any terrorist attack, to reroute the emergency exit, etc.

Emergency Evacuation: Consider a large building like an airport, hospital or a university building. At the time of any emergency situation like a natural disaster or a terrorist attack the rapid-evacuation of the public become the most important event in the initial seconds. At that time, people having 3D model of that building in their smartphone can not only evacuate themselves but also can help others to navigate.

Response to Fire: In a fire situation, the fire fighter mostly do not have the idea of exact locations in the fire building. Using the automatic information extraction feature they can identify the number of particular floor or room or entrance so that they can do a targeted operation without wastage of time.

3 Conclusion

Different researches have been done using different technologies to visualize geo-spatial data in a 3D environment. In this research CityGML 3D city model of Stuttgart (Germany) has been used with the game engine's technology. The main idea was to evaluate the support of both the CityGML and the game engine to each other, to develop a user/system friendly application and to examine the use of application in favor of disaster/emergency management.

The additional features of the game engine like lights, shades, camera and shadows can also be blended with existing 3D city model. Using Unity game engine new algorithms can be implemented to perform additional tasks or functions that does not provided by the game engine by-default. Another, one of the most important advantage of using the Unity game engine is its ability to develop cross-platform application in a convenient way.

4 References

- Agugiaro, G. et al., 2012. a Web-Based Interactive Tool for Multi-Resolution 3D Models of a Maya Archaeological Site. *ISPRS - International Archives of the Photogrammetry, Remote Sensing and Spatial Information Sciences*, XXXVIII-5/(March), pp.23–30.
- Engel, J. and Döllner, J., 2009. Approaches Towards Visual 3D Analysis for Digital Landscapes and Its Applications. *Digital Landscape Architecture Proceedings 2009*, pp.33–41.
- Manyoky, M. et al., 2014. Developing a GIS-Based Visual-Acoustic 3D Simulation for Wind Farm Assessment. *ISPRS International Journal of Geo-Information*, 3, pp.29–48. Available at: <http://www.mdpi.com/2220-9964/3/1/29/>.
- Map 3D and Murphs Law, (2010). A History Class. [online] Available at: <https://map3d.wordpress.com/2010/08/09/a-history-class/> [Accessed 20 Jan. 2015].
- Valient, A.M., 2001. 3D Engines in games - Introduction. *Conversion from HTML article written in april 2001*, (April), p.20. Available at: http://www.dimension3.sk/downloads/3d_engines_in_games.pdf.

ACKNOWLEDGMENT

The authors wanted to exhibit their truthful appreciation to Mr. Mohl from Stadtmessungsamt Stuttgart, Germany to provide 3D textured data of city of Stuttgart. He not only provide the data but also provide the initial advisement on this research regarding data structure.

Development Of An Integrated GIS-Based Emergency Response System

Moses Murimi Ngigi

Dedan Kimathi University of Technology (Kenya)

KEY WORDS: *Emergencies, emergency response system, GIS, GPS, network analysis*

ABSTRACT:

Emergencies occur day in day out with pre-warning or no warning, this call for emergency preparedness which involve laying down plans on how to deal with emergencies and developing systems to enable emergency communication and deployment of response services to incident location. There exist problem in emergency communication such as delayed reporting, problem in determining incident locations, issues with evaluating expected ground conditions among others in emergency management. This issues lead to delays in response services which then result to loss of lives and property. Emergency response systems are dedicated for communication of incidents or disasters to an emergency response centre that monitor incoming requests. GIS, GPS, Web and Android technologies can be used to integrate the different and related response facilities and help in decision based on closest facility to incident location and efficient emergency services deployment. This has made it possible to improve the overall emergency response by capitalizing on emergency reporting and response in timely manner, thus reducing suffering and prolonged exposure of victims to life threatening situations. This project has come up with web application (incident reporting and responders), and android application which will facilitate incident communication and support by analysis based on closest facility and shortest paths to location of incident as well as dispatch of this information to other supportive team. With this system, emergency management is possible with great effect and thus reduction of loss of lives and property when these incidents occur and also help in realizing the Millennium Development Goals and Kenya Vision 2030 on effective emergency and disaster response and preparedness.

1 Introduction

1.1 Background

Kenya, like the rest of the world, is faced with a wide range of emergencies such as road accidents, collapsed buildings, terrorist attack, disease outbreak, and natural hazards (Wachira, 2016). Emergency response can be seen as actions taken to contain or respond to dangerous, expected or unexpected property destructions and life threatening incidents with a goal of mitigating the impact of the incident to citizens, property and the environment. However, quick and effective response to the emergencies is hindered by a range of issues: late reporting, inefficient free toll call system, ambiguity in location names and route identification challenges.

Kenya has, at various instances, been caught unaware by disasters; leading to elevated loss of life and property to these incidents. Slow response services, have seen incidents escalate to become major ones to which without international assistance the country could not efficiently and effectively manage (Kirchenbaum, 2004). Therefore, a need to develop and adopt emergency preparedness systems for the country is paramount in addressing any kind of disaster irrespective of its magnitude. Emergency response systems are designed to provide emergency and rescue services to citizens or members of the public to ensure public health and safety. These systems provide means for reporting the occurrence, a monitoring system for detecting and alerting response teams about incident details and means of reaching incident location within the shortest time after the incident was reported.

Currently GIS technologies have become widely used in many fields all over the world (MacFarlane, 2005). GIS, GPS, Web and Android technologies can be integrated with these emergency response systems and utilized to optimize deployment of response teams based on the nearest relive team or centre and also to provide directions to the incident location taking into account shortest route as a factor of time which is vital in emergency response.

1.2 Problem Statement and research objectives

Effective emergency and disaster response and preparedness are a vital part in achieving both Vision 2030 and the set Millennium Development Goals (MDGs) as per the Kenyan Constitution. Emergency response teams have had hard times in dealing with the incidents, especially in determining the exact location of incidents scene, shortest route to which rescue teams can use to reach the scene, and coordinating the rescue teams involved in the rescues mission among other challenges. Absence of integrated emergency response systems in Kenya and weak cooperative efforts to contain incidents has been a major drawback in effective response to incidences.

Emergency responders exist independently thus inadequate coordination among various emergency response departments even after coming up with the National Disaster Operation Centre (NDOC). When a disaster or emergency strike it has been difficult to coordinate the different responders with each receiving the news at different times, leading to uncoordinated response. Secondly, there exists a big issue with emergency communication (reporting) due to poor communication intervention and late incident reporting. In Kenya, most emergencies are not reported in time and this result to delayed response by stakeholder to scenes leading to increased clearance time and loss of property and life due to prolonged exposure of victims and property.

The largest problems are: the existing communication channels are inefficient and are set under old technologies, failure of the set organizations to prioritize emergency calls and messages, and wrong or conflicting disaster communication location. In Kenya there exist locations with the same or almost similar names; this makes it difficult for responders to precisely locate incidents location. This then result to a bigger challenge that require continuous communication between the incident reporter and responder. This calls for a smart disaster communication (reporting) system that can avoid conflict in incident location by providing detail on exact location in coordinates, thus narrowing down on the search area radius. Additionally, the problem of determining the shortest and effective route to incident location in emergency response is a major factor that determines time for the relief team to reach destination of incident. Response teams need a system that can guide them to incident scene effectively for quick response and relief to citizens affected.

The main objective of the project was to develop a geographical information systems based integrated emergency response system which can facilitate fast response to incidences through effective and accurate location of the incident, efficient route identification to the incident location, and coordinated approach to incident relief activities with improved communication/reporting capabilities. This project consisted of creating an Android application for reporting emergency occurrences and web application for displaying incidents and their details on a dynamic web map based on Google maps, a system for conducting routing using Google API and finally a map for displaying and analysing real-time incident rates.

2 Methodology and System Development

2.1 Overview

An integrated emergency system developed consisted of an incident reporting unit, a responder unit, combined together to provide the emergency response system (Figure 1). The system was continuously tested during the development. Each aspect of the project was independently developed and compiled for each individual unit. The units were developed using JavaScript, hypertext mark-up language (HTML), extensible mark-up language (XML), Hypertext Processor File (PHP), cascading style sheet (CSS) programming languages and Notepad++ and Android studio. XAMPP was used as a server to facilitate communication and storage of incident information between incident reported and responder.

The system testing was done in Nyeri County and some parts of Nairobi County, Kenya. The database was populated with the following data: administrative boundaries, roads, health facilities/hospitals, police posts, fire stations/centres, and incident scenes as reported/simulated. The accuracy of the reported incidents ranged from 0 to 30 meters, depending on the environmental factors that affect GPS signal and structures that blocked the GPS signal.

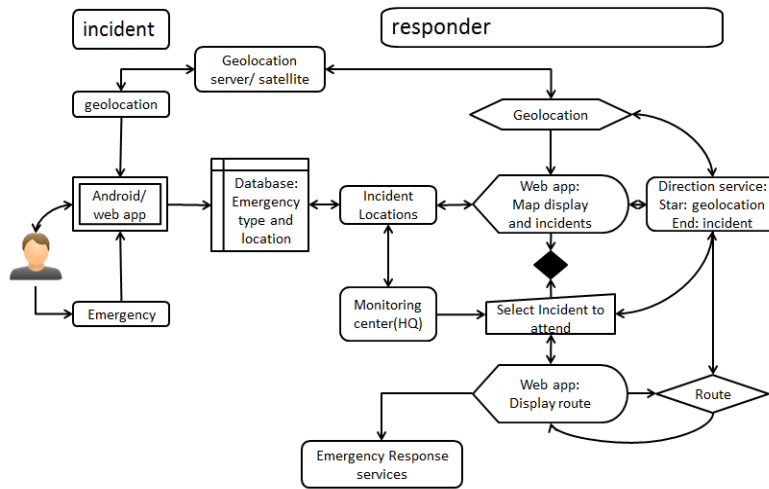


Figure 4: The emergency response system functionality flow

3 Results and Discussion

This project achieved the following: an Android application for reporting emergency incidents, a web application for reporting emergency incidents, a web application for response teams and bodies to identify and reach incident location.

3.1 Android application for reporting emergency incidents

This is an android application dedicated for reporting emergencies. It is here where location (latitude and longitude) of an incident are determined, and user interface for inputting name of incident, area name, and extra information that can help responder determine the expected ground condition, severity, and any other information(Figure 2). It is on the interface of this application where the user can ascertain their location based on visual interpretation from a hybrid map from Google and submit to a database that is accessible to the responders or emergency response teams (Figure 3).

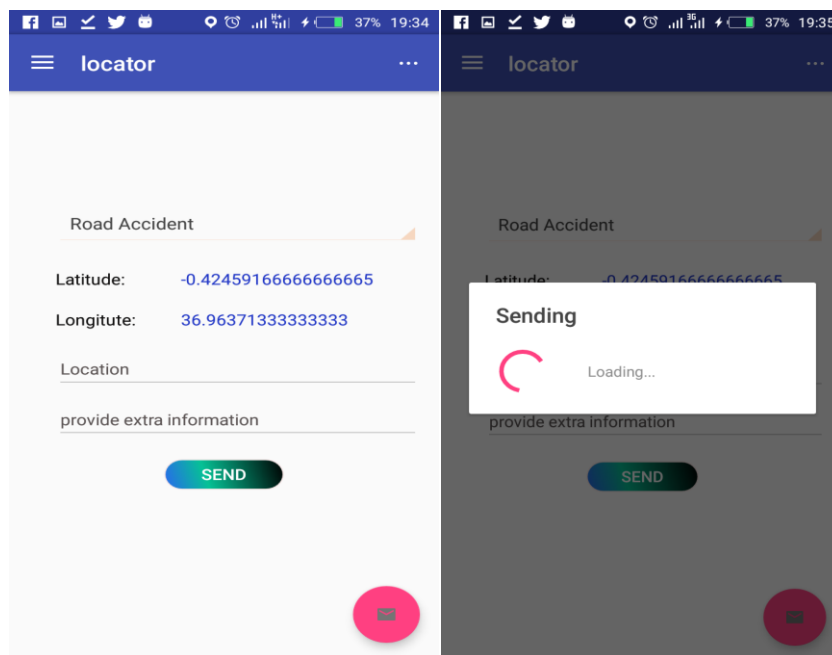


Figure 2: The emergency response system interface for incidence submission

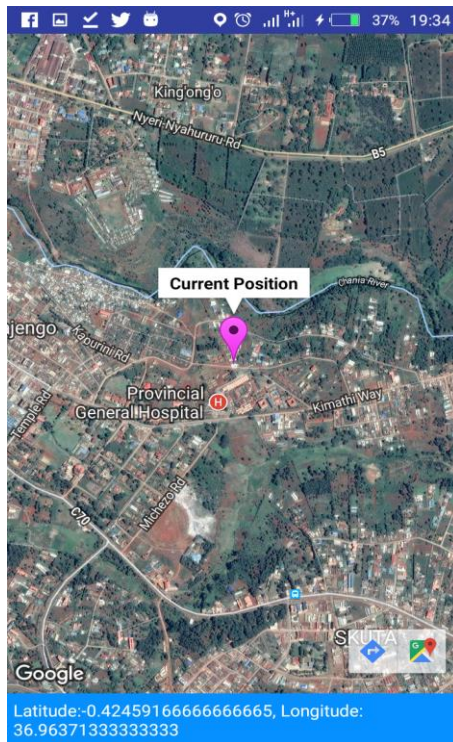


Figure 3: Map showing users current location

3.2 Web application for displaying emergency incidents

The other unit of the emergency response system application was designed for use by emergency responder in attending to the different incidents as reported or updated from the Android application users Figure 4: Emergency incidents display on Google maps) (Figure 4), routing to incident destination (Figure 5), incidents analysis and filtering, and enabling communication among responders. This is aimed at ensuring that incidents are addressed in a well-coordinated manner, thus ensuring that involved response teams work together. The web application has also the capability of displaying the variation in reported incident rates; ranging from green to red as the number of incidents rise (Figure 6 and 7)

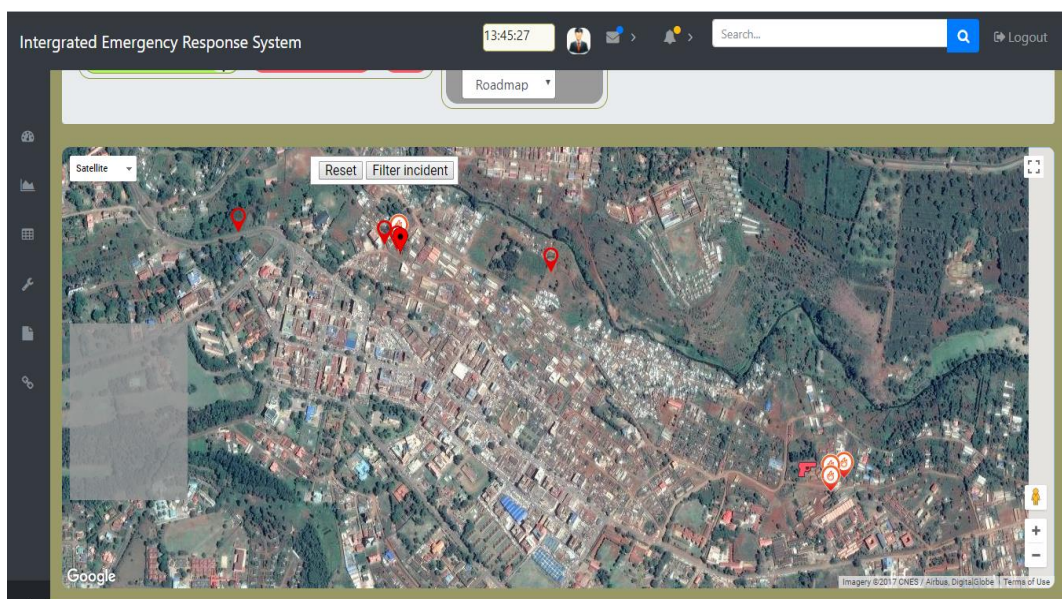


Figure 4: Emergency incidents display on Google maps

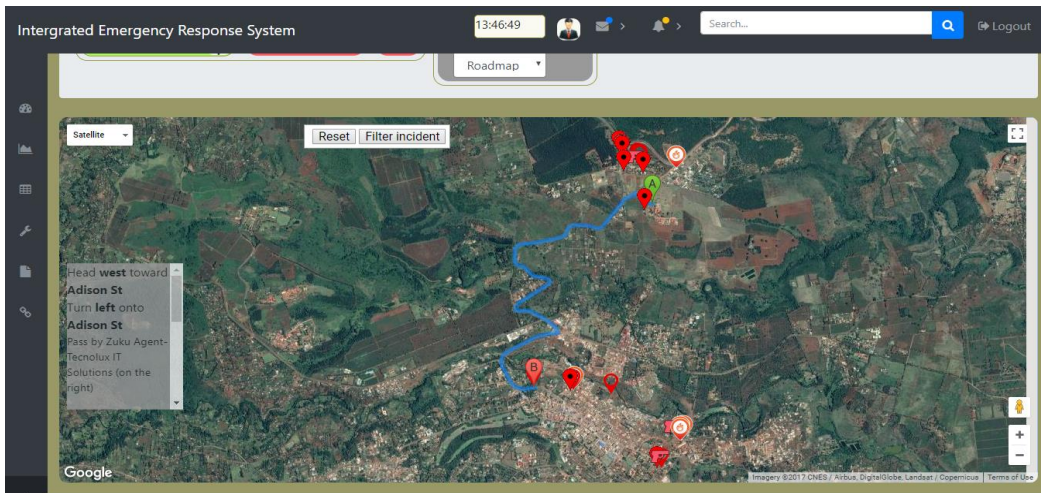


Figure 5: Routing to incident location using direction service

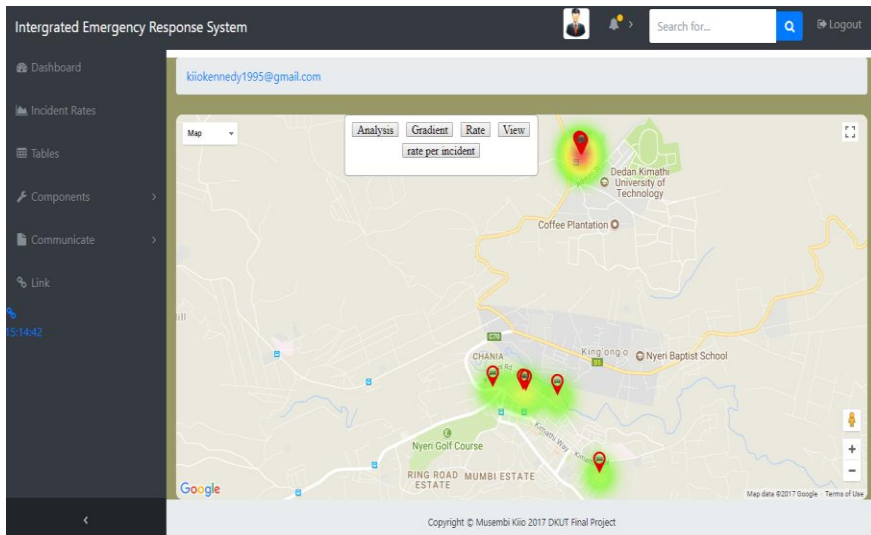


Figure 6: Road accident rates and display on the responders web application

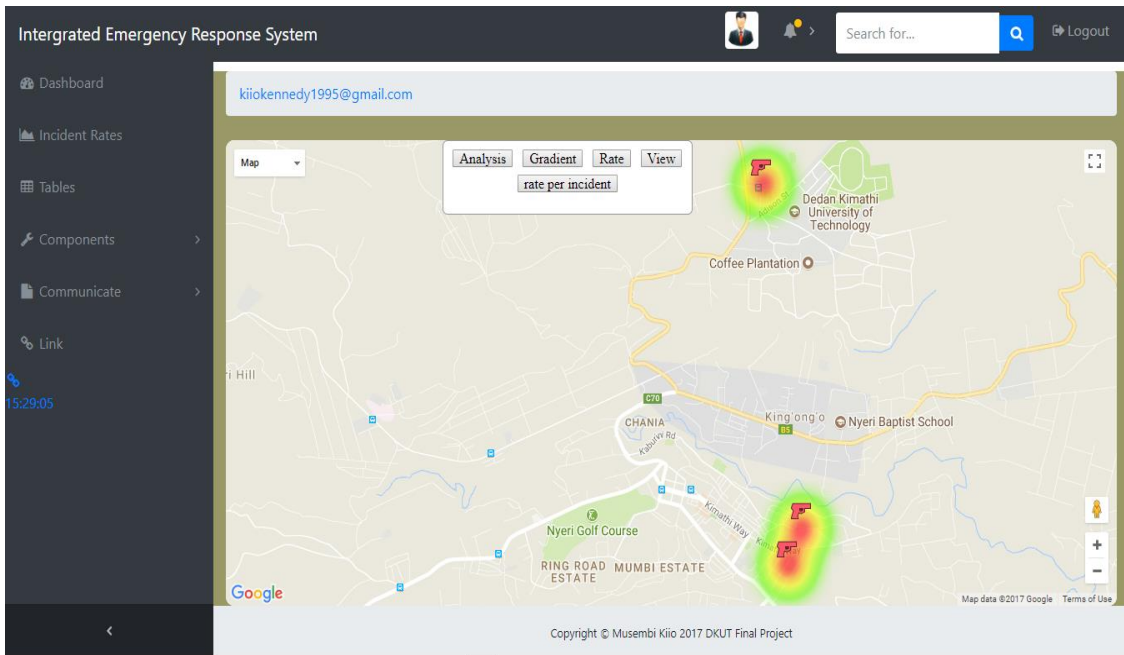


Figure 7: Medical emergency incidents display and rates in the web application

4 Conclusions and Recommendations

Effective emergency and disaster response and preparedness are a vital part in achieving both Vision 2030 and the set Millennium Development goals as per the Kenyan constitution. This call for more research to be done on this field and development of better effective and efficient response systems for realization of these Vision 2030. This project developed only a prototype emergency response system that was tested on simulated data. It demonstrated how GIS, mobile, and web technologies can be harnessed to improve in the reporting, geo-location, and response to emergencies.

The system developed used GIS, Android, and web technologies. The integration of these technologies made it possible to realise an integrated GIS-based emergency response systems that can enable citizens to report emergencies in real time, and get response with immediate effect. GIS helps the system development in generation of shortest route, mapping and displaying incidents in real time, and in performing spatial searches to identify incidents within the set radius of coverage assigned to each responder. Web technology ensures that occurrence can be displayed in web maps based on Google map API, and analysis of incident rates in real time to show areas that experienced high rates of incident occurrences. In addition the web maps provide the incident responder with basic information on expected ground condition and to evaluate the number or type of response service to deliver as well as the teams expected to coordinate to contain the issue.

The Android technology provided a means for communicating emergency incidents to the responders and data to be used to evaluate the type, location and details of emergency incident. The location information is obtained from Global Positioning Satellite (GPS) signals received by fused-in GPS receivers and the mobile network location provider technology (GSM positioning). The information uploading was done using HTTP (Hypertext Transmission Protocol) to a server where it could be relayed to the web platform.

This project can be enhanced by further integration of vehicle tracking system in the emergency response vehicles, and incorporation of location based reporting system based on short messages (SMS) system that is widely used by the citizens. Other messaging systems that are being used in communication such as *WhatsApp* should also be incorporated in the system to report emergency incidences, and populate the emergency response system database for improved services.

5 References

- Business Daily. (October 15, 2015). Kenya lacks a comprehensive disaster management policy. <http://www.businessdailyafrica.com/news/Kenya-lacks-comprehensive-disaster-management-policy/539546-1032972-ewxrp0/index.html>. [Accessed 28.08.2018]
- Cloutier, M., and Cushmac, G., 2016. *Emergency Response Guidebook*. J.J. Keller, Assoc.
- Kirchenbaum, A. ,2004. *Chaos Organization and Disaster Management*. CRC Press
- Leinhos, M., Qari, S. H., and Williams-Johnson, M., 2014. Preparedness and Emergency Response Research Centers: Using a Public Health Systems Approach to Improve All-Hazards Preparedness and Response. *Public Health Reports*, 129(Suppl 4), 8–18.
- MacFarlane, R., 2005. *A Guide To GIS Applications In Integrated Emergency Management*. Cabinet Office.
- Wachira, B. and Smith, W., 2013. Major Incidents in Kenya: the Case for Emergency Services Development and Training. *Prehosp Disaster Med*. 28(2).pp 1-4.

Geospatial support in the context of internal displacement caused by natural disasters

Christine Broenner

Geoinformation Management and Interoperability Expert, Germany, broenner@whenmapsmatter.com

KEY WORDS: Internally Displaced Persons (IDPs), internal displacement, natural disasters, geospatial support, interoperability, disaster risk reduction, displacement risk.

ABSTRACT:

Millions of people are internally displaced worldwide every year through natural disasters such as floods, earthquakes, landslides, storms and wildfires. Countries affected aim to support displaced people by responding to their immediate shelter and other needs, by helping to restore their sustainable livelihoods in their home place or at a new location and reducing the risk of new displacement. The paper sets the scene for geospatial applications that effectively inform and support response and development efforts in the context of internal displacement. It illustrates the opportunities for GIS solutions, which foster common ground for understanding and decision-making in these complex multi-stakeholder and multidisciplinary settings. The paper first introduces terminology regarding internal displacement. It then describes different contexts in which geoinformation management can inform strategy development and decision-making in support of internally displaced persons and of understanding disaster displacement risks and their development over time. Finally, it highlights some practical issues for providing GIS support to those using internal displacement applications in practice.

1 Definition and scale of Internal Displacement

According to the United Nations Guiding Principles on Internal Displacement, Internally Displaced Persons (IDPs) are “persons or groups of persons who have been forced or obliged to flee or to leave their homes or places of habitual residence, in particular as a result of or in order to avoid the effects of armed conflict, situations of generalized violence, violations of human rights or natural or human-made disasters, and who have not crossed an internationally recognized state border” (UN, 1998).

According to the Internal Displacement Monitoring Centre (IDMC), people may become internally displaced during or following the impact of a sudden-onset hazard, if their homes are rendered uninhabitable or they lose their livelihoods or access to basic services. Internal displacement numbers also include displacement that takes place in order to avoid the potential impacts of a hazard before it strikes, often in the form of pre-emptive emergency evacuations. These can be planned, ordered or recommended and facilitated officially, or be the spontaneous response of exposed populations based on their own information and perceptions of risk (IDMC, 2017b). In 2016, evacuations accounted for more than eight million, or over a third of the displacements associated with disasters that were reported over the year (IDMC, 2017c). Planned evacuations can often be found in countries that are regularly or frequently affected by recurring disasters, such as monsoon floods or typhoons.

In 2017 18.8 million people were newly internally displaced through natural disasters. Also, 11.8 million people were newly internally displaced through conflict in 2017. Of those people displaced through disasters, 18 million were weather-related such as floods, droughts and wildfires. Other causes of disaster displacements were geophysical ones such as earthquakes and volcano eruptions (IDMC, 2018). These numbers are in addition to those regarding people who had been internally displaced by natural disasters in previous years and had not been able to return to their homes yet or settle down in a new location and establish a sustainable livelihood there.

Internally displaced people remain under the responsibility of the country's Government authorities when it comes to response to, and resolution of, displacement. There is no binding convention or specific UN agency responsible for IDPs; the international aid community plays a complementary role (OHCHR, 2018). In terms of capturing, managing and disseminating spatial data concerning IDPs, their immediate needs after disaster has struck and those to return to sustainable livelihoods, there are many different actors and approaches. GIS can play a vital role in bringing together and analysing information in an integrated way. In disaster situations input data often stem from a wide variety of sources and are in different formats that require flexible design solutions for which some requirements will be described in section 4 of this paper.

2 Prevention of, preparedness for and mitigation of Internal Displacement

People are at risk of internal displacement to various degrees in different parts of the world. Risk analysis is used to identify the people and places most at risk and, therefore, reduce and manage the threat posed by a disaster. Estimations of risk generally include the consideration of hazard events that could occur and the exposure to these events, the vulnerability of communities towards these hazards and the degree of coping capacity of communities, local and national governments and other stakeholders (JRC, 2015). These influencing factors are multi-disciplinary, interrelated and location-dependent. Knowledge and understanding of their main drivers are the foundation for defining effective measures to reduce future displacement risk (IDMC, 2017b), and for assessing whether, in line with wider development goals, displacement risk has decreased or increased over time.

Kälin (2015) advocates that displacement could often be avoided or at least mitigated by taking appropriate disaster risk reduction measures. The international community has developed disaster risk reduction strategies in the Sendai Framework on Disaster Risk Reduction 2015 – 2030³. The Framework moves away from disaster management to focusing on the underlying drivers of disaster risk and spells out priority for action for reducing the human impact of natural disasters (Wahlström, 2015). It also specifically acknowledges the large number of disaster displaced persons in recent years as one of the devastating effects of disasters (Kälin, 2015). Furthermore, it stresses the need to promote “the incorporation of disaster risk management into post disaster recovery and rehabilitation processes, facilitate the link between relief, rehabilitation and development, use opportunities during the recovery phase to develop capacities that reduce disaster risk in the short, medium and long term, including through the development of measures such as land-use planning, structural standards improvement and the sharing of expertise, knowledge, post-disaster reviews and lessons learned and integrate post-disaster reconstruction into the economic and social sustainable development of affected area. This should also apply to temporary settlements for persons displaced by disasters” (UN, 2015, pp 21 and 22). Implementing this in practice entails the inclusion of displacement figures in the development of disaster risk reduction strategies.

A variety of examples of GIS applications exist for evaluating locations at risk. These are used for designing and implementing measures intended to reduce disaster risks and plan for mitigation measures and recovery in case disaster strikes. A lot of GIS application research goes into the evaluation of risks in thematic approaches, such as the evaluation of the factors affecting the generation of erosion processes and torrential floods, in order to provide effective erosion control and torrential flood protection described by Ristic et.al. (2017). Other GIS systems have been proposed for the entire risk management cycle such as the Decision Support System for Emergency Response in Taiwan that was developed for supporting the preparedness and response to typhoon hazards (Hsu et.al., 2005). Participatory GIS applications have been successful in risk mapping by local communities, where local spatial risk information provided for a better understanding on how household-level flood hazard, exposure, and vulnerability interact, such as in the case of flooding in Nepal (Liu et.al., 2018).

³ “The Sendai Framework for Disaster Risk Reduction 2015-2030 was adopted at the Third UN World Conference in Sendai, Japan, on March 18, 2015. It is the outcome of stakeholder consultations initiated in March 2012 and intergovernmental negotiations from July 2014 to March 2015, supported by the United Nations Office for Disaster Risk Reduction at the request of the UN General Assembly.” (UN, 2015, p.5)

3 Internal Displacement in Disaster Response

IDPs, whether in collective camps or in makeshift temporary accommodation have needs in terms of the provision of water supply, health services and sanitation facilities, food supply, shelter and non-food items, protection, and school education for children during their displacement. These needs have to be assessed. Displacement, and especially protracted displacement also affects host communities in terms of access to services, limited accommodation and changing housing prices, labour opportunities etc. and of governments and regional and local authorities with the increased pressure on infrastructure and service provision such as health and education.

The number of displaced persons and their needs and vulnerability in their current location tend to be assessed and monitored over time in the response phase by dedicated actors, either part of a national emergency response system or external entities. There is a range of methodologies used for capturing the extent of and monitoring the displacement. This includes new actors that have emerged in the form of huge numbers of people who collect and submit spatial information with new technologies such as social media, mobile technologies and, at times, dedicated crowdsourcing platforms. With it comes the possibility to benefit from location-related information - though of varying reliability - that otherwise would not have been captured. Crowdsourcing events to support evacuation efforts have for example been described for the response following Hurricane Harvey that affected Florida in 2017 where a platform enabled residents to report on the flooding situation in their area near-real time (GIM, 2017).

Where internally displaced people have been identified, their temporary locations of people captured and monitored these can be mapped, as can the needs these people have, and any response be informed accordingly. This support also includes establishing the return-home options for people, as often, one of the needs that displaced people have is information regarding the situation in their home place, which likely requires information input from other stakeholders than the response people.

IDMC (2017a) reports that especially in rapid-onset disasters movements of people are often complex and hard to track. Also, IDPs often move several times during their displacement, which makes support for them difficult to grasp.

Not all displaced people are counted; IDPs who seek shelter with family, in remote areas with little information available, and in general outside established or dedicated camps are often not recorded and hence their needs and return intentions are not known. This, and the discontinuation of monitoring, for example because of a lack of resources or when displacement becomes protracted, can lead to a lack of appreciation of when displacement ends. Often, there are also assumptions about rapid return when this may not be the case (IDMC, 2017a).

Regarding the ending of internal displacement situations, The (non-binding) Guiding Principles on Internal Displacement spell out three solutions an IDP should have the right to choose from:

- Return to the place of origin; though, as Ferris (2008) points out, in some natural disasters, IDPs do not have the option of return, such as when entire riverbanks get eroded by flood events;
- Integration into the place of displacement;
- Settlement in another part of the country (UN, 1998).

All of these options pose responsibilities for government authorities and require the capacity to plan for and enable returnees, the newly to be integrated and resettled people to attain sustainable livelihoods in line with disaster risk reduction and development planning intended to decrease vulnerability to risks. These are very different tasks from response operations and entail relevant data and information on displacement and its effects that was collected during the response phase, to be integrated in a meaningful way. The next section will discuss some of the necessary capabilities in spatial information management that would enable the continuity of understanding, and therefore of usage, of relevant displacement data that was collected during a response for planning purposes between heterogeneous actors in the longer term.

4 Outline of the nature of integrated geospatial application support in the context of internal displacement

Both the displacement response and the recovery phase and day-to-day spatial planning processes involve a variety of organisations and authorities, each with their own geospatial data and information requirements, role, requirements, capabilities and capacities in the information management domain. Interoperable capability, to discover and share what has become available, can have its uses if its value and utility has been recognised in advance and can be realised in practice (Broenner, 2012). The necessity to comprehend the scale and context of internal displacement caused by natural disasters and to understand the interrelationships between actors in the response and beyond is important in setting up geo information management solutions. This is because displacement information, especially on protracted displacement, and the monitoring of displacement risk inform recovery activities and also, necessarily, the development of disaster risk reduction strategies. The significance to include displacement information in spatial planning was furthermore highlighted on the occasion of the 20th anniversary of the Guiding Principles on Internal Displacement in 2018 in their GP20 Plan for action through the suggested action “Support the analysis of internal displacement within a broader context including investigating the impact of internal displacement on social and economic indicators, urban systems, governance and the policy environment with the overall goal of including IDPs in local and national development plans” (UN, 2018, p6).

From the humanitarian side, it has been recognised that long-term considerations are critical in meeting needs of displaced people (ICRC, 2018). There is also the realisation that needs assessments tend to favour humanitarian indicators but are not guiding tailored development strategies. Rather, a nuanced analysis of the impact and causes of displacement is advocated, especially for protracted displacement situations, where a lack of sufficient analysis of IDPs and their situation in the context is perceived (UNOCHA, 2017). The kind of information and knowledge to help create situational awareness and understand the vulnerability to displacement *is* often available from those who work with disaster risk reduction measures or from stakeholders involved in spatial planning tasks. This information can be exploited practically if suitably flexible GIS applications are provided.

Bringing the information and analysis together in a meaningful way for developing an understanding of displacement situations and their drivers over time, enabling continuity in the support of displaced people and preventing new internal displacement through reducing displacement risks, opens opportunities for GIS-supported working. These users require flexibly designed systems to be developed, or existing ones adapted, to accommodate the information provision, reception, integration and analysis when and as long as needed, before, during or after crises.

These designs entail but are not limited to:

- Acknowledging that varying degrees of interoperable capabilities are required - in order to accept data from different sources and in different formats as and when needed. Interoperability can be achieved between systems and applications that have been developed based on user interactions and processes that take place within the organisation on a day-to-day basis and other systems. Data exchange with known response collaborators can be enabled for such systems using open source standards or using pre-agreed proprietary standards established through prior formal agreement. Systems that, through their design, are able to collaborate and exchange services as part of a federation, in a plug-and-play manner when and as long as needed, do so entirely through the use of open standards (Broenner 2012). Such systems can enable users to collaborate in a federated manner as long as needed.
- The development and availability of meaningful metadata is necessary in a way that allows users to find out which data is available and judge the appropriateness of the data for their own purpose. This is vital in the displacement context, as data collected and recorded by another entity has often been developed for a different purpose than one’s own, yet may be relevant for the own work and useful to have. Therefore, descriptions that go beyond referring to the technical details of the data (such as scale, time of collection etc.) and describe the data content and attributes is necessary. Open standards-based, but not rigidly standardised, description and documentation of data (and the alternative meanings ascribed to them) enables the querying of information. This augments human understanding, and not just provides machine-to-machine interoperability (The abaci Partnership, 2012).

- The review of policy and operational frameworks in which geospatial applications and systems are embedded is useful so that the sharing and use of relevant geoinformation from a range of potential stakeholders on-the-fly during the response or in the longer-term planning is possible beyond existing institutional agreements and proprietary rights.

Systems designed or adapted following such principles can efficiently and effectively support the work of ad-hoc communities of interest in the field of displacement. They take into consideration that these communities are formed of heterogeneous actors with different skills, equipment and data collection tasks and needs, and area working to different time scales, yet can facilitate collaboration by adapting or designing systems that are fit-for-purpose for data sharing and dissemination if needed to develop common understanding.

5 Summary

Internal Displacement caused by natural disasters is a situation that affects millions of people worldwide every year anew. Efforts are underway to analyse space in terms of locations where populations are exposed and vulnerable to disaster, and what the risk mitigation options are in these areas. Once disaster has struck, the immediate efforts of the responder community dealing with the displaced persons are of different nature; they count them and assess and monitor their needs and vulnerability over time. Geospatial support in both situations has been developed and is effective to varying degrees; some countries do roll out disaster management schemes that provide integrated approaches of disaster management cycles. In other cases, often in disaster-prone less developed countries, these processes are not as well developed and interrelationships of dealing with displacement before, during and after disaster less addressed. This paper has provided insights, on the need for flexible geospatial support for those involved in this field of work, with the intention of helping practitioners 'join up the dots' for effective GIS-based support in what is a complex, dynamic, ambiguous and often intangible multi-stakeholder context, where all efforts ultimately are intended to save human lives.

6 References

- The abaci Partnership, 2012. Organisation forms and Contextual Complexities. <https://complexitydemystified.wordpress.com/2012/08/07/organisation-forms-and-contextual-complexities/> [Accessed 31.08.2018]
- Broenner, C., 2012. Appropriate Interoperability - From technical to socio-technical. In: Behr F.-J., Rahman A.A., Zimmermann M., Pradeepkumar A.P. (Editors): *Geoinformation – Catalyst for planning, development and good governance. Proceedings of Applied Geoinformatics for Society and Environment 2012*, pp 203-210.
- Ferris, E., 2008. Displacement, Natural Disasters, and Human Rights. The Brookings Institution. <https://www.brookings.edu/on-the-record/displacement-natural-disasters-and-human-rights/> [Accessed 25.07.2018]
- GIM International, 2017. Crowdsourced Mapping Projects Aid Post-Harvey Disaster Management - 31/08/2017. <https://www.gim-international.com/content/news/crowdsourced-mapping-projects-aid-post-harvey-disaster-management> [Accessed 28.07.2018]
- Global Platform for Disaster Risk Reduction, 2017. 2017 Global Platform for Disaster Risk Reduction Proceedings. https://www.preventionweb.net/files/55465_globalplatform2017proceedings.pdf [Accessed 27.07.2018]
- Hsu, P-H., Wu, S-Y. and Lin, S-T., 2005. Disaster Management Using GIS Technology: A Case Study in Taiwan. https://www.researchgate.net/profile/Feng_Tyan_Lin/publication/228626036_Disaster_Management_Using_GIS_Technology_A_Case_Study_in_Taiwan/links/552856460cf2779ab78dffc0/Disaster-Management-Using-GIS-Technology-A-Case-Study-in-Taiwan.pdf?origin=publication_detail [Accessed 27.07.2018]
- ICRC, 2018. Displaced in Cities : Experiencing and Responding to Urban Internal Displacement Outside Camps https://reliefweb.int/sites/reliefweb.int/files/resources/4344_002_Displaced-in-Cities_web.pdf [Accessed 10.08.2018]

- IDMC, 2018. GRID 2018 Global Report on Internal Displacement. <http://www.internal-displacement.org/global-report/grid2018/> [Accessed 27.07.2018]
- IDMC, 2017a. 2016 Africa Report on Internal Displacement <http://www.internal-displacement.org/sites/default/files/inline-files/20171206-Africa-report-2017.pdf> [Accessed 10.07.2018]
- IDMC, 2017b. Global Disaster Displacement Risk - A baseline for future work <http://www.internal-displacement.org/sites/default/files/publications/documents/201710-IDMC-Global-disaster-displacement-risk.pdf> [Accessed 27.07.2018]
- IDMC, 2017c. GRID 2017 Global Report on Internal Displacement. <http://www.internal-displacement.org/global-report/grid2017/pdfs/2017-GRID.pdf> [Accessed 27.07.2018]
- JRC, 2015. Index for Risk Management – INFORM. JRC Scientific and Policy Reports. <http://www.inform-index.org/Portals/0/InfoRM/2016/INFORM%20Concept%20and%20Methodology%20Version%202016%20updated%20cover.pdf?ver=2015-11-26-123614-937> [Accessed 31.08.2018]
- Kälin, W (2015): Sendai Framework: An important step forward for people displaced by disasters. The Brookings Institution. <https://www.brookings.edu/blog/up-front/2015/03/20/sendai-framework-an-important-step-forward-for-people-displaced-by-disasters/> [Accessed 31.08.2018]
- Liu, W. et.al., 2018. Integrated Participatory and Collaborative Risk Mapping for Enhancing Disaster Resilience. In: ISPRS International Journal of Geo-Information, 7, 68. <http://pure.iiasa.ac.at/id/eprint/15141/1/ijgi-07-00068-v2.pdf> [Accessed 27.07.2018]
- OHCHR, 2018. Questions and Answers about IDPs. <https://www.ohchr.org/en/issues/idpersons/pages/issues.aspx> [Accessed 10.10.2018]
- Ristic, R. et.al., 2017. Disaster Risk Reduction Based on a GIS Case Study of the Čađavica River Watershed. In: *South-east European forestry* 8 (2), pp 99-106. https://www.seefor.eu/images/arhiva/vol8_no2/ristic/ristic.pdf [Accessed 15.08.2018]
- UN 2018. 20th Anniversary of the Guiding Principles on Internal Displacement: A Plan of Action for Advancing Prevention, Protection and Solutions for Internally Displaced People. 2018 – 2020. <https://www.ohchr.org/Documents/Issues/IDPersons/GP20PlanOfAction.pdf> [Accessed 21.10.2018]
- UN, 2015. Sendai Framework for Disaster Risk Reduction 2015–2030. https://www.unisdr.org/files/43291_sendaiframeworkfordrren.pdf [Accessed 27.07.2018]
- UN, 1998. Report of the Representative of the Secretary-General, Mr. Francis M. Deng, submitted pursuant to Commission resolution 1997/39. Addendum: Guiding Principles on Internal Displacement. <http://www.un-documents.net/gpid.htm> [Accessed 31.08.2018]
- UNOCHA, 2017. Breaking the Impasse. Reducing protracted internal displacement as a collective outcome. OCHA Policy and Studies Series. <https://www.unocha.org/sites/unocha/files/Breaking-the-impasse.pdf> [Accessed 27.07.2018]
- UNOCHA, 2018. Tackling the issue. <https://www.unocha.org/ending-protracted-internal-displacement/tackling-issue> [Accessed 31.08.2018]
- Wahlström, M., 2015. New Sendai Framework Strengthens Focus on Reducing Disaster Risk. In: *International Journal of Disaster Risk Science*, 6: pp 200–201 <https://link.springer.com/content/pdf/10.1007%2Fs13753-015-0057-2.pdf> [Accessed 31.08.2018]

Deriving Vegetation Health Index in Hong Kong and Colombian Amazon by using Sentinel 2 and Landsat 8 in Google Earth Engine

Andres Felipe Ramirez[†], Yuk Kit Chang[†] and Michael Hahn[‡]

[†] M.Sc. Student. Fakultät Vermessung, Informatik und Mathematik, Hochschule für Technik Stuttgart, Germany.

[‡] Professor Dr. Ing. Fakultät Vermessung, Informatik und Mathematik, Hochschule für Technik Stuttgart, Germany.

KEY WORDS: Google Earth Engine, Sentinel, Landsat, Vegetation Health Index (VHI), Vegetation Condition Index (VCI), Temperature Condition Index (TCI).

ABSTRACT

This project investigates the use of Google Earth Engine in computing vegetation condition index (VCI) and vegetation health index (VHI) with open remote sensing data for Hong Kong and Colombian Amazon. VCI is computed using Sentinel 2 data, while VHI includes a correction of temperature condition index (TCI), obtained from Landsat 8 thermal data. JavaScript is used to develop scripts for processing the data and displaying the results as thematic maps in a web based platform.

1 Introduction

Google Earth Engine is a cloud-based platform for processing several kinds of remote sensing data. It has a Code Editor which is an online integrated development environment for rapid prototyping and visualization of spatial analyses using Applications Programming Interface (API) (Goerlick et al., 2017). Moreover, it allows access to an archive of public available remotely sensed imagery such as Landsat and Sentinel collections (Google Inc., 2018) and other already processed data. Due to Google Earth Engine cloud base data storing and processing nature, it is not necessary for users to have a powerful computer, install additional software nor maintain any data by themselves. All users' needs are a computer with internet connection and registration of a Google Earth Engine account. This tool is free for research, education, and nonprofit use.

Due to the combination of high amount of satellite imagery available with the power of Google cloud servers, Google Earth Engine is getting more and more popular in the research and education areas. To get familiar with this tool, studies of finding VCI and VHI based on (Kogan, 1995) approach, in Hong Kong and in Colombian Amazon with open data are conducted by using Google Earth Engine.

2 Objectives

- i. Develop a script in Google Earth Engine for computing VCI and VHI in Hong Kong in 2017.
- ii. Develop a script in Google Earth Engine for computing VCI and VHI Colombian Amazon (2015 -2018).
- iii. Compare VHI and VCI results for both study areas.

3 Study Areas

(a) *Hong Kong*

There are over 7.40 million inhabitants in Hong Kong where the land extension is around 1.104 km² in which over 40% of land are country parks and nature reserved areas (Government of Hong Kong, 2018). Although the need of land for urban expansion is putting some pressure over the limits of the cities and forest areas, these areas remain protected by the government and have high environmental value to the local citizens. Figure 1 shows a false color composition (RGB 843) of Sentinel 2 satellite images in which forest areas are represented by the bright red color and urban areas by gray or bright tones.

(b) *Colombian Amazon*

For this investigation, Colombian Amazon region is defined by merging three departments (Amazonas, Vaupés and Guainía) with an average of 95% of forest coverage (IDEAM, 2016). The area has an extent of around 230.000 km² and it is located at the South-East part of the country. Due to its geographical location, it is not affected by seasonal weather, instead, it holds a constant tropical weather throughout the year. Figure 2 shows a false color composition (RGB 843) of Sentinel 2 satellite images in which forest is represented by the bright red color.

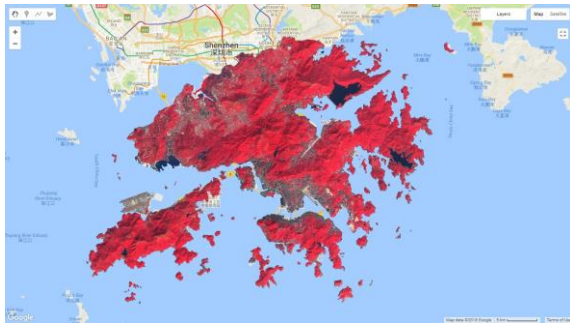


Figure 1: Hong Kong. False color (RGB 843) Sentinel 2.

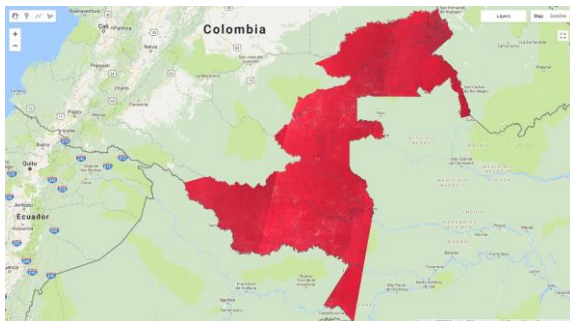


Figure 2: Colombian Amazon. False color (RGB 843) Sentinel 2.

4 Data

Two different datasets of satellite imagery are used: Sentinel 2 for the multispectral images, and Landsat 8 for the thermal images which are open data and available through Google Earth Engine dataset catalog. For the Hong Kong area the analysis is divided into two seasons: cold (October to February) and hot (March to September) and only images with cloud coverage less than 10% are used. Taking into account these conditions, for the cold season 30 Sentinel 2 and 6 Landsat 8 images are collected, meanwhile, for the hot season 23 and 10 Sentinel 2 and Landsat 8 images are collected respectively. For Colombian Amazon, the analysis is done seasonal separation due to its atmospheric conditions, thus, the time span for image collection is expanded (2015-2018) resulting in 113 and 67 Sentinel 2 and Landsat 8 images respectively. Table 1 summarizes the number of images used in each area.

	Sentinel-2	Landsat 8
Hong Kong	53	16
Colombian Amazon	113	67
Total	166	83

Table 1: Number of images used

4.1 Sentinel 2 (Multispectral)

Images taken by Sentinel-2 Multispectral Instrument (MSI), measure the Earth's reflected radiance in 13 spectral bands from 0.443 μm (Coastal) and 2.190 μm (SWIR). Computations of VHI and its individual components are done using visible and NIR bands with a spatial resolution of 10 m. Images are processed and delivered by the European Space Agency in Level-1C and projected to cartographic coordinates using a Digital Elevation Model and resampled with a constant Ground Sampling Distance of 10, 20 and 60 m depending on the native resolution of the different spectral bands (ESA, 2015). Pixel radiometric measurements are provided in Top of Atmosphere reflectance and additional information, such as Cloud Masks is also included.

4.2 Landsat 8 (Thermal)

For the thermal data used in the computation of VHI is obtained from Landsat 8 Thermal Infrared Sensor (TIRS) Tier 1 dataset. This dataset contains the corrected surface reflectance from the Landsat 8 OLI/TIRS sensors and contains 5 visible and near-infrared (VNIR) bands and 2 short-wave infrared (SWIR) bands processed to orthorectified surface reflectance, and two thermal infrared (TIR) bands processed to orthorectified brightness temperature. These bands were originally collected with a resolution of 100 m and has been resampled using cubic convolution to 30 m (USGS, 2017). TCI value is computed by using B10 that stores surface temperature in Kelvin sensed between 10.60-11.19 μm .

5 METHODOLOGY

5.1 Vegetation Indices

The normalized difference vegetation index (NDVI) is a remote-sensed indicator to measure photosynthetic activity of vegetation (Petorelli, 2013).

The NDVI is calculated as the normalized ratio of the spectral reflectance measurements acquired in the near-infrared band and visible red band.

$$NDVI = \frac{NIR-RED}{NIR+RED} \quad (1)$$

From equation 1, NIR is the near-infrared band and RED is the visible red band. NDVI varies between -1.0 and +1.0. Generally, high NDVI indicates a favorable condition for vegetation growth (Huete et al., 2000), which is associated with highly photosynthetically active vegetation. In contrary, a low NDVI shows there is little photosynthetic activity, which means the vegetation maybe dead or stressed. Kogan (1995) further enhanced the application of NDVI for drought monitoring by introducing the VCI which separates weather-related signal in the NDVI from the long-term ecosystem changes. VCI is defined by equation 2 where $NDVI$, $NDVI_{max}$ and $NDVI_{min}$ represent the smoothed seasonal NDVI, their absolute maximum and minimum values within a period of time, which is 1 year in this project.

$$VCI = 100 \times \left(\frac{NDVI - NDVI_{min}}{NDVI_{max} + NDVI_{min}} \right) \quad (2)$$

Based on VIC, VHI was developed through a combination of VCI and temperature condition index (TCI) (Kogan, 1995 and 2011). In equation 3, BT is the smoothed Brightness Temperature within a specific period of time. Since the temperature change within a year in Colombian Amazon is not distinctive, the computation of TCI is done for the length of the time span. For Hong Kong, it is divided into hot (March to September) and cold (October to February) seasons for the computation of TCI. BT_{max} and BT_{min} are the absolute maximum and minimum of the BT within year 2017 respectively.

$$TCI = 100 \times \left(\frac{BT_{max} - BT}{BT_{max} + BT_{min}} \right) \quad (3)$$

Value of the weighting factor (a) for the contributions of vegetation condition and temperature to vegetation health in equation 4, which often assumed as 0.5 for simplicity, is determined by experience; VCI, TCI and VHI, vary from 0 to 100, with the VHs between 40 and 60 reflecting normal vegetation conditions (Kogan, 2011).

$$VHI = a \times VCI + (1 - a) \times TCI \quad (4)$$

Due to different geographical and atmospheric conditions between the two study areas, weight factor (a) must be different as well. Assuming constant weather conditions in the Amazon region and seasonal weather conditions in Hong Kong, values of (a) factor are defined as follows: $a = 0.8$ for Amazon and $a = 0.5$ for Hong Kong.

5.2 Post-processing

All the computations detailed in section 5.1 are carried out for each pixel of every image. However, considering the theoretical definition of VCI, it is possible for a pixel with very low NDVI (i.e. non-vegetation) to have a high value of VCI when the pixel has a low dispersion in NDVI throughout the sampling period. It is important to ensure the VCI values are computed for vegetation only.

NDVI values close to 1 represent dense vegetation while values close to 0 represent no green leaves (Weier & Herring, 2000). This leads to a post processing masking operation applied to the NDVI results defined by the following condition:

$$VegetationPixel : NDVI > 0.3 \quad (5)$$

5.3 Coding

Google Earth Engine is accessed through API for JavaScript or Python. The API is available as a client for sending requests to Google servers. The JavaScript API is already available online through the code editor which is an Integrated Development Environment (IDE) for rapid prototyping and visualization of spatial data. An extra installation to work with Python API is required and available through GitHub.

JavaScript API is used to conduct this investigation.

5.3.1 Accessing data

Assets: Imported files stored on personal Google drive or shared files owned by another user.

Datasets: Imported datasets stored on Google Earth Engine's public catalog (on the cloud).

Each Dataset has its own ID⁴ and properties that can be accessed through JavaScript code.

5.3.2 Earth Engine structures and methods.

To handle geospatial data such as images and features (raster and vector), Google Earth Engine defines its own data structures in which each data type stores specific components. Most important data types are images, features, imageCollection and featureCollection. In order to be able to work with the data, it is necessary to use

⁴ Sentinel 2: COPERNICUS/S2. Landsat 8: LANDSAT/LC08. High resolution: USDA/NAIP/DOQQ

the Earth Engine methods which are specifically developed by Google and identified by the prefix *ee* (E.g: *ee.Image*, *ee.ImageCollection*).

5.3.3 Mathematical operations and Reductions.

Basic mathematical operations⁵ are performed pixel wise when pixel has a valid value in all images involved in the computation. For visualization purposes or to simplify computations, an *ImageCollection* can be reduced by composing a single image representing a statistical⁶ value from all the images integrating the collection.

5.3.4 Map method and Customized functions.

Loops are not used in Earth Engine coding, instead the map method allows to iterate over single items belonging to a collection. Functions can be created to fulfill specific needs using JavaScript syntax. First, the function must be defined and then it must be invoked by passing the input as parameter.

5.3.5 Visualization.

Results of operations and computations are not displayed automatically, in order to visualize layers, the method *Map.addlayer()* must be used in which several parameters are set to achieve good visualization effects.

6 RESULTS

For both study areas a discrete representation for VCI is displayed with a color palette where green and red, represent high and low values respectively. In addition a comparison between VHI and VCI is shown in line plots.

Due to the seasonal weather and atmospheric conditions, the influence of TCI is higher in Hong Kong than in Colombian Amazon where conditions remain constant over the whole year. Final VHI values are highly affected by thermal data from Landsat 8 TIRS band. If no Thermal data is available, then the VCI weight is 1 and therefore the final VHI will be only influenced by NDVI values.

6.1 Hong Kong

In order to compute the VHI in Hong Kong, the weight factor (*a*) is set to 0.5 as described in equation 6. Table 2 describes the three different categories for VHI values (Kogan, 2011).

$$VHI = 0.5 \times VCI + 0.5 \times TCI \quad (6)$$

Values	Description
60 – 100	Favorable condition
40 – 60	Normal condition
0 – 40	In stress

Table 2: Vegetation Health categories

⁵ Arithmetic (Add, Subtract, Multiply, Divide, Modulus, Exponent), comparison (Equal, Not Equal, Less Than, Greater than), logical(And, Or, Not, Xor) and conditional

⁶ Among others: min, max, mean, median or standard deviation

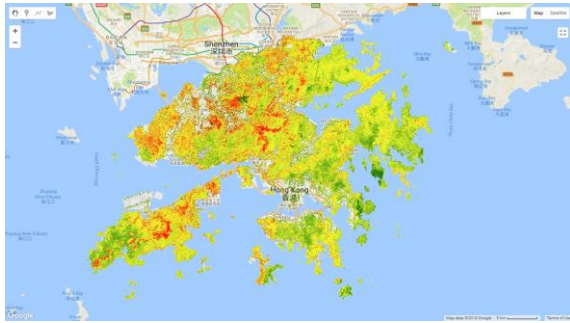


Figure 3: VHI Hong Kong - Winter.



Figure 4: VHI Hong Kong - Summer.

Figures 3 and 4 show the result of VHI in cold season (winter) and hot season (summer) respectively. Summer is dominated by high values represented with green color while values for winter are lower. Usually summer is affected by clouds which are colder than land surface; the presence of clouds decreases the temperature recorded by TIRS bands and therefore VHI values are lower. On the other hand winter is cloud free, however the land surface temperature is lower than in summer; these conditions also make the final VHI values low.

Figures 5 and 7 show the VHI thematic maps in 2017 of the Hong Kong International Airport in which the healthier the vegetation, the greener the map is. It is clear that the vegetation health during summer is better than that of during winter. By reading the charts of VHI (Figures 6 and 8), it is clear that in summer the VHI is always above 60 while in winter it can be under 60. This result is convincing since vegetation growth is usually better in summer than in winter due to the exposition of the vegetation to the sun. Figure 9 shows the visualization of VHI in winter of a detailed view of Kowloon Park located in Hong Kong's downtown and figure 10 shows the timeline comparison of VHI and VCI from a vegetation spot located on this park. Values displayed on the graph show values between 60 and 100 which are considered as non-stressed vegetation. However, there are outlier values lower than 60 in mid-December 2017 and mid-February of 2018 derived from very low NDVI values coming from atmospheric effects.



Figure 5: VHI Hong Kong - Winter. Detailed view (airport area).



Figure 6: VHI and VCI. Hong Kong - Winter. Airport area.



Figure 7: VHI Hong Kong - Summer. Detailed view (airport area).



Figure 8: VHI and VCI. Hong Kong - Summer. Airport area.

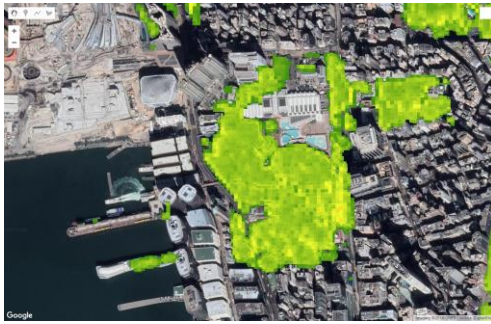


Figure 9: VHI Hong Kong - Winter. Detailed view (Kowloon Park).

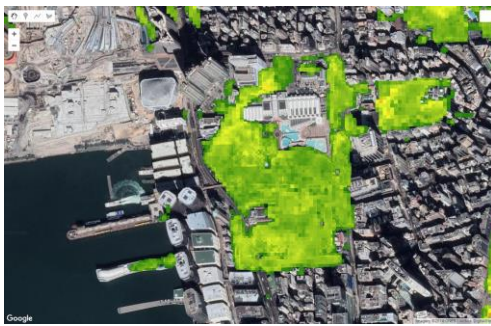


Figure 10: VHI and VCI. Hong Kong - Winter. Kowloon Park

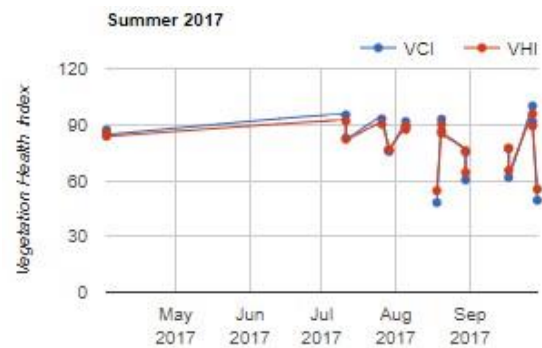


Figure 11: VHI Hong Kong - Summer. Detailed view (Kowloon Park).

Figure 12: VHI and VCI. Hong Kong - Summer. Kowloon Park.

Figure 11 shows the same park but for summer. Greener areas are present in the result which represents healthier vegetation than in winter. Figure 12 shows the VHI and VCI values over time during summer. Most of the values are between 60 and 90, which is similar to winter. Generally, the vegetation in the park is non-stressed.

6.2 Colombian Amazon

Due to constant weather conditions and data availability, VHI in Amazon is computed with a different weight factor (a) as described in the equation 7 and in figure 13, and between a longer period of time (2015 - 2018). Although atmospheric influence is visually evident, it still does not affect the overall VHI classification remaining higher than 60 (non-stressed).

$$VHI = 0.8 \times VCI + 0.2 \times TCI \quad (7)$$

Temperature data from Landsat images plays a big role in this area, boundaries from Landsat individual scenes can be easily identified on the VHI results shown in figures 13 and 14. Figure 15 shows VHI values from a spot in Puinawai Natural Reserve which is covered almost 100% by dense forest; most of the VHI values are focused around 90-100 as expected in the area. Despite some outliers are present, those values are still higher than 70, which according to table 2 are still considered as non-stressed vegetation.

Figure 16 shows the city of Leticia and its surroundings located in the southernmost point of the country where the Amazon River is a common boundary among Colombia, Brazil, Peru and Ecuador. Urban areas and rivers are identified to some extent but there are still green pixels over the water surface that are classified as non-stressed vegetation. This misclassification can be explained by the influence of thermal data in the computation of VHI.



Figure 13: VHI Colombian Amazon.

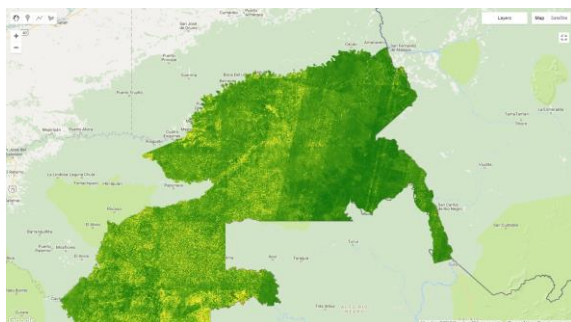


Figure 14: VHI. Colombian Amazon. Detailed view (Natural Reserve Puinawai).

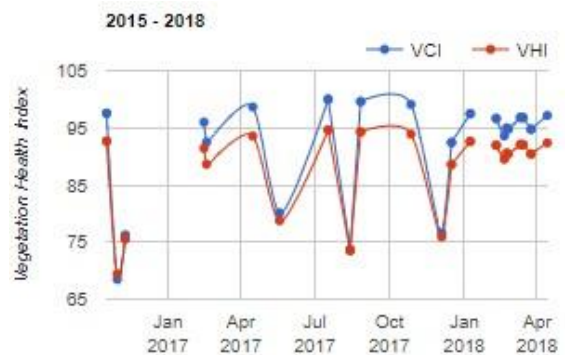


Figure 15: VHI and VCI. Colombian Amazon. Natural Reserve Puinawai.



Figure 16: VHI. Colombian Amazon. Detailed view (Leticia).



Figure 17: VHI and VCI. Colombian Amazon. Leticia.

Figure 17 shows VHI and VCI values of a dense vegetation spot located in the surroundings of Leticia. For this specific area, temperature has an influence on the final VHI values of almost 20 points which are represented in the graph by the difference between blue and red lines (if temperature data TCI is discarded, VHI equals to VCI). VHI values for this dense vegetation area are expected to be near 100 and this assumption is correct if TCI is discarded. On the other hand VHI values with TCI are still high and are classified as non-stressed vegetation according to table 2.

6.3 Atmospheric Effects on VHI

VHI is computed according to a weight factor (α) given to TCI and VCI, in which TCI is highly influenced by atmospheric conditions, especially clouds. To avoid the effect of clouds on the computation of VHI, initial query is applied to filter out images with more than 20% cloud coverage in the Landsat 8 dataset. However, since there is no cloud mask available in this dataset, the effect of clouds on VHI can still be identified. Figure 18 shows a region with dense and healthy vegetation but with low VHI, which can only be identified in the hot season, when cloud coverage is high. This low VHI region could be an effect of the presence of cloud in the Landsat 8 dataset.

In order to reduce the cloud effects, a possible approach to handle this problem is to create a cloud mask for the Landsat 8 dataset by computing an extra index from the multispectral bands of Landsat. Furthermore, other thermal data less affected by clouds, or with a cloud mask included can be used instead of Landsat data.

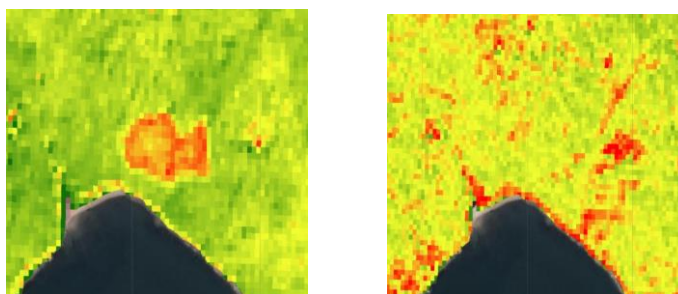


Figure 18: VHI season comparison (left: Hot, right: Cold). Hong Kong.

7 CONCLUSIONS

Google Earth Engine allowed us to process large amount of satellite and vector data in a very simple way. No installation nor data download is required but only a registration to the platform. We found out that some intermediate programming skills (JavaScript) are required in order to take full advantages of the capabilities of the platform. In this specific case we consider that our learning curve to reach the required skills was shorter than expected which allowed us to continue the study of vegetation health analysis. We developed a single script (appendix) which contains all the processing steps as well as the customized tools to work each study area independently.

Through result analysis, it was found that the effect of temperature plays a big role in VHI. In Hong Kong, its effect in urban areas is larger than that in rural area. Moreover by comparing both areas, it is evident that atmospheric influence in Colombian Amazon is stronger than in Hong Kong. To reduce or increase the influence of these atmospheric effects on the results, weight factor (α) can be modified when computing the overall VHI; for most of the Amazon area TCI lowered the VHI values in almost 20 points but this difference did not affect classification of stressed or non-stressed vegetation. Considering that the correction of TCI does not affect the classification of vegetation health categories in Amazon, TCI can be neglected and only the VCI can be considered as an indicator of Healthiness. VCI formulation is a ratio of two subtractions involving actual, maximum and minimum values; because it does not differentiate between vegetation and non-vegetation, high values of VCI in water or in clouds can be expected when computing final VHI will produce a high value as well. This issue is solved by excluding non-vegetation pixels from all the computations by setting a threshold based on NDVI and applying it as a mask to the remaining computations.

8 DISCUSSION

8.1 Availability of Cloud-free Data

One of the major difficulties when conducting this project was the limited number of cloud-free data in the study areas which lead us to the decision to compare the monthly or seasonal VHI of the study areas. Hong Kong is very cloudy in summer as well as Colombian Amazon throughout the year, thus, the number of available images within a month or three months was very limited and not sufficient for the comparison. In Hong Kong it is very common to have images with over 80% cloud coverage, that drove us finally to compute the VHI according to hot and cold seasons with contains a period of about 6 months ensuring enough number of images for study and comparison. On the other hand, for Colombian Amazon, the time span was longer (2015-2018) in order to have enough data to manage the analysis.

In terms of thermal data, the number of images available is lower than that of multispectral because most of the data is affected by atmospheric effects or by data noise, especially in the overlapping areas of images sensed in different dates.

8.2 Google Earth Engine

Through this project, we found that Google Earth Engine is a very convenient tool. Its cloud processing capability enables users to perform complex computation and analysis in an ordinary laptop or desktop computer, no powerful workstation is required. Moreover, users are able to share their codes or resources via the cloud easily, enabling effective work allocation and collaboration within development group. The open data collections in Google Earth Engine are very comprehensive and up-to-date. With the help of filters, users can find required data very easily. However, there is no graphical user interface in Google Earth Engine, all commands have to be written in codes. For users without programming knowledge, this tool can be challenging to use. Furthermore, special JavaScript syntaxes are designed for Google Earth Engine, which must be learnt by users even they are familiar with JavaScript. Regarding quantification of areas, we found that for very large areas, the request of pixel counting or area calculation is not possible. It is because when the computation time is too long, Google server breaks the connection. If large area statistics are required, results must be exported locally first and then processed by another software.

8.3 Further Study on TCI and MSI

Soil with higher moisture should have lower temperature, therefore, we can assume that there should be a correlation between TCI and Moisture Stress Index (MSI), which is commonly to estimate soil moisture variability. Further study can be done in this aspect to find out whether a more precise VHI can be obtained with the help of MIS.

8.4 Accuracy Assessment

Although the obtained results seem convincing from a thematic perspective, there is no ground truth data to assess the accuracy. As an additional research, field data should be collected as control data to assess the quality of the results by means of a confusion matrix or kappa κ coefficient.

9 References

- Bokushevaa, R., Koganb, F., Vitkovskayac, I., Conradt, S., Batyrbayevac, M., 2016. Satellite-based vegetation health indices as a criteria for insuring against drought-related yield losses. *Agricultural and Forest Meteorology*, Vol 220, p 201.
- Fengsong, P., Changjiang, W., Xiaoping, L., Xia, L., Kuiqi, Y., Yi, Z., Kun, W., Li, X., Gengrui, X., 2018. Monitoring the vegetation activity in China using vegetation health indices, *Agricultural and Forest Meteorology*, 2018, p 218.

- Google Inc., Google Earth Engine API. <https://developers.google.com/earth-engine/> [accessed June 2018]
- Google Inc., Google Earth Engine. <https://earthengine.google.com/faq/> [accessed June 2018]
- Gorelick, N., M. Hancher, M. Dixon, S. Ilyushchenko, D. Thau and Moore, R., 2017. Google Earth Engine: Planetary-scale geospatial analysis for everyone. *Remote Sensing of Environment*, Vol 202, pp 18-27.
- GovHK, Honkong – The Facts. <https://www.gov.hk/en/about/abouthk/facts.htm> [accessed June 2018]
- Huete, A., Didan, K., Miura, T., Rodriguez, E.P., Gao, X. and Ferreira, L.G., 2000. Overview of the radiometric and biophysical performance of the MODIS vegetation indices. *Remote Sensing of Environment*, Vol 83, pp 195–213.
- Instituto de Hidrología, Meteorología y Estudios Ambientales – IDEAM, 2016. Mapa de Bosque - No Bosque Área continental.
- Karnieli, A., Bayasgalan, M., Byarjargal, Y., Agam, N., Khudulmur, S. and Tucker, C.J., 2006. Comments on the use of the Vegetation Health Index over Mongolia. *International Journal of Remote Sensing*. Vol 27, No 10.
- Kogan, F., 1995. Application of vegetation index and brightness temperature for drought detection, *Adv. Space Res.* 15 (11), 91–100.
- Kogan, F., Vargas, M., Ding, H. and Guo, W., 2011. VHP Algorithm Theoretical Basis Document, NOAA NESDIS Center for Satellite Applications and Research, Version 1.0.
- Nguy-Robertson, A., Gitelson, A., Peng, Y., Viña, A., Arkebauer, T. and Rundquist, D., 2012. Green Leaf Area Index Estimation in Maize and Soybean: Combining Vegetation Indices to Achieve Maximal Sensitivity. *Agronomy Journal*. Volume 104, Issue 5.
- Pettorelli N., 2013 *The Normalized Difference Vegetation Index*. First Edition (Oxford University Press), p 193.
- The European Space Agency, 2015. Sentinel-2 User Handbook, ESA Standard Document, ESA Sentinel Online, Issue 1 Rev 2.
- U.S. Geological Survey, 2018. Product Guide - Landsat 8 Surface Reflectance Code (Lasrc), LaSRC Product Guide, Version 4.3.
- Weier; J. & Herring, D., 2000. Measuring Vegetation (NDVI & EVI). NASA Earth observatory. <https://earthobservatory.nasa.gov/Features/MeasuringVegetation/> [accessed June 2018]

Geodatabase of Base Map for Structure Plan of Adama City, Ethiopia

Yonas Asefa Fufa

Addis Ababa University, asfgeneral09@yahoo.com

KEY WORDS: *Database; Topographic map; Base Map; Urban Planning; Structure plan; ArcGIS*

ABSTRACT:

Base map is a map serving as the foundation for subsequent planning showing all physical features and existing land-use/built-up area of the area/city. Urban planning maps cannot do without a topographic base map. As in many other thematic mapping applications use is often made of already existing base map layers, but, ideally, the topographic base should be better adjusted to purpose and use, scale of representation and the planning information layer that is projected on it. Base map can be prepared by ground survey, aerial photographs or remote sensing. Structure plan needs base map for existing situation analysis and land use proposal. Adama structure plan base map was prepared by ground survey using Sokkia GRXII GPS and Aerial photographs taken by Intelligence Network Security Agency which sponsored by Adama Science and Technology University. Base map geodatabase was created to store both spatial and non-spatial data. The contents of the geodatabase (Feature data set and feature classes) were determined based on the importance of the features needed for structure plan preparation. This paper explains what literatures recommend contents of base map geodatabase, what Adama base map look like and the order of layers in ArcGIS.

1 Introduction

Base map is a map serving as the foundation for subsequent planning showing all physical features and existing land-use/built-up area of the area/city.

Physical planning maps cannot do without a topographic base. As in many other thematic mapping applications use is often made of already existing base map layers, but, ideally, the topographic base should be better adjusted to purpose and use, scale of representation and the planning information layer that is projected on it.

A base map is the graphic representation at a specified scale of selected fundamental map information; used as a framework upon which additional data of a specialized nature may be compiled (American Society of Photogrammetry, 1980). Within the multipurpose cadastre, the base map provides a primary medium by which the locations of cadastral parcels can be related to the geodetic reference framework; to major natural and man-made features such as bodies of water, roads, buildings, and fences; and to municipal and political boundaries. The base map also provides the means by which all land-related information may be related graphically to cadastral parcels.

By the state-of-the art, spatial data of Adama base map was collected by different methods: ground survey, aerial photographs or remote sensing. In addition, secondary data, i.e. existing map/ digital data were also used. The instruments used for ground survey is Sokkia GRXII GPS. Aerial photographs at 10cm ground sample distance were taken by Intelligence Network Security Agency (INSA) by sponsor of Adama Science and Technology University (ASTU).

The collected spatial data and non-spatial data were stored in base map geodatabase. This paper will explain what type and content of geodatabase was created.

2 Literature Review

To develop a structure plan base map, different reference materials were explored. As bench mark thematic layers case of Nepal, ESRI geodatabase, USGS Digital map data Contents and Adama city geodatabase were studied. The content of each geodatabase are explained as follows.

2.1 Thematic layers case of Nepal

There are various thematic layers which are required to prepare geodatabase of urban area and nine layers are commonly prepared. Four other thematic layers are used for some municipalities. Each thematic layer is briefly described as following:

- Base Map-Control Points: includes trig. points, BMs, new establishes points, main features
- Administrative Boundary: includes District, VDC/ municipality, ward, national parks, services area,
- Topographical And Hypsographic Features: peak, pass, pit, land slide, embankment, escarpment, cliff, landslide, cutting, contour, depth contour, hill shading,
- Transport: Road- category, surface types, width, status, name; airport- category, surface types, status, name; bridge- category, structure and crossing types, width, name; railway category, width, status, name;
- Hydrography: River, lake, ponds, canal, dam, sluice gate, spillway, weir, and snow covered area, glacier, crevasse,
- Land Use: cultivation, orchard, nursery, plantation, forest, shrubs, grass land, river/stream, sand and gravel bed, lake /pond, snow covered area, other, tree species, cultivation type, intensity, functional use zones,
- Infrastructures: water supply-scheme type, house hold served, capacity, name, organization, source, reservoir, treatment plant, pipeline, water valve, hydrant, other source; sewerage- pipe line, storm water, manhole, treatment plant; electricity- electric line, pylon, transformer; Telephone- line, cabinet and poles,
- Buildings: Functional category, functional use, other structures
- Environment: watershed, hazards, flood hazard, flora and fauna,
- Cadastre: administrative boundary, parcel number and its boundary, ownership data
- Street Names And House Number: Street names decision, metric house number,
- Socio-Economic Data: Population, literacy, health and occupation status, metric house number, status of infrastructure,
- Linkage Of Data With Tax System: cadastral parcel, building, ownership data, and tax system

2.2 ESRI Geodatabase

According to ESRI GIS (Arctur and Zeiler, 2004), common thematic layers are:

- Transportation: includes roads, railways, transportation infrastructure, and cartographic features.
- Boundaries: these include administrative boundaries, such as municipal and other legal jurisdiction.
- Cultural: includes any cultural features in not in other themes, such as hospitals, schools, Museums, and other significant buildings and landmarks.
- Hydrography: surface waters and features for managing waters, such as rivers, lakes, canals, wells, and water treatment plants.
- Hypsography: includes elevation points, contour lines, TINs, DEMs, and shaded reliefs based on DEMs.
- Surface Overlays: could have any number of different features, depending on purpose of the map.
- E.g: land covers (vegetation), Soil type, and surface geology
- Image Base: include raster data of satellite image and orthophotos, scanned maps, etc.
- Reference: include map grids or graticules, and other labeled tics at map's edge
- Page Layout Design: includes North arrow, legend, source attribution, inset or locator maps, etc.
- Cross-Cutting Themes: Labels, Place names, etc

2.3 USGS Digital Map Data Contents

This data base will initially contain 11 types of base-map data as follows (National Academy of Sciences, 1983):

- Reference Systems: geographic and other coordinate systems except the Public Land Survey System.
- Hypsography: contours, elevations, and slopes.

- Hydrography: streams and rivers, lakes and ponds, wetlands, reservoirs, and shorelines.
- Surface Cover: woodland, orchards, and vineyards.
- Nonvegetative Features: lava rock, playas, dunes, slide rock, and barren waste areas.
- Boundaries: political jurisdictions, national parks and forests, and military reservations.
- Transportation Systems: roads, railroads, trails, canals, pipelines, transmission lines. Bridges and tunnels.
- Other Significant Man-Made Structures: buildings, airports, and dams.
- Geodetic Control, Survey Monuments, Landmark Structures.
- Geographic Names.
- Orthophotographic Imagery.

2.4 Existing Adama City Geodatabase

INSA was developed geodatabase for Adama town. The layers of this geodatabase are as follows:

- Cadastre: contains “LandParcels”, “NeatLine” and “Projectlimit”
- Cultural: contains cemetery, open area, park garden, playground, religious buildings and swimming pool.
- Hydrography: contains water features and drainage systems.
- Relief: Relief is a feature data set which contains height information and Ground Control points
- Structures: contains any buildings, fences and tukuls Structure.
- Transportation: includes bridges, culvert, public square, road centerline, road paved, road under construction, road unpaved, sidewalk and track.
- Utilities: includes telecommunication and electrics facilities.
- Vegetation: includes cultivated land, horticulture, trees, tree line and wood land

3 Methodology

Geodatabase of Adama structure Plan base map was developed using the following methodology. Four geodatabases were compared and final geodatabase was developed with some amendments.

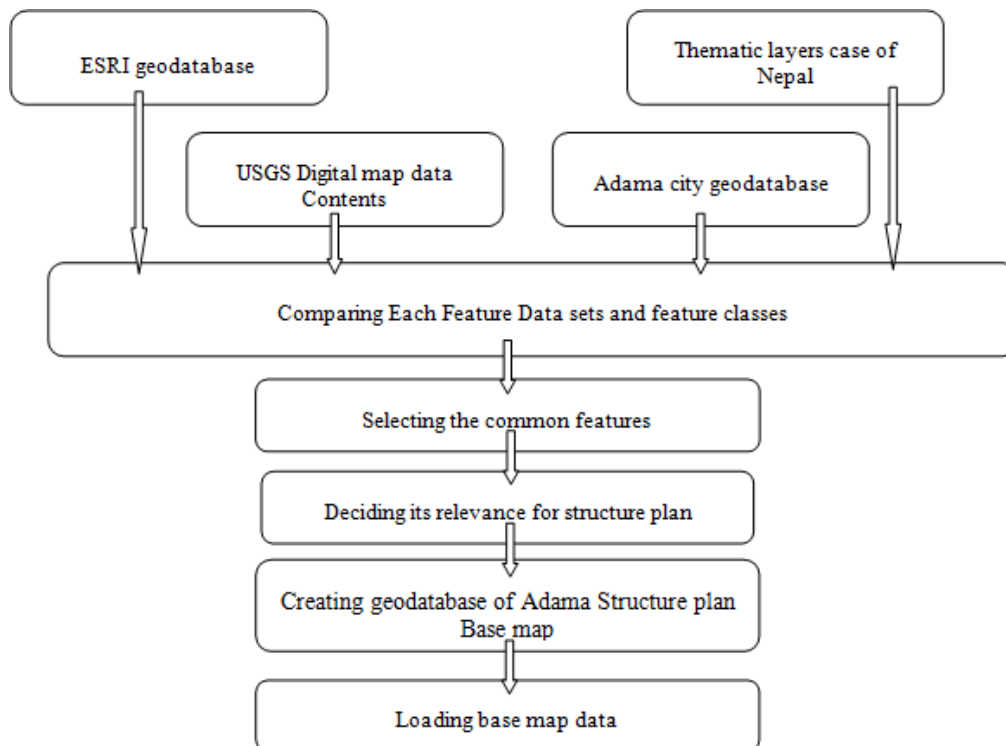


Figure 1; Adama Base Map's Geodatabase Methodology

4 Adama Base Map Geodatabase

4.1 Comparison of different Geodatabases

As explained in literature review the summary of each geodatabase are shown in Table .

Base Map Thematic Layers, Nepal	Common Themes by ESRI	USGS Digital map data Contents	ADAMA Cadaster by INSA	Proposed Thematic layers for Structure Plan Base Map
Base map-control points	Geographic Names	Geographic Names		Control Points
Administrative boundary	Boundries	Boundaries	Cadastral	Boundries
Topographical and hypsographic features	Hypsography/Elevations	Hypsography	Relief	Hypsography
Transport	Transportation	Transportation Systems	Transportation	Transportation
Hydrography	Hydrography	Hydrography	Hydrography	Hydrography
Land use	Surface Overlays/Land cover	Surface Cover	Vegetation	LandUse
Infrastructures			Utilities	Infrastructures
Buildings		Other Significant Man-Made Structures	Structures	Blocks
Environment				
	Cultural features		Cultural	Cultural
	Orthoimagery	Orthophotographic Imagery		Orthoimagery
	Landsat 7 satellite imagery			
		Reference Systems		
		Nonvegetative Features		

Table 1: Summary of Four geodatabase

4.2 Geodatabase of Adama Structure plan base map

The followings are thematic layers of Structure Plan Base Map

Control Point

It includes:

Bench Marks(Name, MonumentType, EstablishedBy(EMA, OUPI, & Land), E, N, H, Photo) : There are two main types of benchmarks that exist – “vertical control points” and “horizontal control points”. Vertical control points contain a precisely measured Easting, Northing and Elevation. The elevation is usually measured as height above sea level. Horizontal control points simply contain Easting and Northing values.

GCPs(Name, E, N, H, MonumentType, Photo): are crucial for orthorectifying, which is the geometrical correction of aerial and satellite images.

LandMarks (Name, Type of Services) any significant buildings, Structures and landmarks.

Boundary:

It includes Index map (Index number is provided for printing purpose), Adama Project boundary and Kebele Boundary.

Hypsography

Elevation points, Contour lines, Gorges, and DEMs are included in hypsography.

Name	Type
Boundaries	File Geodatabase Feature Dataset
BuildingOrBlocks	File Geodatabase Feature Dataset
ControlPoints	File Geodatabase Feature Dataset
Hydrography	File Geodatabase Feature Dataset
Hypsography	File Geodatabase Feature Dataset
Infrastructures	File Geodatabase Feature Dataset
LandCover	File Geodatabase Feature Dataset
PointData	File Geodatabase Feature Dataset
SocialService	File Geodatabase Feature Dataset
Transportation	File Geodatabase Feature Dataset

Figure 2: Geodatabase of Adama City

Transportation

Transportation includes roads, railways and transportation infrastructures. Roads are classified by surface materials. These are Expressway, Asphalt, Cobble Stone, Walkway, Gravel, and Unpaved Road. Transportation infrastructure contains bridge, Culvert, and pipes.

Hydrography

In hydrography, river represents water bodies which is not seasonal; Stream represents any channel in which water flows; pond represents water stored in small area and Marshy Swampy Area represent any wet lands

Land-Cover

Land cover is generalised as an Agriculture, Quarry site, Trees and Vegetations

Infrastructures

They include:

water supply(source, reservoir, treatment plant, pipeline, water valve, hydrant, other source);

sewerage(pipe line, storm water, manhole, treatment plant);

electricity(electric line, Pole, pylon, transformer, Wind Farm and Substations);

Telephone(line, cabinet and poles),

Building/Block

It includes prominent Buildings, Blocks (Block Function) and Fence (Service Type)

Cultural/Social Service

Anything that is common in some culture is a cultural feature. It contains hospitals, Schools, Cemetery, Open Space, Religious Building, Playground, Museums, Military Camp/Police Station and Universities

AdamaMosaic_2017

This is the place where mosaic ortho photo of Adama was stored.

Adama_DTM_2017

Adama Digital Terrain Model (DTM) generated from aerial photograph of 2017 was stored under this raster data set.

4.3 Adama Geodatabase Data

Spatial data of Adama Structure plan was digitized from aerial photographs. But ground topographic surveying was also done for some special services and features which were not identified from the image. The digitization was done for each feature classes of the geodatabase.

Static GPS positioning was carried out for determining ground control points (GCPs). The processed final coordinates of the GCPs were loaded into GCPs feature classes. 160 GCPs made up of reinforced concrete were fixed on the ground. The majority of the GCPs were distributed in expansion areas.

4.3.1 Methods of Data Collection

Data were collected by ground survey and aerial photographs. Available secondary data were also used.

4.3.2 Instrument Used

Twelve GNSS GPS Receivers (Atlas and Leica) were used. Lap tops and Hand held GPS Receiver are also used.

4.3.3 Ground Control Points

Thirteen ground control points were established from Primary Control Points. Static reading was taken for two hours. The processing was done by INSA. The final coordinates given by INSA is shown in table 2. The coordinate system is UTM and Adindan datum.

ID	X	Y	Z
AD01	540108.599	958473.785	1547.232
AD02	547347.615	953888.840	1466.047
AD03	541730.545	950919.673	1466.952
AD04	543370.975	943036.126	1512.066
AD05	533708.243	951327.030	1672.189
AD06	527474.426	954321.649	2103.232
AD07	520721.839	946045.963	1876.159
AD08	525289.239	940574.424	1614.559
AD09	534036.568	941142.172	1619.078
AD10	539991.959	937371.954	1599.484
AD11	533255.196	929805.111	1541.662
AD12	526380.556	931945.816	1541.106
AD13	515581.958	938099.086	1651.854

Table 2: Ground Control Points

4.3.4 Mosaic Photographs

The aerial survey was done by INSA in 2017. The processed result was used for this structure plan. New mosaic photographs cover an area of 31,000 ha.

4.3.5 Digital Elevation Model

Digital elevation model (DEM) was generated from aerial photographs by INSA. It covers an area of **31,000 ha**.

4.3.6 Drawing Order of Layers

The layer list in Fig. 3 shows the drawing order of layers on the map—layers higher in the table of contents are drawn on top of those that are lower.

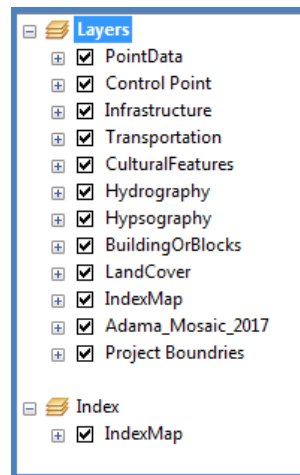


Figure 3: This picture shows the order of drawing

The final output base map of Adama city is shown in Figure 4.

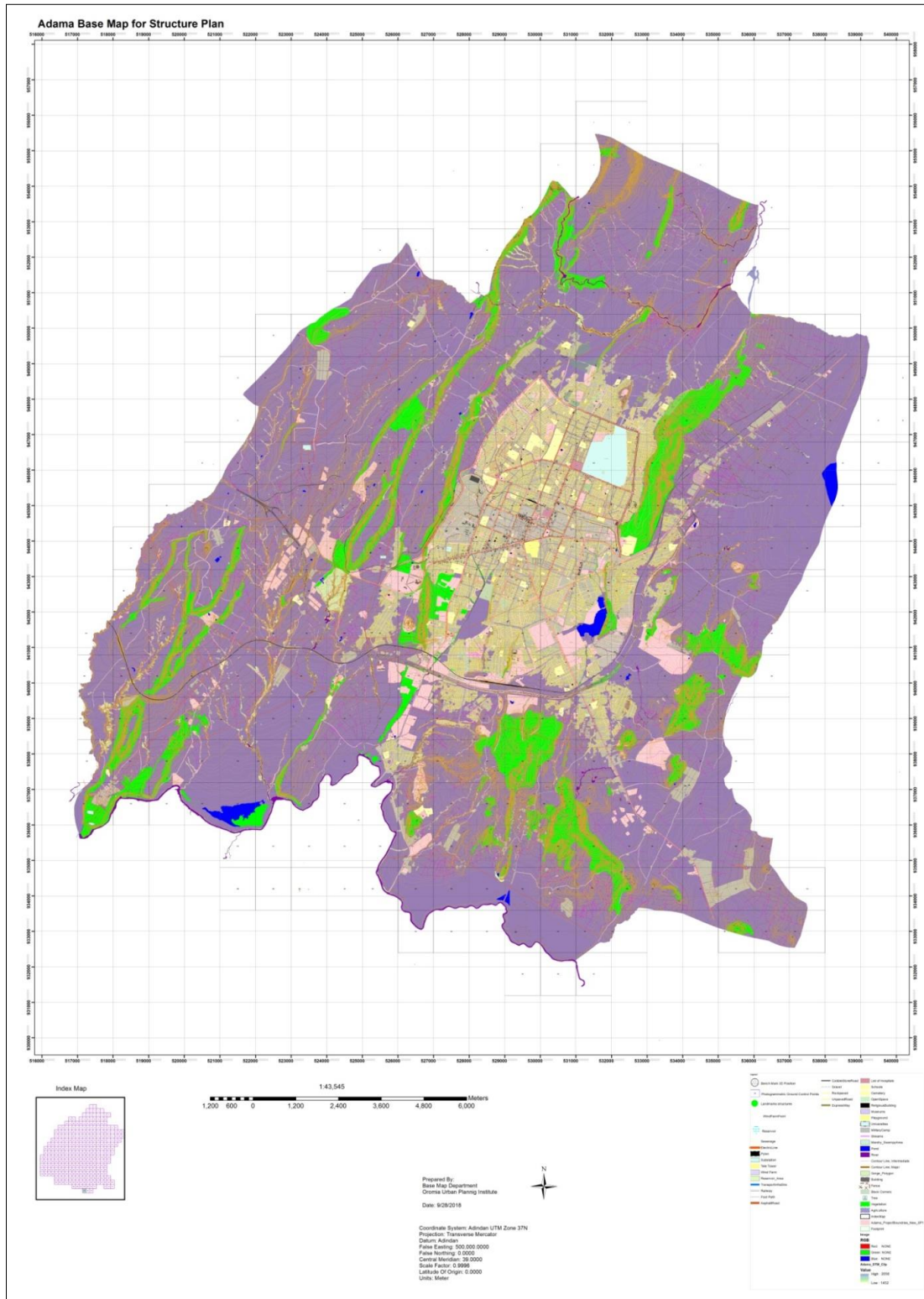


Figure 4: Base map of Adama City

5 Conclusion

The content of geodatabase feature data set depends on the purposes of the database. The minimum data sets for base map, which used for structure plan, have to include control point, building/block, infrastructure, transportation, cultural features, hypsography, hydrography, land cover and imagery. Each data set contains a

number of feature classes. The number of data sets and feature classes depend on accuracy level, time available and money.

6 References

- Aston, F., & Mackenzie, A., 2014. *Structure Plans, Outline Development Plans, Area Plans, Master Plans – Demystifying the Jargon*. <http://www.astonconsultants.co.nz/article-structure-plans-outline-development-plans-area-plans-master-plans-ndash-demystifying-the-jargon.html> [accessed July 2017]
- Arctur, D. and Zeiler, M., 2004. *Designing Geodatabases*, Esri Press. pp 308 - 373
- National Academy of Sciences, 1983. *Procedures and Standards for a Multipurpose Cadastre*. The National Academies Press. <https://www.nap.edu/read/11803/chapter/5#52> [accessed 26 July 2017]

Assessing the use SEPAL cloud based system to perform remote sensing tasks for development REDD+ Projects

Gillie Cheelo

Department of Geography and Environmental, School of Natural Sciences, University of Zambia, Great East Road, Lusaka (Zambia), - gillie.cheelo@gmail.com

KEY WORDS: *Cloud based system, Verra (VCS), REDD+, Remotes Sensing, VM0015, SEPAL*

ABSTRACT:

There are a number of cloud based remote sensing applications that have been developed in the recent years. Some of the well-known applications include Google Earth Engine (GEE), SEPAL, Hadoop, Ge-grid, Sentinel-Hub Platform. The advantages of these cloud based systems are that work is done on the browser instead on the desktop applications. Most cloud based system are now relatively simple to work with. Nonetheless, to work with cloud based system such as GEE requires some basic scripting skill in R, JavaScript or Python. The needs for users to have some basic scripting skills to work with remote sensing cloud based system tends to discourage potential less/ non programming users to work with these cloud system systems despite their obvious advantages. As a way of bridging this gap and reducing the time it takes to prepare remote sensing data before performing the actual analysis, Food and Agriculture Organization (FAO) is developing SEPAL application which is being tested. In this workshop/paper SEPAL was tested to ascertain if it can be used to develop REDD+ Projects. The assessment was based on testing the functionalities, access to data sources and documentation against the VM0015 Methodology in REDD+ Project development using a real REDD+ Project development in Zambia. The remote sensing requirements from VM0015 Methodology were identified tested in SEPAL cloud based system. My findings are that SEPAL cloud based system is very simple to use without any need to know basis scripting skills to perform advanced analysis as compared to other cloud based system such GEE. It has all the remote sensing functionality to help REDD+ project developer satisfying the VM0015 requirements. Therefore, remote sensing fraternity needs to embrace the use of cloud based remote sensing system to benefit from the existing advantages that cloud based system provides. SEPAL like other cloud based remote sensing system will greatly reduce the time it takes for preprocessing especially if you are using desktop remote sensing application. SEPAL cloud based application is certainly the answer to users who are intimidated by need to code or pay (Sentinel hub Platform) in order to perform advanced remote sensing analysis on the cloud. On the other hand, the challenges of low internet speed are not a factor as the processing is done on the server side and the analysis continues even when you have logged of.

1 Introduction

This paper intends to show that SEPAL application can be used to development REDD+ Project as it is able to meet all the remote sensing requirement provided by VM0015 Methodology. To contextualize this paper, the background of cloud based system, overview of REDD+, description of what SEPAL is and its architecture has been presented in this section.

1.1 Background

In the 21st century the cloud computing has gain ground due to improved IT, internet service technology. The high performing computers which provide high speed computing capacity have increase and becoming accessible not only to users from well-funded organization in developed countries. The advantages of cloud based system is that they are efficient, provide increase collaboration and accessible anywhere, they remove the need to purchase/install or maintenance software and hardware. However, the two key draw back are concerns on data security and need for reliable internet (Jozczuk–Januszewska, 2011; Maryam & Nasim, 2018).

They are also a number of cloud based remote sensing applications that are being or have been developed. These applications include but not limited to Google Earth Engine, SEPAL, Ge-grid, Hadoop (White et al., 2014). The set-up of GEE has been revolutionary and has really open up the accessibility and use of the cloud based system for remote sensing work. GEE enables access to large earth-observatory satellite data and high performing computing resources for processing large amount of data without having to suffer the need for to purchase and manage high speed computers (Gorelick et al., 2017; Xiong et al., 2017). Some of datasets available are Landsat, Sentinel-2, SAR. GEE has successfully been used by both scientist and operators especially from developed country who have the technical skills. Cloud based system like GEE have eliminated the need to download large files, need to manage enormous storage volume or purchase expensive high speed processing computers to undertake heavy analysis. Padarian et al., (2015) showed effectiveness and efficiency of the GEE whilst analysing 654,178 Landsat 7 scenes which occupies an equivalent of 707 petabyte of storage space. Ordinarily, it could have taken 1,000,000 hours to processed such volume of data but through cloud computing in GEE it took only 100 hours.

However, to use cloud based system such as GEE basic scripting skill is required either in JavaScript or Python. The need for GEE users to have scripting skills tends to put off potential users even with the existing helpful published examples, tutorials, training videos and functioning. In response to the needs, Food and Agriculture Organization (FAO) is developing SEPAL application which is being tested. In this workshop will show how SEPAL can be used to develop the REDD+ Project, discuss accessible dataset, SEPAL's functionalities against the critical remote sensing tasks and documentation needed for REDD+ project development.

1.2 REDD+ Overview

REDD is stand for reducing emission from deforestation and degradation. It was built by the Technical Experts from FAO, UNEP and UNDP under the UN-REDD programme launched in 2008 focusing on developing countries. It was developed based on the rationale that tropical deforestation and degradation are accumulative responsible for net 10-15% of net global deforestation (Parker, et al., 2009) and that the traditional methods to combat deforestation had failed. It was developed to provide an incentive to keep the existing forest standing. The plus in REDD+ was introduced to include a comprehensive approach to mitigating against climate change by introducing REDD contribution to poverty reduction, conserving biodiversity and sustaining vita; ecosystem services. REDD+ militate against climate change by stopping deforestation and degradation and supporting sustainable forest management (UN-REDD) (ibid).

2 Overview of SEPAL and its Architecture

SEPAL is a cloud computing-based platform for autonomous land monitoring using remotely-sensed data. The SEPAL acronym stands for System for Earth Observation Data Access, Processing and Analysis for Land Monitoring. It is a web based graphical user interface which allows users to access powerful cloud-computing resources to query, access, process satellite data quickly and efficiently without the need to learn how to script.

SEPAL was inspired by a need to create a system/platform that made accessing and using satellite data easier by eliminating the need for the user to spend a lot of the time finding, downloading, and pre-processing the satellite data before being ready for analysis. SEPAL was designed to work in conjunction with modern spatial data infrastructures (like Google Earth Engine) and other open-source software (like R) to lower the barriers to using remotely sensed data and to enable everyone, everywhere to focus on solving problems and answering questions with ready-to-use data. The SEPAL architecture is a combination of Google Earth Engine and open

source software such as ORFEO Toolbox, GDAL, R, R Studio Server, R Shiny Server, SNAP Toolkit, and OpenForis Geospatial Toolkit. It allows and provided a web based graphical user interface which allows users to powerful cloud-computing resources to query, access and process satellite data and perform advanced analyses without really the need to learn how to script as is the case for GEE. SEPAL is a project of the Forestry Department of the United Nations Food and Agriculture Organization (FAO) funded by the Government of Norway (Lindquist, 2018).

SEPAL's architecture is organized basing on four modules; search, browse, process and terminal modules. The search module enables searching, selecting, mosaicking, undertaking classification based on random forest algorithm and performing analysis such as change detection and time series analyses. It also has an export utility to export analysis results either to SEPAL itself or Google Earth Engine as an asset. Vector dataset to determine the extent are inputted as fusion tables. The second model is the browse module which is used to search for saved resources on SEPAL and for downloading. The third module is the process module where all advanced analysis are performed such as sample design for ground truthing, accuracy assessment, Time Series, Geoprocessing tools, SAR data processing .

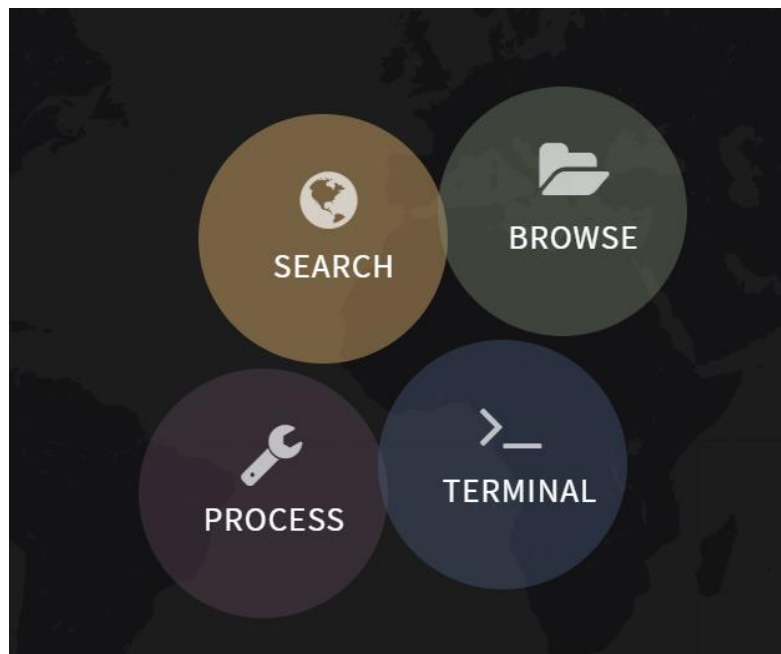


Figure 1: SEPAL Modules

<https://sepal.io>

SEPAL has also another external module called SEPAL-CEO. This module help to captures training data for image classification and image based ground truthing data based on the set sample design. SEPAL CEO has functionalities to set up the project for both training data and ground truthing data collection. In SEPAL CEO application has functionality to enable possibility to connect to available online other baseline such as Digital Globe, Planet and assets saved in GEE.

ceo-sepal add project

name	type	date created	username			
GroundTruthing_20_June_2018	CEP	6/20/2018, 11:02:03 AM	gcheelo	edit	collect	delete
2016_trainigs	TRAINING-DATA	4/5/2018, 5:18:00 PM	gcheelo	edit	collect	delete
Training_2006_v2	TRAINING-DATA	1/16/2018, 3:00:38 PM	gcheelo	edit	collect	delete

Figure 2: SEPAL CEO Set Up

<https://sepal.io/ceo/>

3 Methodology

3.1 Methodological Process

We used the VM0015 requirement to extract the remote sensing requirements and the requirements were assessed against the functionalities available in SEPAL application. These functionalities were also used for the real cases scenarios of using SEPAL to development the remote sensing component of the REDD+ project in the Eastern Part of Zambia. The study area for the preparation of the REDD+ was approximately 7,000, 0000 known as reference region⁷ in RED+ language. The remote sensing work needed to be prepared for the reference region. Then these requirements were compared with what SEPAL is able to provide in section 4 (Analysis and Discussion). Section 3.1 discusses the remote sensing requirements from VM0015 methodology under the VCS.

3.2 Remote Sensing Requirements using the Verra (VCS) – VM0015 Methodology

These requirements provide guidance on the data to be used and the type of analysis to be perform in the development of the REDD+ project. To implement REDD+ Project and be able to sell carbon credit the project development need to be transparent, scientifically sound, well document for another person to follow and get the same result. To achieve this goal, they are a number of the standards that has been developed to guide the REDD+ Project development and monitoring. Some of the REDD+ standard that can be used are Forest Carbon Portal, Climate Community and Biodiversity Alliance (CCBA), Verra (formerly Verified Carbon Standard, Plan Vivo, Carbon Development Mechanism (CDM), Gold Standard, Code REDD (<https://www.cifor.org/gcs/redd-map/>)).

Verra has a number of approved methodologies for REDD+ Project developers and each has different applicability conditions to consider. For our interest will look at the VM0015 Methodology. The VM0015 Methodology was developed by World Bank Biocarbon Fund, IDESAM, the Amazonas Sustainable Foundation and Carbon Decision International for REDD+ Project activities (Shoch et al., 2011). This methodology was approved in 2011 and its quite useful for mosaic projects with multiple sites which requirement use of remote sensing technology as it can be too costly to use point interpretation to undertake image classification. This standard full lists of criteria for the full REDD+ development but for the interest of this paper it is restricted to the remote sensing specific requirements. These requirements are;

- Requirement 1: Analysis of historical land use change and land cover change. This involve collection and used of satellite imagery with the minimum spatial resolution of 10m to 10m up to the maximum of 100m x100m from optical and non-optical sensors system such as (but not limited to) Landsat, SPOT, ALOS, ASTER IRS Sensors, RADAR covering a past 10-15 years. The used satellite needs also to be well documented in terms of satellite used/sensor, spatial resolution, spectral resolution, coverage, acquisition date, image ID for each scene summarized in a table as shown below.
- Requirement 2: Well performed and documented preprocessing of the satellite imagery which is very important especially for change analysis or time series analysis, such as geometric correction, shadow removal, haze reduction and radiometric correction.
- Requirement 3: Interpretation and classification: support either the post or pre-classification change detection.
- Requirement 4: For training classifier training and validation data use high resolution data from remote sensors with of spatial resolution (< 5 meters' x 5 meters) to both train and undertake ground truthing posterior analysis. Well described type of data used, coordinates and sampling design.
- Requirement 5: Map accuracy verified and well documented map accuracy that meet the accuracy requirement of 90% for the forest class and 85 % overall accuracy. This is necessary to produce credible baseline (Pedroni, 2012)

The requirement includes the data that can be used, the preprocessing, analysis and accuracy assessment to be performed. These step are document into the methodology annex which is presented to the Auditor and the

⁷ The boundary of the reference region is the spatial delimitation of the analytic domain from which information about rates, agents, drivers, and patterns of land-use and land-cover change (LU/LC-change) will be obtained, projected into the future and monitored. (Pedroni, 2012)

Auditor will need to be able to use the description and re-run the process and get the same result. This could take a day or more depending on what software you have used and how the workflow is well documented for repeatability.

Biocarbon Partners has used SEPAL to development the REDD+ Project covering more than 1,000,000 hectares of Land in Eastern and Lusaka Provinces of Zambia. Specifically used SEPAL to select and preprocess Landsat scenes covering the project area, created composites, undertaken image classification, perform change analysis and perform accurate sampling scheme and the error matrix. SEPAL also comes with another model which is used to collect both training data and ground truthed data. In this workshop will shared my experience working and testing SEPAL cloud based system against the VM0015 remote sensing requirements.

4 Analysis and Discussion

4.1 Analysis – Test SEPAL against the VM0015 Requirements

The analyses were done based on each of identified requirement in section 3.2.

Requirement 1: Used the SEPAL's search module find access the needed satellite imagery from the Google Earth Catalogue according to the requirement such as Landsat 4 and 4, Landsat 7, Landsat 8 and Sentinel-2 to use to create mosaics for your area of interest as shown in the figure below.

Figure 3: Search for Landsat Scenes

The scenes for near the selected dates are used to create a default composites and users have the opportunity to choose which scenes to use. The Landsat scenes are displayed with calculated information on the cloud cover, ID, row/path, number of days away from the set target date, satellite name, date the image was capture as shown below in Figure 4. This information is used to populate the VM0015 methodology documentation required during project verification under the Verra (VCS). Hence the requirement 1 is well met with SEPAL's functionalities of having access to Landsat (30m), Sentinel-2 (10m)-these are within the set range of minimum spatial resolution of 10m to 100m spatial resolution for either optical and non-optical sensors system. SEPAL enables access to PALSAR datasets.

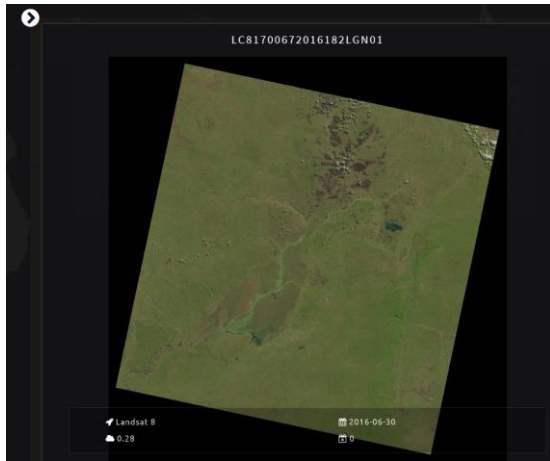


Figure 4: Landsat Scene

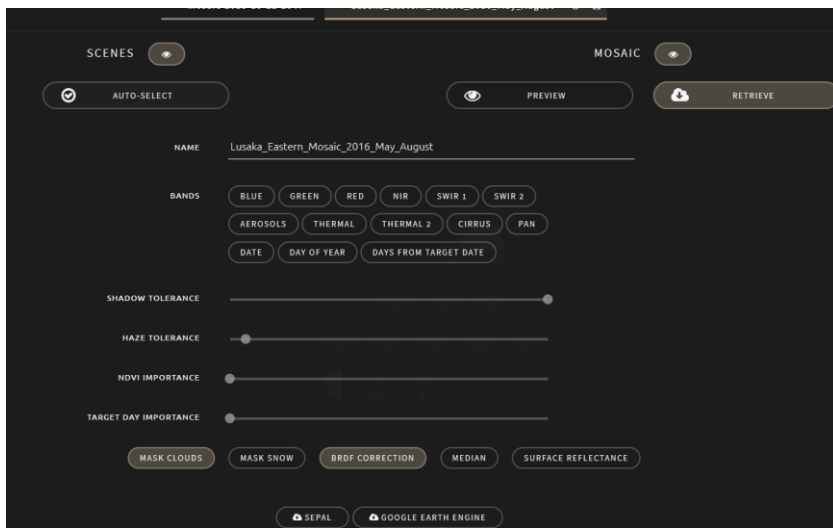


Figure 5: Preclassification

After the composite is created spectral band of interest can be exported to GEE as an asset or SEPAL.

Requirement 2: When finished with creating a composite mosaic. The composite based on the provided area of interest is preprocessed to create a finished composite. Each mosaic with these setting can be saved as a recipe be re-used later. Figure above the are tabs that have algorithm underneath that enables preprocessing such as cloud mast, BRDF correction, Shadow tolerance, haze reduction and calculation of the surface reflectance to radiometric correct the scenes. With regard to geometric correction all the Landsat imagery are co-registered with an accuracy of less than a pixel hence cannot cause errors during the change detection and time-series analysis.

Requirement 3: SEPAL has the tools to undertake image classification using the default random forest algorithm and training point collected from SEPAL CEO application illustrated in requirement 4.

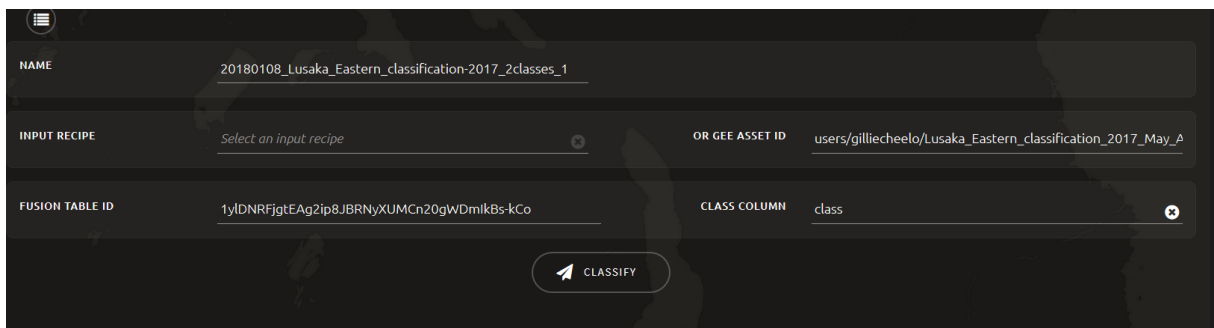


Figure 6: Image classification in SEPAL

SEPAL support pre-classification change detection and post classification. The figure below shows two mosaics exported to GEE as assets for two periods-2006 and 2016 and a fusion table with collected training points.

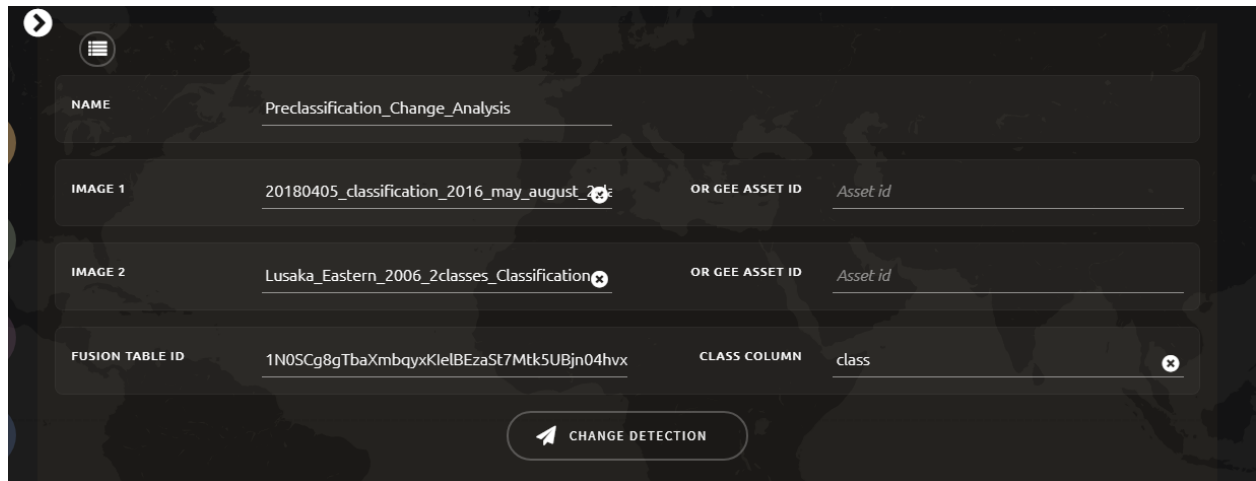


Figure 7: Pre-classification change analysis setting 2006 and 2016

Can also undertake the similar analysis to identify area for training using time series analysis. Post-classification change detection is don't done on SEPAL instead was easily done using QGIS/ArcGIS using raster algebra (substraction).

Requirement 4: SEPAL CEO application has access to high resolution Digital Globe imagery (50cm to 60cm) which was used for training the classifier and also for ground truthing as shown in Figure 8 below. Your own high resolution satellite imagery can also be uploaded in the gee account and accessible to SEPAL CEO to be used quality training and ground truthing.

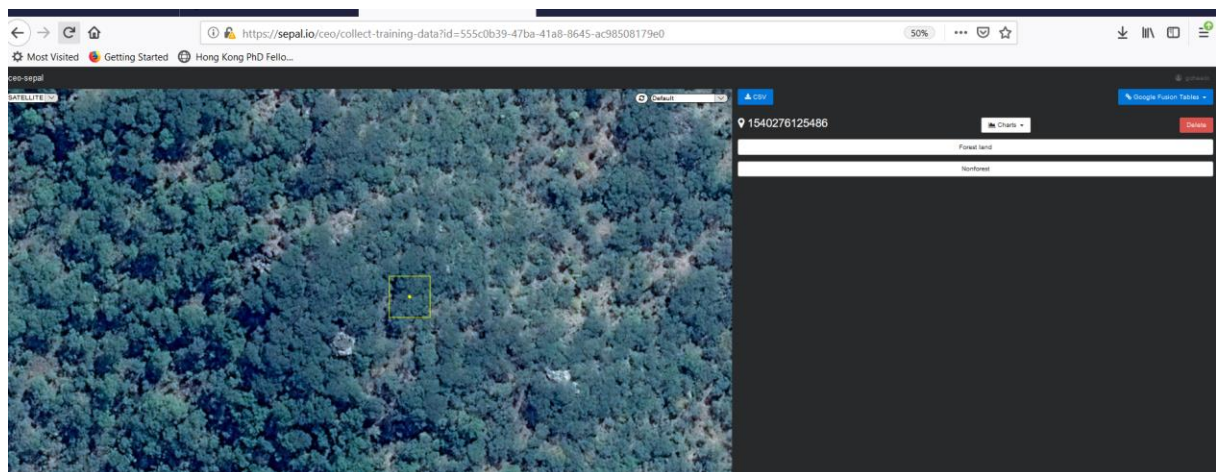


Figure 8: Capturing Ground Truthing Data in SEPAL CEO

In SEPAL CEO it is also possible to access on satellite imagery and stored in GEE as assets, access to Digital Globe Cloud Services, Globe Imagery Browser Services (GIBS), GeoNetwork and GeoServer as web map service. SEPAL in the search module enables us to undertake the classification using the random forest the default classifier using the obtained training points from SEPAL CEO application and produce the classification result below Figure 9.

We started off with having using the IPCC classes of Forest, Grassland, Cropland, Wetlands, Settlement and other but due to poor results we finally opted for only to classes –forest and non-forest. The result of the 2007 classification is shown in Figure 9



Figure 9: Random Forest Classification Results

Requirement 5: The SEPAL's processing module stratified area estimator-design tool which helps to defined statistically samples aimed to me the desired overall accuracy based on the classification results available classes. These sample designed is used to estimate the areas and also used to estimate the estimate the uncertainties (confidence intervals) for the areas for each class (Olofsson, et al., 2014).

Stratified random sampling was used for the designing the ground truthing locations. The ground truth sampling design was set to get sample and their distribution that enables us to get results that meets the minimum accuracy requirements of at least 90% for the forest class and 85 percent overall accuracy. The expected classification results were set in the sample design for forest to be slightly higher (0.95) expected user accuracy confidence and 0.9 for overall results as shown in Figure 10.

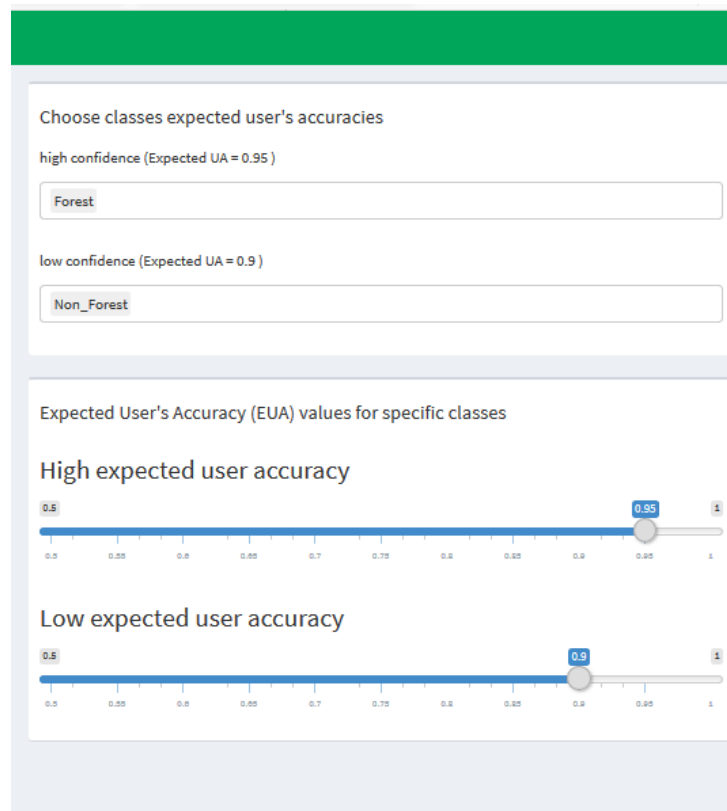


Figure 10: Setting the expected accuracy for the ground truthing points

From these setting at total of 663 point were generated; These point where ground truthed using most recent Digital Globe satellite data in the SEPAL CEP application and start assigning the points according to what Land cover seen on the digital globe data.

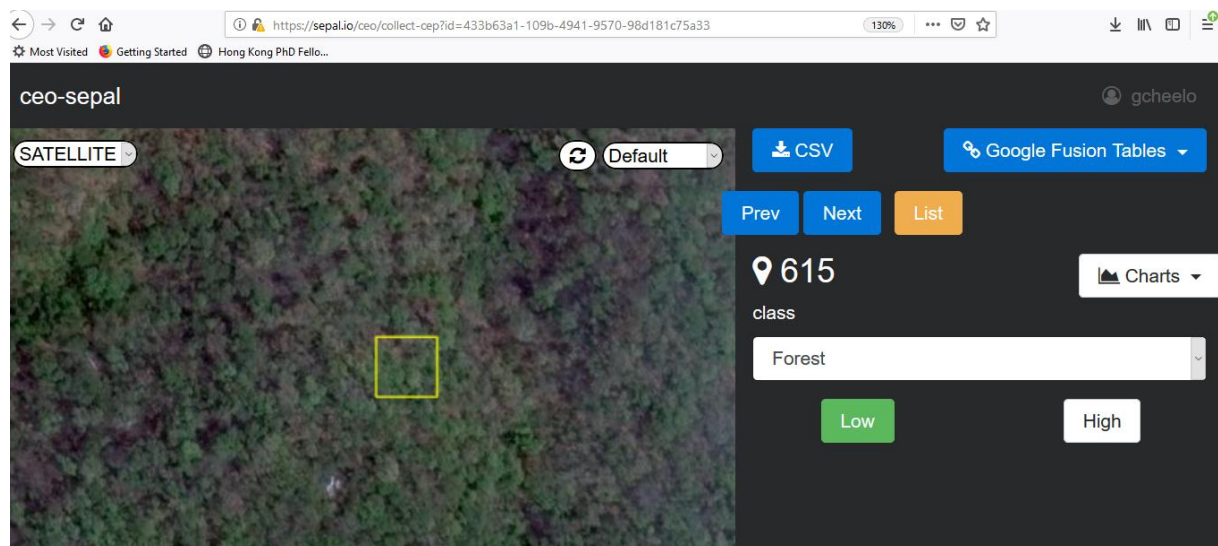


Figure 11: Capturing of training data using SEPAL CEO application

After this the data was exported from SEPAL CEO as CSV file and loaded in the stratified area estimator-analysis tool in SEPAL process module. The aim of the stratified analysis tool is to analyse the results from the stratified sampling designed that can be used for area estimates. The accuracy assessment for the 2017 and use classification were as follows in Table .

	Forest	Non Forest	Row total	User accuracy	Error of commission
Forest	327	14	341	95.89442815	4.105571848
Non Forest	25	297	322	92.23602484	7.763975155
Total Column	352	311	663		
Prodcuer accuracy	92.89772727	95.49839228	624		
Error of omission:	7.102272727	4.501607717			
				Correctly classified:	624
	Overall accuracy:	94.11764706			

Table 1: Map Accuracy assessment

Based on the accuracy assessment above the area of forest and non-forest is estimate in consideration of these results instead of just have the pixel count which does not give information on the uncertainty in the results. Below table shows the table of the area estimates. The estimate area takes into account the level of uncertainty caused by the miss classified pixels.

users_accuracy	map_pixel_count	strRS_area_estimate	strRS_standard_error	strRS_confidence_interval	number_samples
0.958944282	81863455	84458391.11	1445280.021	2832748.841	352
0.922360248	76711980	74117043.89	1445280.021	2832748.841	311
					663

Table 2: Area estimates calculation based on the accuracy assessment results

4.2 Discussion

SEPAL makes it easier to show the VCS verifier that you followed all the right procedure when developing the remote sensing part of the REDD+ Project development. Just available the SEPAL account detail the VCS verified can easily replicate the processes performed and ascertain its accuracy. SEPAL makes it easier to prepared the baseline methodological annex which is required for verification.

The use of Digital Globe imagery basemap used in SEPAL should be used whilst Google Earth application is open so that you know the true date of the imagery used. However, SEPAL is still a project under development hence the developers are very flexible in taking into consideration any useful comment. At first SEPAL had no option to include your own area of interest but now this functionality was included. With regards to classification algorithm SEPAL currently only has on algorithm available by default- random forest it would be great to include more algorithm option. SEPAL does not only have functionalities for the analysis suitable for REDD+ Project, it has also other advance analysis to perform post classification change analysis, image segmentation and other analysis under development. To access SEPAL create need to go to <http://tinyurl.com/fao-sepal> enter your email address, name, institution or country and a brief explanation of why you want to use SEPAL.

5 Conclusion

The remote sensing fraternity needs to embrace the use of cloud based remote sensing system to benefit from the existing advantages that cloud based system provides. Currently they are a number of free cloud based platforms. The cloud based system provide access to vast satellite data, remote sensing analysis algorithm at a very fast speed (in few minutes) - which could take from hours to weeks/months if done on desktop remote sensing application. Cloud based system have removed the complexities of handling large volume of satellite data, removed the need to download large files, manage obscure formats, the need to purchase expensive high performing computers or the need to maintain hardware and software. SEPAL address the barriers that scripting poses to less skill user as it eliminates the need to script to perform advance analysis. Therefore, users especially in developing countries can also perform large project more efficiently and focus or analysis than data preparation. The user should take advantage of sepal it has easy manual developed and it was developed to support REDD+ development.

7 Acknowledgements

Acknowledgements of support from Erik Lindquist, PhD- Forestry Officer from the National Forest Monitoring (NFM) Team, REDD+/NFM cluster, Forestry Department Food and Agriculture Organization of the United Nations.

6 References

- Gorelick, N., Hancher, M., Dixon, M., Ilyushchenko, S., Thau, D., & Moore, R. (2017). Google Earth Engine: Planetary-scale Geospatial analysis for everyone. *Remote Sensing of Environment*, 202, 18-27.
- Joszczuk-Januszevska J. (2011) The Advantages of the Use of Cloud Computing in Intelligent Transport Systems. In: Mikulski J. (eds) Modern Transport Telematics. TST 2011. Communications in Computer and Information Science, vol 239. Springer, Berlin, Heidelberg.
- Lindquist, E. (2018, January 11). *wiki*. Retrieved October 3, 2018, from <https://github.com:https://github.com/openforis/sepal/wiki>
- Olofsson, P., Foody, G. M., Herold, M., Stehman, S. V., Woodcock, C. E., & Wulder, M. A. (2014). Good practices for estimating area and assessing accuracy of land change. *Remote Sensing of Environment*, 148, 42-57.
- Padarian, J., Minasny, B., & McBratney, A. B. (2015). Using Google's cloud-based platform for digital soil mapping. *Computers and Geosciences*, 83, 80-88.
- Parker, C., Mitchell, A., Trivedi, M., Mardas, N., & Sosis, K. (2009). *The Little REDD+ Book*. Oxford: Global Canopy Programme.
- Pedroni, L. (2012, December 3). *Approved VCS Methodology VM0015*. Retrieved October 20, 2018, from <https://verra.org:https://verra.org/wp-content/uploads/2018/03/VM0015-Avoided-Uplanned-Deforestation-v1.0.pdf>
- Shoch, D., Eaton, J., & Settelmyer, S. (2011). *Project Developers Guidebook to VCS REDD Methodology*. California: Conservation International Carbon Fund.
- Verma P., Gupta., Sambya R.S., (2018) Security Issues and Challenges in Cloud Computing: A review, National Conference on advancement in Computer Science and IT, 1, 2 (189-196)
- Whitman, R.T., Park, M.B., Ambrose, S.M., Hoel, E.G., 2014. Spatial indexing and analytics on Hadoop. *Proceeding. 22 ACM SIGSPATIAL*. pp. 73–82.
- Xiong, J., Prasad, S., Murali, T., Gumma, K., Poehoelt, J., Congalton, R. G., et al. (2017, April). Automated Cropland Mapping of Continental Africa using Google Earth Engine Cloud Computing. *ISPRS Journal of Photogrammetry and Remote Sensing*, 225-244.

Assessment of Fire Induced Forest Degradation in Heterogeneous Forest Type of Nepal using Remote Sensing data with Google Earth Engine

Raja Ram Aryal¹ and Nishanta Khanal²

¹ Department of Forest Research and Survey, Ministry of Forest and Environment, Nepal

² International Centre for Integrated Mountain Development, Kathmandu, Nepal

KEY WORDS: Forest Fire, Google Earth Engine, Fire Severity, Burn Severity, differential Normalized Burn Ratio (dNBR)

ABSTRACT:

Forest fire is a global phenomenon as a part of ecological process which alters the ecosystem pattern from forest species distribution, its structure to complete destroys of its existence. Those consequences reduce the goods and service provided from forest and leading towards its degradation. There are different drivers of forest degradation, among them forest fire is most prevalent worldwide and come in second position in Nepal after grazing. Nepal like United Nations Framework Convention on Climate Change (UNFCCC) representative countries should have to identify and quantify the proximate and underlying drivers of forest degradation at a national level to implementing REDD+ strategies and action plans. Nepal's Emission Reductions Program Document (ERPD) has already built up and accepted. In this situation, it is inevitable to assess fire induced forest degradation as a direct driver of forest degradation in Nepal. Remote sensing has been used extensively to map severity from fire as burn severity and fire severity separately on the basis of broad spectral changes due to burning from the use of several spectral indices (combinations of different sensor bands) such as Normalized Burn Ratio (NBR), the difference in the Normalized Burn Ratio between pre- and post-fire images (dNBR), and the Normalized Difference Vegetation Index (NDVI). In this study, forest degradation due to fire was assessed by sentinel 2 and Landsat 8 satellite imageries analysis in Google Earth Engine cloud based platform through image differencing techniques for calculating fire and burn severity area separately using dNBR value within a different forest type of Nepal. Fire severity analysis was carried out within six severity classes. However, it was clearly observed that severity did not reach up to maximum (Higher) severity in each and every case. Overall, burn severity is lower than fire severity obtained from both satellites imageries but that forests areas under different severity class are dramatically altered. From Landsat 8 image analysis, it was found that *Cupressus torulosa* and *Tsuga dumosa* forest type are found in highest level of low severity burn class and moderate low severity class severity among 15 forest type and *Acaicia catechu* and *dalbergia sissoo* in lowest level within those classes during fires severity analysis. Whereas, in burn severity analysis, highest level was found on *Betula utilis* forest type and *Pinus roxburghii* in lowest level. Almost, similar result was obtained from Sentinel 2 image analysis only the *Picea smithiana* forest type show lowest level severity during burn severity analysis. From the analysis of Landsat 8 and Sentinel 2 derived severity due to fire reflects that Nepalese forests are in the verge of degradation. Forest fire is acting as one of the drivers of forest degradation which rate is highly fluctuating within different forest type in Nepal. In this research we were not able to include field level severity data. Furthermore, generating of field based Composite Burn Index (CBI) or GeoCBI is inevitable to derive co-relation with remote sensing burn indices for estimation of carbon emission from forest fire in future.

1 Introduction

Forest fire is a critical issue for natural resource managers and policy makers because of the potential environmental, societal and economic consequence. It is vital ecological processes which influence global ecosystem patterns from spatial distribution, structure and carbon cycle of vegetation to climate change process (Bowman et al., 2009). It is one of a direct driver of forest degradation.

Forest degradation is a global phenomenon in which goods and services derive from forest declined in terms of their value and production due to alteration from several changes. Various natural and human induced disturbances are the source of such change which may vary in extent, severity, quality, origin and frequency (FAO, 2009). Nepal like United Nations Framework Convention on Climate Change (UNFCCC) representative

countries should have to identify and quantify the proximate and underlying drivers of forest degradation at a national level to implementing REDD+ strategies and action plans (Kissinger et al., 2002). In Nepal, The REDD Readiness Program Proposal of the country has identified nine major drivers of deforestation and degradation which are spatially and temporally varied and intricate. One of them is forest fire which is interconnected with others (MoFSC, 2010). Forest fire is one of the major direct drivers of forest degradation in Nepal.

Severity database from the fire damage are very poorly maintain in Nepal. Especially, the severe impact of fire in different forest type is not available due to insufficient information from field (Fire prone area). However, some studies such as spatial and temporal interannual variability in burnt area (Parajuli et al., 2015), trends in the burnt-area relating climatic data (Khanal, 2015), spatial fire risk index was developed using fuel availability, temperature and ignition potential (Mir et al., 2017) have been studied. Fire degradation emission for ER program area was derived from Global fire degradation emissions based on MODIS burned area maps using the Global Fire Emissions Database (GFED). However, burned area estimates from this model do not represent true burned area and found overestimated than actual emissions from fire due to thermal anomalies of MODIS pixel size (Facility and Team, 2018). Furthermore, low resolution remote sensing data without validation from field measurement data are not significant in the ER Program's carbon accounting.

Multispectral satellite data have a capacity to detect change in ecosystem. Such change detection technologies have become a common technique used in the burned area mapping (Brewer et al., 2005; Cocke et al., 2005; Epting et al., 2005; Key & Benson 2006; Miller & Yool 2002). Satellite imageries acquired from the same sensor before and after the forest fire events have been used to quantify ecological changes induced by fire through the differences in reflective properties of vegetation (Jakubauskas et al., 1990; Landmann, 2003). Remote sensing has been used extensively to map burn severity on the basis of broad spectral changes due to burning from the use of several spectral indices (combinations of different sensor bands) such as Normalized Burn Ratio (NBR), the difference in the Normalized Burn Ratio between pre- and post-fire images (dNBR), and the Normalized Difference Vegetation Index (NDVI) (Lentile et al., 2006; Key & Benson, 2006). NBR and dNBR are widely used to infer fire severity from remotely sensed data (Van Wagtendonk et al., 2004; Cocke et al., 2005; Falkowski et al., 2005; Smith et al., 2005; Roy et al., 2006).

Fire effects measurements have some temporal gradient. The term burn severity is used interchangeably with fire severity. Fire severity is usually associated with immediate short term post-fire effects measures in terms of vegetation structure, vegetation consumption, vegetation mortality and soil alteration, whereas burn severity relates to the amount of time necessary to return to pre-fire levels or function and long-term fire effects measured in the following year on the ecosystem response on forest successional stages (Lentile et al., 2006; French A et al., 2008; Morgan et al., 2014).

Forest degradation monitoring process should be carried out from mainly two approaches i.e. detection of canopy cover or proxies change and quantification of above ground biomass loss (Mitchell et al., 2017). Due to the lack of field level burned index such as Composite Burnt Index (CBI) and Geo-CBI, this study focused on remote sensing based analysis of forest degradation which has a visible impact on the forest canopy. Despite this relevance, quantitative national-level information on drivers and activities causing deforestation and forest degradation are widely unknown. For example, the question of how much or what fraction of deforestation (emissions) in a country is caused by a specific driver (i.e. expansion of agriculture versus infrastructure) cannot be answered from Nepal. The degree of post-fire change may vary depending on heterogeneous forest type, annual differences in growing season weather, and overall time since fire (White et al., 1996; Cocke et al., 2005; Hudak et al., 2006). For this reason, stratification among vegetation types, comparison of images with similar vegetation phenology, and image differencing techniques for calculating fire and burn severity separately within a different forest type of Nepal was carried out to assess fire effects and ecological change in this research.

2 Materials

2.1 Study area

This study covered the whole area of Nepal (26° 20' 53"– 30° 26' 51" N latitudes and 80° 3' 30" – 88° 12' 5" E longitudes). The total land area of the country is 147 181 km². Forest covers occupied 5.96 million ha (40.36%), Other Wooded Land covers 0.65 million ha (4.38%) and Other Land covers 8.16 million ha (55.26%). Forest and

OWL together comprise 44.74% of the total area of the country (DFRS 2015). Forests are the main source of timber and fuel wood, and also a major source of fodder for livestock. Nepal is home to 35 forest types, 75 vegetation types and 118 ecosystems, along with four global biodiversity hotspots (By and Forests, 2014).

Forest Resource Assessment (Nepal) classified 15 major forest types was used as a mask input in Google Earth Engine. The forest type was defined according to basal area and threshold was more than 60% during FRA. Classification and Regression Tree (CART) approach was used for forest type classification using Landsat 8 imageries and forest inventoried forest type data as trained sample. Classified forest type showed that Terai Mixed Hardwood (TMH) forest type has the highest coverage (24.61%) followed by the Upper Mixed Hardwood (UMH) (18.23%) and Lower Mixed Hardwood (LMH) (17.06%). *Shorea robusta* has highest coverage with 15.27% and followed by *Pinus roxburghii* with 8.45% and so on (DFRS 2015). Those forest type data was used for generating severity level from fire within those forest types.

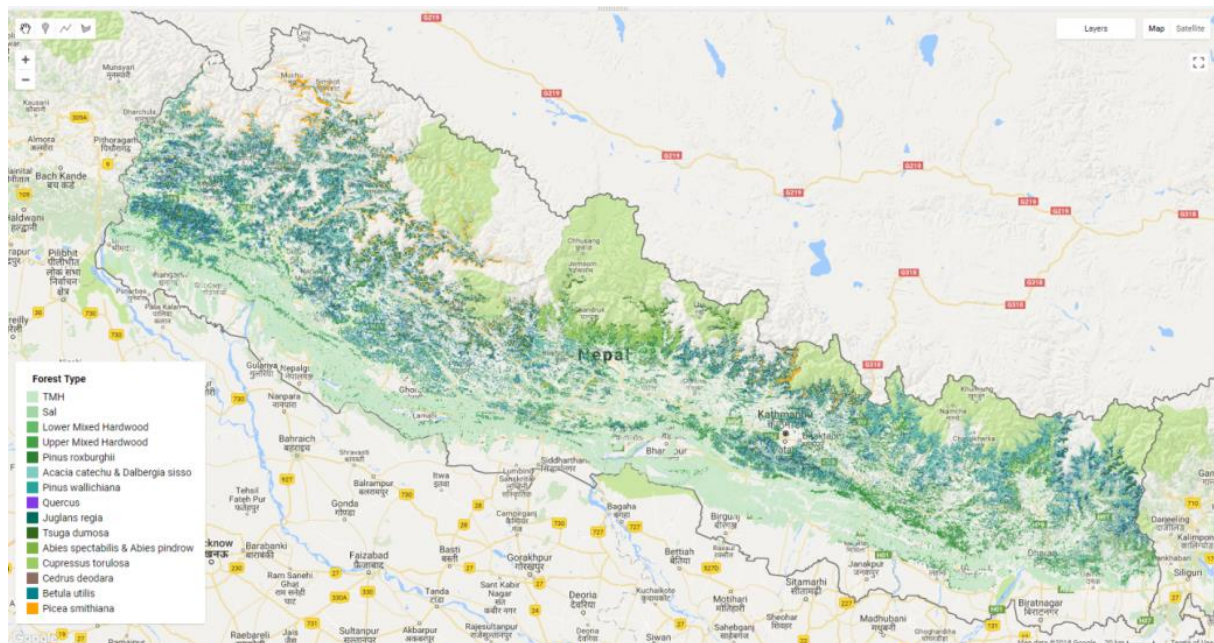


Figure 1 Study Area Map

2.2 Google Earth Engine Platform

Google Earth Engine is a cloud based geographical data processing and analysis platform created by Google. It combines multi-petabytes of archived satellite imagery datasets with a high-performance computation service. To access, process and analyze these datasets, earth engine provides users with application programmable interface (API) in JavaScript and Python programming languages. The JavaScript API can be accessed via a web application interface. Using this interface, users can create, run and share scripts written in JavaScript (Gorelick et al., 2017).

There is a vast amount of geospatial dataset in earth engine. These include satellite imageries with optical and non-optical wavelengths, weather and climate forecasts and hindcasts, topographic and socio-economic datasets, environment variables and land cover data. The images from frequently used freely available satellite images Landsat, Sentinel and MODIS are also available in the data catalog. The catalog is continuously updated at a rate of nearly 6000 scenes per day from active missions with a latency of around 24 hours from scene acquisition time. In case of a dataset that is unavailable in the catalog; users can upload the dataset themselves. They can even request new datasets to be added to public catalog.

3 Methods

3.1 Generating Burn Indices

Severity measures the amount of site alteration from the effects of change agent in a forest. In this study, forest fire is taking as change agent. Forest fire alters the reflectance value of vegetation through reduction of water level in leaf and canopy, destroying chlorophyll, exposing underground soil and altering soil moisture by increasing reflectance value in visible spectrum and decreasing in the near infrared (NIR) region (Escuin et al., 2008). After fire, green vegetation is partially or totally destroyed and soil surface superimposed which decreased absorption in the visible and SWIR wavelengths. Thus, these wavelengths are sensitive to plant cell structure and have been used effectively to monitor forest mortality due to fire (Rogan & Yool 2001). The NBR relates to vegetation moisture content has been developed by combining NIR with SWIR reflectance (Equation (1)) and bi-temporal differenced of pre and post fire NBR produce a distinction between burned and unburned forest area (Key & Benson 2006).

$$NBR = \frac{NIR - SWIR}{NIR + SWIR} \dots\dots\dots \text{Equation (1)}$$

Within GEE, mean pre-fire and post-fire NBR values were calculated using the Landsat 8 TOA Reflectance Tier 1 datasets and Sentinel-2 MSI level 1-C datasets as well. In order to do this, areas covered by cloud in the image were masked using QA bands which contains values that can help us identify whether each pixel is clouds or not. In case of Landsat, these data are produced by implementing a multi-pass algorithm (called 'CFMask') based on decision trees and is described in detail by Foga et al. The QA band named "BQA" was masked over values [2800, 2804, 2808, 2812, 6896, 6900, 6904, 6908]. Similarly, in case of Sentinel, there is a QA band named "QA60" which was masked over value [1024] as it corresponded to opaque cloud covered value.

After that, fire severity across all scenes was computed by calculating the mean composite pre and post-fire NBR using cloud free images within a certain date range. The date ranges selected for this analysis were 2017/01/01 to 2017/02/18 for pre-fire scenario and 2017/06/01 to 2017/07/18 for post fire scenarios which are most fire prevailing date ranges in Nepal. Similar analysis was done to measure burn severity to see the lasting effects of fire using the date range of 2017/01/01 to 2017/02/18 for pre-fire and 2018/01/01 to 2018/02/01 for post-fire. In Landsat image NBR is calculated using Landsat band 4 (NIR) and Landsat band 7 (SWIR). The resulting pre- and post-fire NBR mean composite images are then used to calculate differenced Normalized Burn Ratio (dNBR) (Equations (2)).

$$dNBR = \text{prefireNBR} - \text{postfireNBR} \dots\dots\dots \text{Equation (2)}$$

Same process was repeated with sentinel 2 A data where band 8 (NIR) and band 12 (SWIR) has been used for generating NBR value.

3.2 Classification of Severity Level

Google Earth Engine has a lot of classification algorithms that make use of its high-performance cloud computing architecture such as Classification and Regression Tree (CART), Random Forest (RF), Support Vector Machine (SVM). However, in this study we classified on the basis of dNBR value thresholds. Severity level of the study site has classified using seven severity thresholds prescribed by Key & Benson (2006) tabulated below. Then, the area under each class of dNBR under each forest type was computed.

SEVERITY LEVEL	dNBR Value (express in 10 ³)
Enhanced Regrowth, High	-500 to -251
Enhanced Regrowth, Low	-250 to -101
Unburned	-100 to +99
Low Severity	+100 to +269

Moderate-low Severity	+270 to +439
Moderate-high Severity	+440 to +659
High Severity	+660 to +1300

Table 1 Severity Level from Forest Fire

4 Results and Discussion

4.1 Severity Mapping

Fire severity map and burn severity map using Landsat 8 and Sentinel 2 were prepared separately in Google Earth Engine platform. The map is presented in figure 2, 3, 4 and 5.

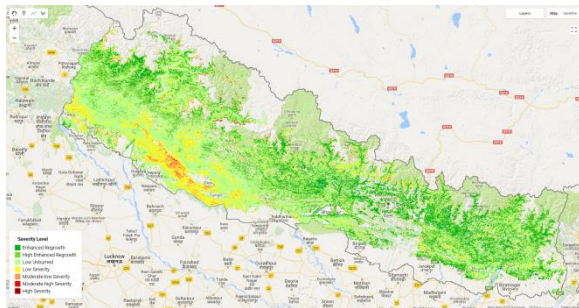


Figure 2 Fire Severity map using Landsat 8

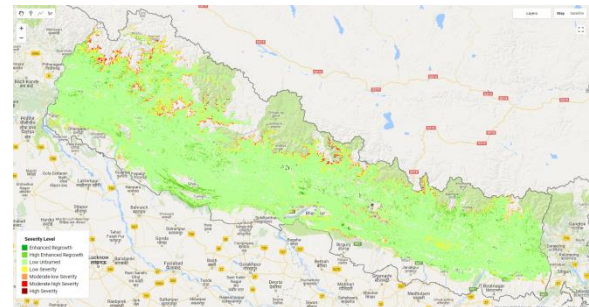


Figure 4 Burn Severity map using Landsat 8

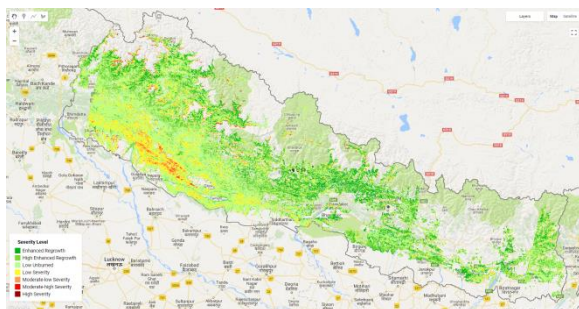


Figure 3 Fire Severity map using Sentinel 2

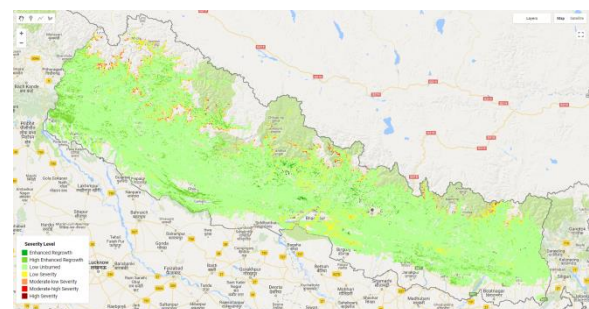


Figure 5 Burn Severity map using Sentinel 2

The above fire severity and burn severity map show the variability within severity class obtained from both Landsat 8 and Sentinel 2. It is clearly observed that severity did not reach up to maximum (Higher) severity in each and every case. Nepal forests have suffered most of the time from surface fire. Only limited crown fire has been observed in some conifer species such as Rani Salla (*Pinus roxburghi*), Gobre Salla (*Pinus wallichiana*), *Cupressus torulosa* and *Abies* species. Most of the forest fires in Nepal are human induced deliberate fire. In some of the cases, it has been out of control and cause more severity. There hasn't been observed wildfire due to lightning and higher severity in those inaccessible areas. Along with that climatic factors such as drought and temperatures are also not extreme in Nepal which also causes to raise severity into peaks or higher level.

4.2 Severity Classification

The histogram observation of dNBR values in each severity class show the normal distribution which provide the basis for classifying severity class and its further analysis within five classes. The area within each severity class due to fire severity and burn severity calculated from Landsat 8 imageries and Sentinel 2 are figured out below (figure 6 and 7).

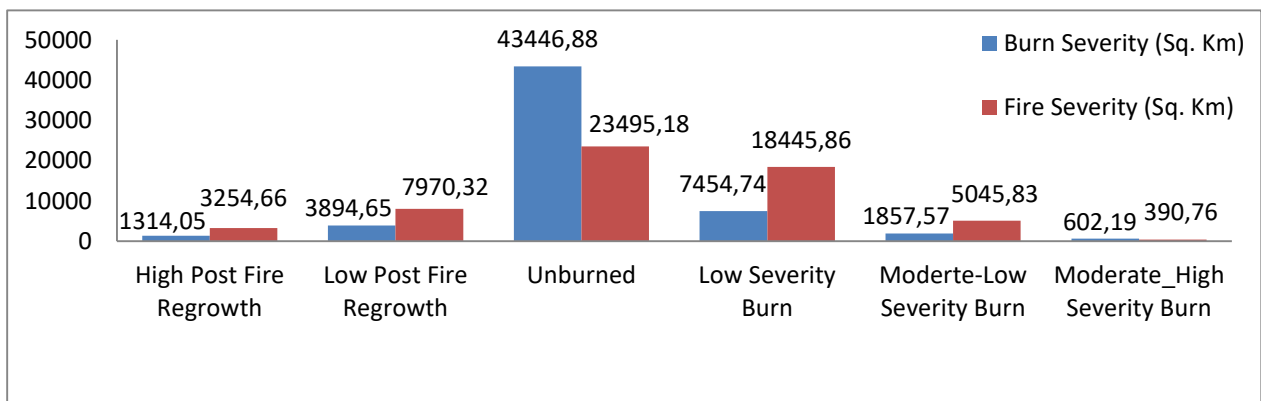


Figure 6 Fire and Burn Severity Level observation from Landsat 8

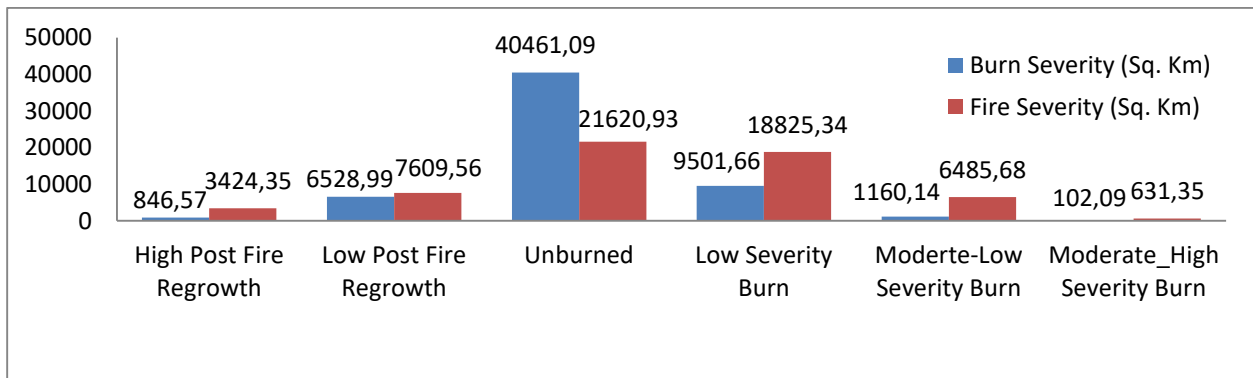


Figure 7 Fire and Burn Severity Level observation from Sentinel 2

Overall, burn severity is lower than fire severity obtained from both satellites imageries. Using Landsat 8 data forest area depicted under fire severity in low severity burn, moderately-low and moderately-high class are 18445.86 Sq. Km, 5045.83 Sq. Km and 390.76 Sq. Km which is drastically reduced in burn severity analysis to 3283.60, 371.15 and 80.77 Sq. Km, respectively. Similar result from sentinel was obtained. It has been observed that 25,942.37 Sq. Km forest area has been degraded from fire severities which is recovered in coming rainy season and remain to 10763.89 Sq. Km forest under degradation after extended assessment. Almost same type of result is found with Landsat 8 image with reduce in severity class.

From the above result, fire severity and burn severity analysis reflect that forests areas under different severity class are dramatically altered. The timing for fire severity and burn severity is the main cause behind such change in forest area in different severity class. For fire severity analysis we used the images just after the fire

or it is initial assessment. After fire severity season, rainy season come which help to recover those burnt area and enabling the environment for sprouting of new seedlings in those area in Nepal. Later on, during extended assessment burnt area effect in forest is low due to regrowth in burnt vegetation and newly appear vegetation which changes its spectral value and convert to unburned area from image analysis.

4.3 Fire and Burn Severity in each Forest Type

Forest Type	Severity Type	High Post Fire Regrowth	Low Post Fire Regrowth	Unburned	Low Severity Burn	Moderate-Low Severity Burn	Moderate High Severity Burn
TMH	FS	6.97	13.2	39.11	33.11	7.42	0.19
	BS	0.61	4.42	70.14	19.47	4.36	1.01
Sal	FS	6.58	13.61	40.79	29.89	8.78	0.36
	BS	0.74	3.78	67.57	19.80	6.41	1.70
LMH	FS	2.93	11.21	41.2	32.96	10.64	1.05
	BS	0.95	3.53	89.85	4.03	0.91	0.73
UMH	FS	5.47	15.78	40.26	29.47	8.32	0.7
	BS	5.60	14.09	67.46	9.89	2.12	0.83
Pinus Roxburghi (PR)	FS	3.41	10.8	40.32	37.77	7.06	0.64
	BS	2.01	4.80	88.85	3.92	0.30	0.11
Acacia catechu and Dalbergia sissoo	FS	13.64	26.99	38.48	16.93	3.65	0.32
	BS	1.38	6.89	77.74	12.83	0.99	0.17
Pinus wallichiana (PW)	FS	3.04	10.96	36.6	32.05	14.62	2.72
	BS	3.88	10.21	62.27	15.51	4.98	3.15
Quercus spp.	FS	7.72	17.3	42.08	26.91	5.74	0.26
	BS	4.73	8.50	77.96	7.41	1.14	0.26
Juglans wallichiana (JW)	FS	2.09	12.9	30.61	34.19	18.15	2.07
	BS	5.41	13.29	72.20	8.43	0.65	0.02
Tsuga dumosa (TD)	FS	0.56	2.97	19.2	39.01	35.08	3.18
	BS	0.62	3.40	71.23	16.20	5.35	3.20
Abies spectabilis and Abies pindrow	FS	3.47	14.87	45.35	28.52	7.1	0.69
	BS	4.00	11.32	50.66	22.80	8.53	2.69
Cupressus torulosa (CT)	FS	0.13	1.38	11.24	31.95	49.44	5.86
	BS	0.01	1.33	75.76	16.53	4.38	2.00
Cedrus deodara (CD)	FS	6.35	15.9	41.62	32.24	3.69	0.2
	BS	5.30	12.04	73.29	8.06	1.06	0.25
Betula utilis	FS	5.92	12.98	32.64	28.96	12.57	6.93
	BS	0.37	2.50	42.32	34.13	14.11	6.57
Picea smithiana	FS	9.64	17.47	40.71	27.31	4.78	0.1
	BS	2.83	5.04	75.65	14.49	1.77	0.22

Table 2 Fire and Burn Severity in each Forest Type using Landsat 8

Forest type wise fire severity and burn severity was calculated in Google Earth Engine Environment using Landsat 8 and Sentinel 2. Relative value (in percentage) of forest area under different severity class in 15 forest type of Nepal is tabulated below (2 and 3).

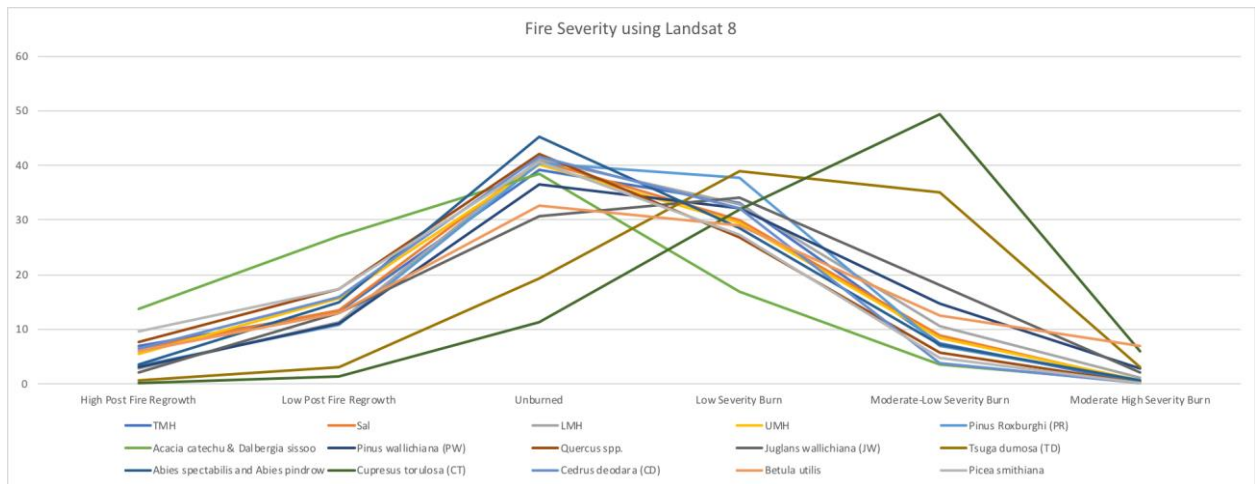


Figure 8 Fire Severity levels on different forest types obtained from Landsat 8

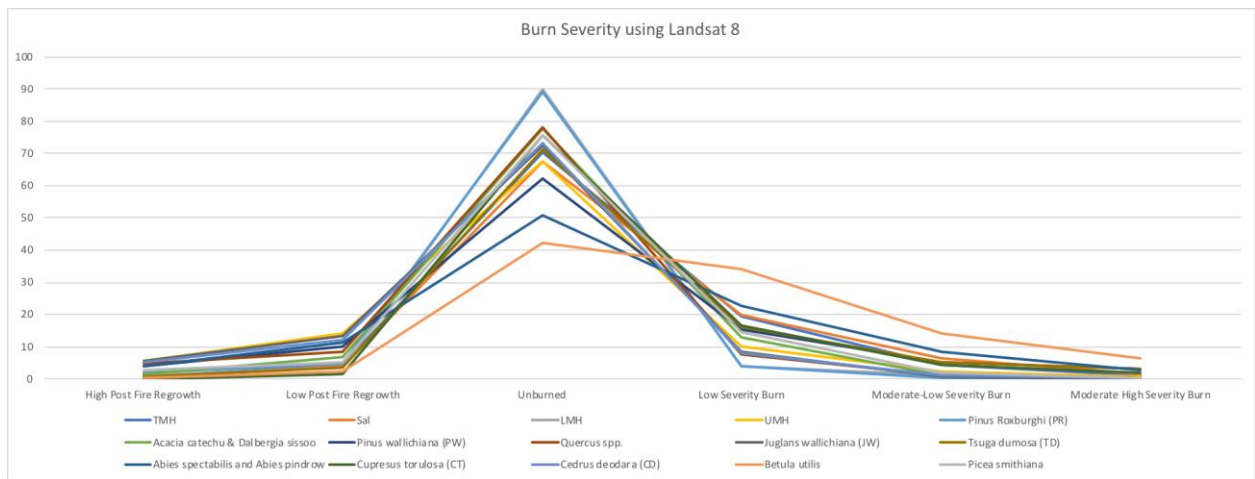


Figure 9 Burn Severity levels on different forest types obtained from Landsat 8

Fire Severity analysis with Landsat 8 shows that TMH, LMH, PR, PW, JW, TD, CT and CD forest type found that greater than 30 % forest area in low severity burn and TD forest Type show the highest level(39.01%) and Acacia catechu and Dalbergia sissoo forest have lowest burnt area percentage(16.93%) and remaining forest type within 20 to 30 % . Similarly, 49.44% forest area of CT has under moderate-low severity class followed by TD (35.08%) with lowest in Acacia catechu and Dalbergia sissoo forest. Whereas, Betula utilis shows highest forest area under moderate-high severity class, followed by CT, TD and PW.

Burn Severity analysis with Landsat 8 shows that Abies species and Betula utilis forest type have greater than 20 % forest area in low severity burn and Betula utilis show the highest level (34.13%) and PR forest have lowest burnt area percentage (3.92%). Similarly, Betula utilis forest type rank in highest forest type under moderate-low severity class followed by Abies species forest type (8.53%) with lowest in PR forest. Whereas, Betula utilis forest type shows highest forest area under moderate-high severity class, followed by TD and PW and so on.

Forest Type	Severity Type	High Post Fire Regrowth	Low Post Fire Regrowth	Unburned	Low Severity Burn	Moderate-Low Severity Burn	Moderate_High Severity Burn
Forest Type	FS	7.25	13.39	35.90	31.92	10.70	0.84

TMH	BS	1.25	9.55	64.37	22.28	2.41	0.14
	FS	8.70	14.35	36.21	29.93	10.02	0.78
Sal	BS	1.18	9.44	59.86	25.57	3.90	0.05
LMH	FS	3.20	10.06	36.44	34.38	14.00	1.93
	BS	2.02	10.87	73.74	12.36	0.95	0.06
UMH	FS	6.25	14.31	35.83	32.24	10.61	0.76
	BS	1.28	12.03	74.31	10.82	1.29	0.27
Pinus Roxburghi (PR)	FS	1.94	8.79	40.26	36.24	11.92	0.85
	BS	1.39	11.99	78.09	7.62	0.86	0.05
Acacia catechu and Dalbergia sissoo	FS	10.69	24.38	40.62	18.95	4.98	0.39
	BS	1.38	11.16	69.97	16.24	1.16	0.09
Pinus wallichiana (PW)	FS	4.04	10.81	37.20	34.93	12.01	1.01
	BS	1.36	13.32	67.31	15.44	2.26	0.30
Quercus spp.	FS	4.80	15.80	41.08	29.06	8.54	0.72
	BS	1.71	14.60	73.54	9.08	0.94	0.13
Juglans wallichiana	FS	5.31	14.52	34.97	31.18	11.85	2.17
	BS	0.91	7.57	71.26	18.86	1.32	0.08
Tsuga dumosa	FS	2.94	10.19	39.30	36.24	10.74	0.60
	BS	3.02	14.71	65.42	14.61	2.01	0.24
Abies spectabilis and Abies pindrow	FS	5.02	12.67	34.08	30.91	13.15	4.17
	BS	1.43	10.75	57.65	22.65	5.83	1.70
Cupressus torulosa	FS	1.35	6.41	36.91	41.47	13.15	0.70
	BS	2.40	16.59	65.98	13.77	1.17	0.10
Cedrus deodara	FS	5.14	14.26	46.44	29.14	4.82	0.20
	BS	3.47	23.70	68.91	3.45	0.42	0.05
Betula utilis	FS	10.24	15.80	31.38	25.74	11.07	5.76
	BS	0.57	13.84	57.90	18.97	6.12	2.59
Picea smithiana	FS	9.60	18.24	34.64	27.84	9.41	0.26
	BS	0.351	20.090	76.435	2.989	0.130	0.005

Table 3 Fire and Burn Severity in each Forest Type using Sentinel 2

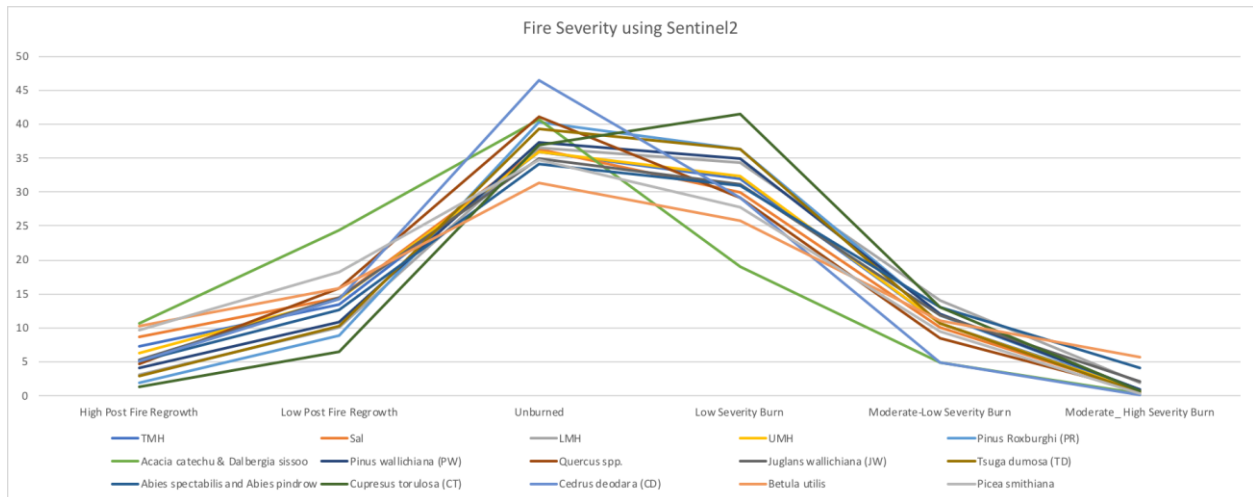


Figure 10 Fire Severity levels on different forest types obtained from Sentinel 2

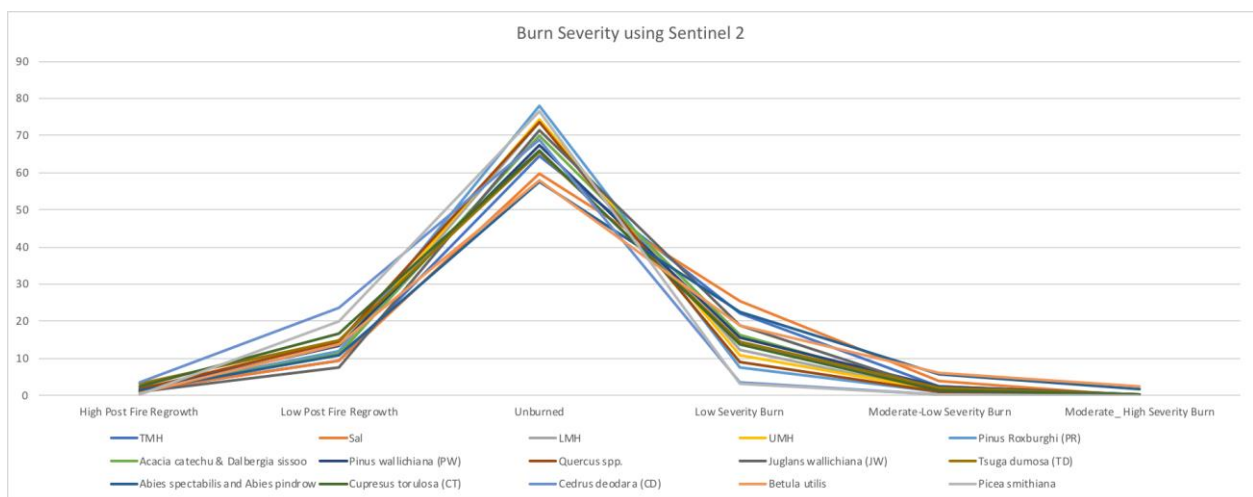


Figure 11 Burn Severity levels on different forest types obtained from Sentinel 2

Similarly, Fire Severity analysis with Sentinel 2 shows that TMH, LMH, PR, PW, JR, TD, Abies species and CT forest type show greater than 30 % forest area in low severity burn and CT forest under the highest level (41.47%) and Acacia catechu and Dalbergia sissoo forest forest have lowest burnt area percentage (18.95%) and remaining forest type within 20 to 30 % . LMH forest type is the highest rank in forest area percentage (14%) under moderate-low severity class and lowest in CD forest type (4.82%) and other remaining in between that range. Whereas, Betula utilis forest type shows highest forest area under moderate-high severity class, followed by Abies species and so on.

Burn Severity analysis with Landsat 8 shows that Sal, TMH and Abies forest type occupy greater than 20 % forest area in low severity burn and Sal forest Type show the highest level (25.57%) and Picea forest have lowest burnt area percentage (2.98%). Similarly, Betula utilis forest type rank in highest forest type with 6.12% under moderate-low severity class followed by Abies species forest type (5.83%) with lowest in Picea smithiana forest type. Whereas, Betula forest type shows highest forest area under moderate- high severity class, followed by Abies species and lowest in Picea smithiana.

The results obtained from Landsat 8 and Sentinel 2 was fairly consistent with each other. As seen on figures 8,9,10 and 11 the graphs for fire severity and burn severity on different types of forests seem similar. While there are some minor differences, one large difference on forest type CT can be observed between graphs 8 and 10. It is believed that this is because of the difference in cloud identification on Landsat 8 and Sentinel 2 products. Because of this more forest area on Sentinel 2 was masked than on Landsat 8.

Severity analysis from forest fire in Nepal using remote sensing burn indices depict that High Mountain and High Himal coniferous forest type are in higher severity than Tropical and Mid-hills broadleaved and conifers. Coniferous trees are on the verge of crown fire and fires were continued for several days in those areas and could not control due to inaccessible from human intervention. The grazers deliberately burned rangeland or grassland to obtain new sprout of grass. Furthermore, in windy and dry days those fires were spread to the nearby forest and destroy whole area which initiates forest degradation in those areas (<http://www.fao.org/docrep/006/AD653E/ad653e51.htm>). Similarly, most of the coniferous trees are more susceptible to fire due to resin contents.

In LMH and Sal forest type accumulated glabrous leaf litter along with naturally seedlings and other associated herbs and shrubs are the fuel source for burning. Trees in those forest types are highly fire resistant and more moisture content so that no crown fire seen in such tropical region which show high fire severity in those forest area and drastically reduces in burn severity analysis.

Among the High Mountain and High Himal conifer forests, *Cupressus torulosa* forest have highest severity rate. During Forest Resource Assessment anthropogenic disturbance analysis, *Cupressus torulosa* forests were found most disturbance forest type and 100% disturbance due to fire (DFRS, 2015). *Acacia catechu* and *Dalbergia sissoo* are riverine forest type and moderately fire resistant (Jackson, J.K. 1994) those characteristics reflect the lowest fire and burn severity among 15 forest types.

5 Conclusion

Google Earth Engine platform for cloud-based analysis of satellite imageries explore its potentiality to assess the driver of forest degradation due to fire. Burn severity indices derive from remote sensing methodology help to map fire and burn severity area as well as its magnitude in different forest type. From the analysis of Landsat 8 and Sentinel 2 derived severity due to fire reflects that Nepalese forests are in the verge of degradation. Forest fire is acting as one of the drivers of forest degradation which rate is highly fluctuating within different forest type in Nepal.

Field derived burn indices will help to validate the result of remote sensing based fire and burn severity. However, in this research we are not able to include field level severity data. Furthermore, generating of field based Composite Burn Index (CBI) or GeoCBI is inevitable to derive co-relation with remote sensing burn indices for estimation of carbon emission from forest fire in future.

6 References

- Bajracharya, K.M., no date. Fire Situation in Nepal. <http://www.fao.org/docrep/006/AD653E/ad653e51.htm> [Accessed 2018/08/16]
- Bowman, D.M.J.S. et al., 2009. Fire in the earth system. *Science*, 324(5926), pp.481–484.
- Brewer, C.K. et al., 2005. Classifying and Mapping Wildfire Severity. *Photogrammetric Engineering and Remote Sensing*, 71(11), pp.1311–1320.
- By, P. and Forests, M.O.F., 2014. NATIONAL BIODIVERSITY STRATEGY AND Government of Nepal. , (July).
- Cocke, A.E., Fulé, P.Z. and Crouse, J.E., 2005. Comparison of burn severity assessments using Differenced Normalized Burn Ratio and ground data. *International Journal of Wildland Fire*, 14(2), pp.189–198.
- DFRS, 2015. *State of Nepal's Forests*, Available at: www.dfrs.gov.np.
- Epting, J., Verbyla, D. and Sorbel, B., 2005. Evaluation of remotely sensed indices for assessing burn severity in interior Alaska using Landsat TM and ETM+. *Remote Sensing of Environment*, 96(3–4), pp.328–339.
- Escuin, S., Navarro, R. and Fernández, P., 2008. Fire severity assessment by using NBR (Normalized Burn Ratio) and NDVI (Normalized Difference Vegetation Index) derived from LANDSAT TM/ETM images. *International Journal of Remote Sensing*, 29(4), pp.1053–1073.

- Facility, T. & Team, M., 2018. Forest Carbon Partnership Facility (FCPF) Carbon Fund Emission Reductions Program Document (ER-PD) ER Program Name and Country : People and Forests - A Sustainable Forest Management-Based Emission Reduction Program in the Terai Arc Landscape , Nepal D. , .
- Falkowski, M.J. et al., 2005. Characterizing and mapping forest fire fuels using ASTER imagery and gradient modeling. , 217, pp.129–146.
- FAO, 2009. Towards Defining Forest Degradation : Comparative Analysis of Existing Definitions. Forest Resources Assessment Working Paper 154, October 2009.
- French A, N.H.F. et al., 2008. Using Landsat data to assess fire and burn severity in the North American boreal forest region: an overview and summary of results. *International Journal of Wildland Fire*, 17, pp.443–462.
- Gorelick, N. et al., 2017. Google Earth Engine: Planetary-scale geospatial analysis for everyone. *Remote Sensing of Environment*, 202, pp.18–27.
- Hudak, A. et al., 2006. Characterizing Stand- Replacing Harvest and Fire Disturbance Patches in a Forested Landscape. *Understanding Forest Disturbance and Spatial Pattern*, (May 2014), pp.209–231.
- Jackson, J.K. 1994. Manual of afforestation in Nepal. Kathmandu: Forest Research and Survey Centre. 2nd edition
- Jakubauskas, M.E., Lulla, K.P. and Mausel, P.W., 1990. Assessment of vegetation change in a fire-altered forest landscape. *Photogrammetric Engineering and Remote Sensing*, 56(3), pp.371–377.
- Key, C.H. & Benson, N.C., 2006. Landscape assessment: ground measure of severity, the composite burn index; and remote sensing of severity, the normalized burn ratio. *FIREMON: Fire effects monitoring and inventory system. Gen. Tech. Rpt. RMRS-GTR-164-CD: LAI-15*, (April 2018), p.51.
- Key, C.H. & Benson, N.C., 2006. Landscape assessment: Sampling and analysis methods. *USDA Forest Service General Technical Report RMRS-GTR-164-CD*, (June), pp.1–55.
- Khanal, S., 2015. Wildfire trends in Nepal based on MODIS burnt-area data. *Banko Janakari*, 25(1), p.76. Available at: <http://www.nepjol.info/index.php/BANKO/article/view/13477>.
- Kissinger, G., Herold, M. and De Sy, V., 2002. Drivers of deforestation and forest degradation: A Synthesis Report for REDD+ Policymake. *Kissinger, G Herold, M De Sy, Veronique*, pp.1–46.
- Landmann, T., 2003. <Characterizing sub-pixel Landsat ETM + fire severity on experimental fires in the Kruger National Park, South Africa_Landmann_South African Journal of Science_2003.pdf>. *South African Journal of Science*, 99(7/8), pp.357–360.
- Lentile, L.B. et al., 2006. Remote sensing techniques to assess active fire characteristics and post-fire effects. *International Journal of Wildland Fire*, 15(3), pp.319–345.
- Matin, M. et al., 2017. Understanding forest fire patterns and risk in Nepal using remote sensing , geographic information system and historical fire data. pp.276–286.
- Miller, J.D. & Yool, S.R., 2002. Mapping forest post-fire canopy consumption in several overstory types using multi-temporal Landsat TM and ETM data. *Remote Sensing of Environment*, 82(2–3), pp.481–496.
- Mitchell, A.L., Rosenqvist, A. and Mora, B., 2017. Current remote sensing approaches to monitoring forest degradation in support of countries measurement, reporting and verification (MRV) systems for REDD+. *Carbon Balance and Management*, 12(1).
- Morgan, P. et al., 2014. Challenges of assessing fire and burn severity using field measures, remote sensing and modelling. *International Journal of Wildland Fire*, 23(8), pp.1045–1060.
- Parajuli, A. et al., 2015. Spatial and temporal distribution of forest fires in Nepal. , (September), pp.7–11.
- Rogan, J., 2001. Mapping re-induced vegetation depletion in the Peloncillo Mountains , Arizona and New Mexico. , 22(16), pp.3101–3121.
- Roy, M. et al., 2006. Genetic inactivation of melanin-concentrating hormone receptor subtype I (MCHRI) in mice exerts anxiolytic-like behavioral effects. *Neuropsychopharmacology*, 31(1), pp.112–120.
- Smith, A.M.S. et al., 2005. Testing the potential of multi-spectral remote sensing for retrospectively estimating fire severity in African Savannas. *Remote Sensing of Environment*, 97(1), pp.92–115.

- Van Wagtendonk, J.W., Root, R.R. and Key, C.H., 2004. Comparison of AVIRIS and Landsat ETM+ detection capabilities for burn severity. *Remote Sensing of Environment*, 92(3), pp.397–408.
- White, J.D. et al., 1996. Remote Sensing of Forest Fire Severity and Vegetation Recovery. *Int. J. Wildland Fire*, 6(3), pp.125–136.

Concept for High-resolution Aerosol Monitoring using Satellite Imagery and Sensor Networks in Stuttgart City

J. Gitahi^a, M. Hahn^a

^a Department of Geomatics, Computer Science and Mathematics, University of Applied Sciences Stuttgart – Schellingstraße 24, D-70174 Stuttgart (Germany), - joseph.gitahi@hft-stuttgart.de, michael.hahn@hft-stuttgart.de

KEY WORDS: Urban Air Quality, Aerosol Optical Depth, Sentinel -2, Sentinel -3

ABSTRACT:

Satellite remote sensing aerosol monitoring products are readily available but limited to regional and global scales. The low spatial resolution makes them unsuitable for city-level monitoring of aerosol concentrations and pollution sources. Freely available satellite images such as Sentinel -2 at relatively high spatial (10m) and temporal (5 days) resolutions offer the chance to map aerosol distribution at local scales. The main goal of the study is to produce high spatial and temporal resolution maps that accurately depict air quality in Stuttgart City. In this paper we examine existing satellite, ground-based aerosol datasets, and Aerosol Optical Depth/Thickness (AOD/AOT) retrieval algorithms which will form the basis of our study project. In the first step, AOD retrieval algorithms will be applied to Landsat 8 (30m) and Sentinel -2 (10m,20m and 60m) satellite images. The AOD results will be evaluated using groundtruth measurements from AERONET stations. The second step will be examining the relationships between satellite retrieved AOD and ground Particulate Matter (PM) measurements. Two sets of ground sensor networks in the study area will be used in this step, the highly accurate but sparsely distributed stations from the local environmental agency and low-cost air quality sensors from a citizen science project that form a dense network but with lower accuracies. In this paper, we look into the various AOD retrieval methods, available air quality datasets and design a workflow for high-resolution mapping of aerosol.

1 Introduction

Aerosols are a mixture of solid and liquid particles of organic and inorganic substances suspended in the atmosphere. Their sources include dust, pollen, forest fires, sea salt, emissions from transport and industrial fuel combustion. Subtypes of atmospheric particles, the particulate matter (PM), are under criticism for their adverse effects on human health. They are often classified as PM₁₀ and PM_{2.5} for particles with a diameter of less than or equal to 10µm and 2.5µm respectively. The study of their concentration in the atmosphere is important due to the role they play in Earth's climate and their adverse effects on human health. In the atmosphere, the particles can either absorb or scatter sunlight affecting Earth's energy budget. Health effects include damage to respiratory and cardiovascular systems with PM_{2.5} posing higher risks owing to their smaller size. The risk is higher in urban regions where an estimated 55% of the World's population live (United Nations, 2019) which is as a result of higher anthropogenic aerosols emissions from transport, industries, power plants and household sources. To reduce the effects on human health, WHO (2006) provides a set of air quality guidelines aimed at reducing the concentration and identifies daily and annual thresholds below which adverse effects do not occur. For PM_{2.5}, a 24-hour mean of 25µg/m³ and an annual mean of 10 µg/m³; for PM₁₀ a 24-hour mean of 50 µg/m³ and an annual mean of 20 µg/m³.

Satellite remote sensing has been used to determine the aerosol concentration in the atmosphere based on the inversion of radiative transfer (RT) equations which model the scattering and absorption of solar radiation by aerosols, gas and water molecules in the atmosphere. The retrieval of columnar aerosol optical depth/thickness (AOD/AOT) forms a crucial step in the atmospheric correction of satellite images to generate surface reflectance products. By using the top-of-atmosphere (TOA) reflectance received by the satellite sensors and known surface reflectances/ bottom-of-atmosphere (BOA), the optical thickness of the atmosphere can be determined. The RT equations generate Look-up-Tables (LUT) which model the relationship between TOA reflectances and AOD in the required electromagnetic spectrum range. TOA reflectances follow the RT equation as expressed in Equation 1.

$$\rho_{TOA} = \rho_{ATM} + \frac{T_{Atm}(z_{Sun}) \cdot T_{Atm}(z_{Sat}) \cdot \rho_{Surf}}{(1 - \rho_{Surf} \cdot R_{HemAtm})} \quad (1)$$

Where ρ_{TOA} is the TOA reflectance, ρ_{ATM} is the atmospheric reflectance, ρ_{Surf} is the surface reflectance, R_{HemAtm} is the hemispheric albedo of the atmosphere, $T_{Atm}(z_{Sun})$ and $T_{Atm}(z_{Sat})$ are transmissions of the atmosphere for sun z_{Sun} and satellite z_{Sat} zenith distances respectively.

AOD is then obtained by subtracting Rayleigh scattering and gaseous absorption influences from the total optical thickness of the atmosphere as shown in Equation 2.

$$\delta_{Aer}(\lambda) = \delta(\lambda) - \delta_{Gas}(\lambda) - \delta_{Ray}(\lambda) \quad (2)$$

Where δ is the optical thickness of the atmosphere at wavelength λ , $\delta_{Aer}(\lambda)$ the AOD, $\delta_{Gas}(\lambda)$ the optical thickness of gaseous absorbers and $\delta_{Ray}(\lambda)$ the optical thickness of Rayleigh Scattering.

One of the algorithms used to estimate AOD is the Dark Object Subtraction (DOS) or Dark Target (DT) method which relies on the presence of dark pixels in an image. For these dark pixels of zero or minimal surface reflectance, TOA reflectances received are a result of atmospheric reflectances $\rho_{TOA} = \rho_{ATM}$. The estimated atmospheric reflectance is subtracted from the entire image scene to calculate the surface reflectance and used in RT models to retrieve the AOD. The assumption of this method is that dark pixels of known reflectances are found in an image scene and that the atmosphere is spatially uniform over the image.

The second approach is the multispectral method which relies on the known constant spectral properties of dark dense vegetation (DDV) in the electromagnetic spectrum (Kaufman and Sendra, 1988; Kaufman *et al.*, 1997). It uses the empirical relationships between surface reflectances in the blue and red bands with the SWIR band $\rho_{Blue} = 0.5 * \rho_{SWIR}$ and $d = 0.25 * \rho_{SWIR}$. This is based on the spectral properties of healthy vegetation where chlorophyll strongly absorbs light at blue and red bands and the moisture content absorption peaks in the SWIR band. The DDV algorithm has been used extensively to retrieve AOD over land surfaces with high precision from images acquired by Moderate Resolution Imaging Spectrometer (MODIS) on board Terra and Aqua satellites. The assumptions of this method are that pixels with low BOA reflectances in the visible spectrum are present such as dark vegetation or water bodies and that the ratio between BOA reflectances at different wavelengths is constant (Gillingham *et al.*, 2012). The application of this approach for AOD retrievals is limited over brighter surfaces and arid regions which have sparse or no vegetation. This approach is also limited by locational, seasonal and angular dependence of visible and SWIR bands surface ratios (Hagolle *et al.*, 2015). Deep Blue (DB) algorithm is used for AOD retrievals over brighter surfaces especially arid and semi-arid regions where there are no dark pixels for the DDV method. In MODIS, this algorithm uses the 412nm band also referred to as the “deep blue” band in which aerosols appear bright and surfaces darker unlike in visible bands where the contrast between aerosols and the surfaces is not easily distinguishable.

AOD can also be retrieved using the multi-temporal method which is based on the assumption that land surfaces change slowly over time and remain relatively constant especially with short satellite revisit times and a constant viewing angles. The changes in reflectances observed from one image to another of the same scene can thus be attributed to the atmospheric aerosols which vary rapidly over time. Based on these assumptions, the approach is less accurate for satellites with longer revisit times and when vegetation in a scene changes rapidly in between acquisitions. The method’s sensitivity to aerosols variation also decreases and the error increases with increasing surfaces reflectances

1.1 Study Area

In the city of Stuttgart, air pollution levels have in the past exceeded the thresholds set by WHO which can be attributed to the high traffic and industrial activities (Osterath, 2016; Nair, 2017). Geographically, the city is located in a valley basin surrounded by mountains which inhibit airflow and further worsen the air quality situation.

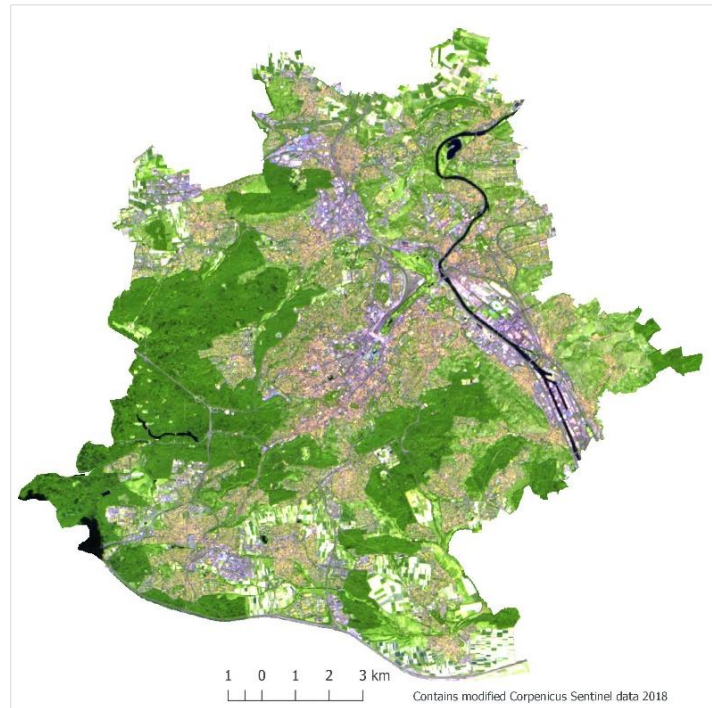


Figure 1: False-colour (urban) Sentinel-2 satellite image of Stuttgart city region acquired on 31st July 2018

2 Datasets

2.1 Satellite products

2.1.1 Moderate Resolution Imaging Spectroradiometer (MODIS) Aerosol Products

National Aeronautics and Space Administration's (NASA) MODIS instrument monitors aerosols and their properties over cloud, snow and ice-free land and ocean surfaces. Two instruments are onboard Terra and Aqua satellites and have been collecting data since 2000 and 2002 respectively. They provide high radiometric sensitivity in 36 spectral bands from 0.4 μm to 14.4 μm , a temporal resolution of 1 to 2 days, and varying spatial resolutions of 250m, 500m and 1000m.

Different algorithms are applied to extract AOD over land, oceanic and inland water bodies. These are: Deep Blue (DB) and Dark Target (DT) Land over land surfaces while DT Ocean is applied over oceanic and inland water bodies (Levy *et al.*, 2013). The DT and DB algorithms use dark or darker surfaces to estimate the atmosphere's contribution to TOA radiances but differ in the way they account for surface reflectance. The DT algorithm uses dark surfaces in two visible channels 0.47 and 0.66 μm and the approximate transparency of the atmosphere at 2.12 μm to obtain an accurate estimation of the atmospheric scattering. This works best over dark vegetation and does not work well over bright land surfaces. The DB algorithm calculates the AOD by using darker surfaces in two blue channels 0.412 and 0.470 μm and little absorption by dust in a red channel 0.670 μm . This works best over bright land surfaces but can also retrieve aerosols over vegetation. The main product of the algorithms is AOD at a wavelength of 550nm namely MOD04. Additional information includes single scattering albedo, aerosol size and quality assurance information. The AOD is produced at a resolution of 10 km X 10 km at nadir for both DT and DB, and an additional 3 km X 3 km resolution for DT Land and Ocean algorithms.

2.1.2 Sentinel Aerosol Products

The Sentinels are part of the European Space Agency's (ESA) earth observation mission, Copernicus Programme, with each mission serving different operational needs. AOD products are derived as the main product of Sentinel-5P and by-products of processing algorithms for Sentinel-2 and Sentinel-3 missions.

Sentinel -5P provides global information on atmospheric trace gases, aerosols and cloud distributions affecting air quality and climate globally on a daily basis. The mission is a gap filler for atmospheric products between SCIAMACHY/Envisat which ended in April 2012, the OMI/AURA mission and the future SENTINEL-5 and SENTINEL-4 missions. The Tropospheric Monitoring Instrument (Tropomi) onboard covers bands in ultraviolet and visible (270–495 nm), near-infrared (675–775 nm) and shortwave infrared (2305–2385 nm) at a spatial resolution of 7 km x 3.5 km.

In Sentinel -2, Level-2A processing is applied to TOA Level-1C orthoimages to produce Bottom-Of-Atmosphere (BOA) corrected reflectance product. The additional outputs include AOD, water vapour and scene classification maps together with associated quality indicators. Each of the products is available at 10m, 20m and 60m spatial resolution and a temporal resolution of 5 days from the two Sentinel -2. The AOD is derived using the Dense Dark vegetation (DDV) algorithm which requires an image scene to contain DDV or water bodies whose surface reflectance is known. The algorithm assumes the vegetation is sufficiently dark and that the ratio between BOA reflectances at different wavelengths is constant. In the absence of dark vegetation or soil, an incremental threshold in the Shortwave Infrared (SWIR) 2190nm band is applied to identify reference areas with medium brightness.

Sentinel -3 mission's main objective is measuring sea-surface topography, sea and land surface temperature, and land and ocean surface colour for ocean forecasting systems, environmental and climate monitoring. Onboard the mission's two satellites are Ocean and Land Color Instrument (OLCI) and Sea and Land Surface Temperature Radiometer (SLSTR). The Sentinel-3 SYN AOD at 300m spatial resolution is one of the synergy products derived from the OLCI and SLSTR sensors. The Sentinel -3 SYN algorithm used to estimate aerosols and surface reflectances uses a synergistic approach to retrieve AOD by combining DOS and multi-view-angle (MVA) methods (North and Heckel, 2010). The DOS method is used for single view AOD retrievals using a correlation of BOA reflectances from known surfaces of dark vegetation and water bodies. Dark pixels are identified by calculating the Normalized Difference Vegetation Index (NDVI) using reflectances in the infrared band (870nm) and the red band (670) Equation 3.

$$NDVI = \frac{\rho_{870} - \rho_{670}}{\rho_{870} + \rho_{670}} \quad (3)$$

The multi-view-angle method assumes a constant angular variation of BOA reflectances across a wavelength which is as a result of Bidirectional Reflectance Distribution Function (BRDF). For the SLSTR sensor, the ratio of BOA reflectances at nadir and off-nadir viewing angles is well correlated between bands. The advantage of this approach over the DOS is that it does not require prior information of BOA reflectances.

2.1.3 Copernicus Atmosphere Monitoring Service (CAMS)

CAMS provides global monitoring and forecasting information on air quality and atmospheric composition with near-real-time analysis and 4-day forecasts (CAMS, 2018). The service uses a combination of satellite and ground-based observations to model the atmospheric conditions. In Europe, a regional model based on seven numerical air quality models by calculating the median outputs of individual models has been developed to provide better estimates of the air quality. The model known as CAMS regional Ensemble has a temporal resolution of one hour, a spatial resolution of 0.1° (7.9km horizontal resolution in the study area) and a vertical resolution of eight levels from the surface to 5000m. The pollutants monitored include O₃, CO, NO₂, SO₂, PM₁₀, PM_{2.5}, birch pollen, grass pollen, olive pollen, PANS, NMVOC, NH₃, NO.

2.2 Ground-based products

Air quality data products are also available from ground-based measuring instruments. The state institute for the environment, Landesanstalt für Umwelt Baden-Württemberg (LUBW, 2018), has a network of monitoring stations in Baden-Württemberg with eight of the stations in the Stuttgart city region. The pollutants measured are benzene, CO, CO₂, O₃, SO₂, NO, NO₂, air pressure, temperature, wind speed, wind direction, PM₁₀ Gravimetry, PM_{2.5} Gravimetry and PM₁₀ Photometry. The PM₁₀ Photometry which is available in real-time is used to only provide timely information to the public while PM gravimetric measurement results are more accurate and available after 10 days. The major issues with the stations are their sparse distribution in the study area and data gaps in some of the measuring stations.

The other set of ground measurements is from the OK Lab Stuttgart citizen science project with a network of around 300 low-cost sensors measuring PM₁₀ and PM_{2.5} (OK Lab Stuttgart, 2018). The sensors upload PM measurements every two and a half minutes to a portal which offers free and open data access. The sensors complement the sparsely distributed LUBW stations and provide relative information about the air quality for civic engagement in air pollution monitoring and control, however, they are not used for regulatory purposes. They suffer from uncertainties in the measured data quality which needs to be addressed to ensure that realistic and indicative measurements are obtained.

The AERONET (Aerosol RObotic NETwork) project established by NASA consists of a global network of sun photometers measuring AOD and aerosol properties and includes stations from national agencies, institutes, universities, individual scientists, and partners. Aerosol measurements and properties from AERONET stations are used for validation and calibration of AOD retrieval algorithms. However, these stations are sparsely distributed globally and hence the need for satellite retrieved AOD for better coverage. Since there is no AERONET station in the study area, aerosol properties will be obtained from LUBW stations and MODIS instrument. Compared to ground-based aerosol monitoring sensors, satellite remote sensing has inherent advantages since the spatial coverage is nearly continuous over large extents and provides high spatial resolution data. However, the sparsely distributed ground-based sensors like AERONET provide the most accurate AOD measurements and are thus considered as ground truth.

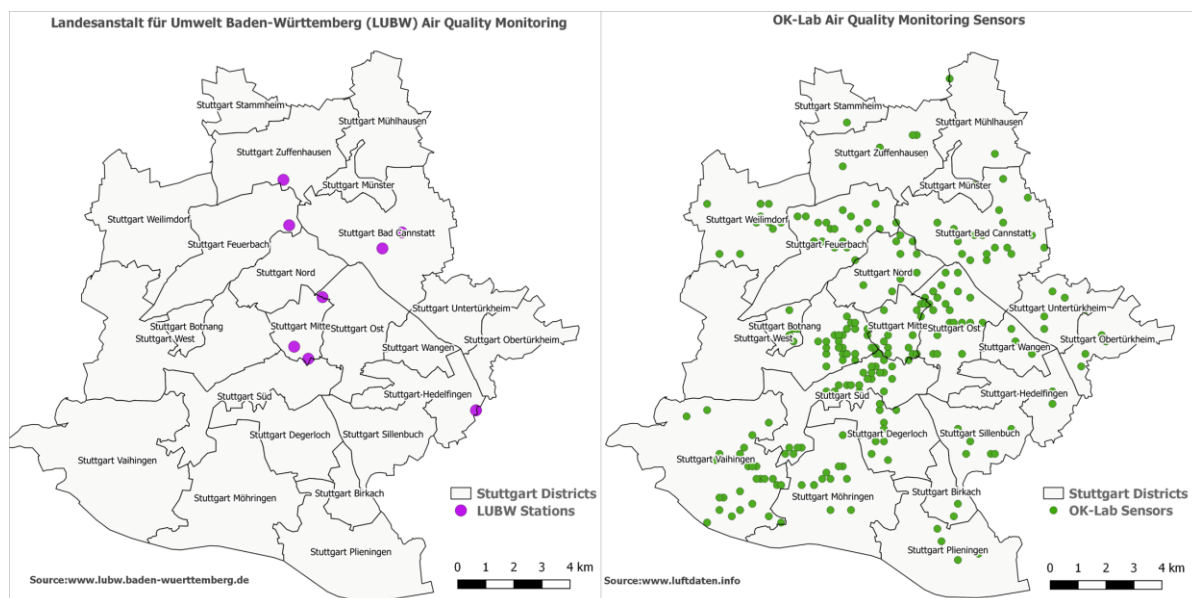


Figure 2: LUBW and OK Lab Stuttgart air quality sensors

3 AOD Retrieval Algorithms

3.1 Sen2Cor

ESA's Copernicus programme provides Sentinel -2 images either as TOA Level-1C or BOA Level-2A products. For the Level-1C products, Sen2Cor processor is freely available for users to perform single-date atmospheric corrections. AOD, water vapour and scene classification bands are created as by-products of the correction process. The by-products are also available readily in Level-2A products. The tool is available either as a standalone or a plugin to ESA's Sentinel Application Platform (SNAP) software. AOD is derived at 550nm using the DDV algorithm based on the SWIR (band 12) and the visible bands red (band 4) and blue (band 2). It requires the presence of dark vegetation, dark soils or water surfaces in an image scene. In the absence of dark pixels, atmospheric correction is performed with a constant AOD specified by a start visibility value at 40km corresponding to an AOD of 0.2 at sea level (Richter *et al.*, 2011; Louis *et al.*, 2016; Main-Knorn *et al.*, 2017).

3.2 MACCS-ATCOR Joint Algorithm (MAJA)

MAJA is an atmospheric correction algorithm combining modules from Multi-Temporal Atmospheric Correction and Cloud Screening (MACCS) developed by CNES and CESBIO and Atmospheric Correction (ATCOR) by DLR (Hagolle *et al.*, 2015). The algorithm, applicable to Landsat -8, Sentinel -2, VENμS and Formosat-2 satellite images, employs different techniques to estimate aerosols for the atmospheric correction process. Using the multi-temporal method, for two consecutive cloud-free satellite observations at dates D and D_T , the algorithm searches for AODs of both dates that minimize the squared differences between the corrected surface reflectances Equation 6.

The setback to this method is that the accuracy is reduced when the AOD is nearly similar for both dates making it impossible to retrieve an absolute AOD value. To improve the AOD retrievals in this scenario, the present image is compared to a reference image from an older iteration of the algorithm in Equation 7. A cost function Equation 4 which is a sum of Equations 6 and 7 errors, and a Levenberg–Marquardt non-linear least mean squares (LMS) algorithm searches for the AOD of D and D_T that minimizes the error.

$$cost_{MT} = \sum_{validpixels} err_{MT}^2 \quad (4)$$

Where:

$$err_{MT}^2 = (K_1^2 err_1^2 + K_2^2 err_2^2) \quad (5)$$

$$err_1 = at_{cor}(\rho_{TOA}(D), \tau) - at_{cor}(\rho_{TOA}(D_T), \tau_T) \quad (6)$$

$$err_2 = at_{cor}(\rho_{TOA}(D), \tau) - (\rho_{Surf}(D_T)) \quad (7)$$

Where at_{cor} is the atmospheric correction function linking TOA reflectances to their corresponding BOA reflectances for a given AOD τ and aerosol model, $\rho_{Surf}(D_T)$ is BOA reflectance from the reference image. The reflectances used in the cost function are from the blue band range which has a lower temporal variation. K_1 and K_2 weight the contribution of err_1 and err_2 where K_2 is set to one and K_1 is proportional to the mean value of the difference of TOA reflectances from dates D and D_T .

The second technique used is the multispectral method which is based on the DDV approach but relying on blue-red bands relationships instead of the visible /SWIR relationships. This adapted method seeks to address issues affecting the DDV approach which are locational, seasonal and angular dependences of visible/SWIR surface ratio. Due to the errors observed when SWIR band is used, the algorithm uses a more robust blue-red relationship which is established for each of the satellite sensors applicable to diverse locations and seasons Equation 8.

$$\rho_{blue}^{surf} = C * \rho_{red}^{surf} \quad (8)$$

Where: C is the blue-red coefficient. For Sentinel -2 $C = 0.45$, B1 is used as the blue band and B4 is the red band.

Since only one equation is used, retrieving both the AOD and the aerosol model is not possible and a constant aerosol model for any given location has to be used. This assumption of a constant aerosol model introduces atmospheric correction errors. MAJA's multispectral method uses a cost function in Equation 9 by summing up the squares of differences between blue surface reflectances after atmospheric correction and the blue surface reflectances predicted from the red band.

$$cost_{MS} = \sum_{validpixels} K^2 \times err_{MS}^2 \quad (9)$$

Where:

$$err_{MS}^2 = at_{cor}(\rho_{blue}^{TOA}(D), \tau) - (A \times at_{cor}(\rho_{red}^{TOA}(D), \tau) + B) \quad (10)$$

Where the weight K is equal to the NDVI to account for better correlation of the blue-red relationship for high NDVI, A and B are gains linking the blue and red BOA reflectances for a particular satellite sensor.

The algorithm uses a third technique which combines the multi-temporal and multispectral algorithms and relies on minimizing the cost function using the LMS algorithm. The cost function combines the multitemporal and multispectral Equations 5 and 10 respectively shown in Equation 11.

$$cost = \sum_{MTvalidpixels} K_{MT}^2 err_{MT}^2 + \sum_{MSvalidpixels} K_{MS}^2 err_{MS}^2 \quad (11)$$

Where K_{MT} and K_{MS} are weighting coefficients for the contribution of the multitemporal and multispectral methods. K_{MT} takes into account the time interval between two consecutive images, whose increase leads to decreased AOD retrieval accuracy due to surfaces changing over time.

For the three approaches, two constraints, a lower and an upper boundary, are applied to limit errors in AOD estimates. The lower boundary being that AOD cannot be negative and the upper boundary estimated using the Dark Object Subtraction (DOS) method. For AOD retrieval, clear pixels with the minimum reflectance in the blue band are selected and checked in previous images to avoid undetected cloud shadows. The two bounds obtained are then added to the cost function. To address the need for constant viewing angles, directional correction is performed in the multi-temporal approach to enable merging a time series of images acquired from different orbits which sometimes is the case with overlapping Sentinel-2 images. This also helps in densifying the time-series. Finally, interpolation of missing AOD retrievals due to masked pixels and smoothing of the image is done to deliver the final output.

3.3 iCOR

iCOR is an atmospheric correction algorithm for both land and water developed by Vlaams Instituut voor Technologisch Onderzoek (VITO) Remote Sensing Unit provided freely as a SNAP plugin for Landsat-8 and Sentinel-2 data (Keukelaere *et al.*, 2018). AOD is retrieved using the method by (Guanter *et al.*, 2005) which is then used as an input to the MODTRAN5 radiative transfer equation used for correcting atmospheric effects. The first step in correcting Sentinel-2 images is water and cloud pixels masking performed using a single band (NIR B8) thresholding for water and multiple threshold levels for the cloud pixels. The algorithm also takes advantage of the present SWIR-Cirrus band (B10) to improve detection of cirrus clouds. The TOA scene is then partitioned into 15 x 15km tiles which are assumed to include high spectral variation and atmospherically homogeneous.

In each of the tiles, the lowest radiance value for each band is selected as the dark target spectrum and the approximate path radiance retrieved using pre-calculated MODTRAN5 look-up-table (LUT). The AOD value leading to the path radiance closest to the dark spectrum is considered the upper boundary for the specific tile. Five reference pixels with high spectral contrast are selected based on their NDVI values from TOA reflectances and used in the next step to refine the estimated AOD through an endmember inversion technique. The technique models surface reflectance of the five pixels as a linear combination of two predefined pure green vegetation and bare soil spectra that act as artificial endmembers Equation 12.

$$\rho_s = C_v * \rho_{veg} + C_s * \rho_{soil} \quad (12)$$

Where: $\rho_s, \rho_{veg}, \rho_{soil}$ are surface reflectances of reference pixels, predefined vegetation and soil spectra, C_v and C_s are independent coefficients weighting vegetation and soil proportions C_v and C_s are free in the inversion resulting in 11 parameters as degrees of freedom; two parameters for each of the five pixels and AOD. The inversion is performed through the minimization of the Merit function δ^2 Equation 13 (Guanter Palomar, 2007).

$$\delta^2 = \sum_1^N \omega_{pix} \sum_{\lambda_i} \frac{1}{\lambda_i^2} [L_{pix,\lambda_i}^{SIM} - L_{pix,\lambda_i}^{SENS}]^2 \quad (13)$$

Where: L^{SIM} is simulated TOA radiance from MODTRAN5 LUT, L^{SENS} is measured TOA radiance, λ_i is centre wavelength of the i -th band and ω_{pix} is weighting factor (2.0 for pure vegetation, 1.5 for mixed and 1.0 for pure soil pixels)

The AOD value leading to the minimum δ^2 value in the inversion is selected for the cell. The last steps in the retrieval process are an interpolation of the missing pixels due to cloud masking and smoothing of the mosaiced tiles. The iCOR algorithm avoids the need for dark targets making it less restrictive than the DDV approach.

3.4 Simplified high-resolution MODIS Aerosol Retrieval Algorithm (SARA)

The low spatial resolution of MODIS MOD04 AOD products limit the application to regional and global scales and is not suitable for urban areas. To overcome this, Bilal *et al.* (2013) came up with a Simplified high-resolution MODIS Aerosol Retrieval Algorithm (SARA) to retrieve AOD over mixed surfaces at 500m resolution over the Hong Kong area. The algorithm achieves this without using a LUT but instead uses aerosol properties from an AERONET station and MODIS products for the RTM calculations. The inputs from the AERONET station are single scattering albedo (SSA) and asymmetric factor. From MODIS, the TOA reflectances are calculated from MOD02HKM, solar and view angles obtained from MOD03 and MOD09GA are used to retrieve surface reflectances.

SARA achieves improved mapping of the aerosol concentration at a higher resolution than MOD04 AOD product at 10km spatial resolution. The retrieved AOD demonstrated high consistency with AERONET ground-based measurements ($R^2 = 0.964$) and better identifies pollution sources in both urban and rural regions.

4 The concept for High-resolution Aerosol Monitoring

In the first step, the AOD retrieval algorithms described in section 3 will be applied to Sentinel -2 and Landsat -8 imagery of the study area. To evaluate their accuracy and consistency, the satellite retrieved AOD will be compared with the AERONET AOD which is more accurate and considered as groundtruth. Statistical analysis will be used to evaluate the spatial-temporal consistency of the different algorithms.

In the next step the PM ground measurements will be analyzed independently before using them to model AOD-PM relationships. The first PM dataset, which is from the highly accurate and reliable air quality monitoring stations from LUBW, will be interpolated for complete coverage of the study area. Due to the few stations, interpolation techniques will be evaluated to find the most suitable taking into account their spatial distribution and the geography of the study region. The crowd-sourced PM measurements from Stuttgart OK-Lab citizen science project will however, require more processing to determine the reliability of the measurements and filter out outliers. Different techniques such as timeseries analysis, calibration and collocation with reference LUBW stations will be employed. Since their distribution is dense and growing daily, the interpolation technique for these sensors will be different from the former. CAMS which provides PM estimates for different vertical levels will also be used in evaluating the performance of these low-cost sensors.

The next processing step is an estimation of both surface PM_{10} and $PM_{2.5}$ concentrations from the retrieved AOD. This will take into consideration the vertical distribution of aerosols and the effects of meteorological parameters; wind speed, humidity and temperature. Modelling AOD-PM relationships will be carried out using retrieved AOD, ground-based PM measurements and meteorological data. Multiple regression and machine learning techniques will be used in this stage. Statistical and quantitative methods will be used to validate

estimated PM concentrations using ground PM measurements from LUBW and OK Lab Stuttgart stations. The final product of the workflow will be high-resolution maps that show detailed spatial variations of PM pollution at a city-level scale. The workflow is shown in Figure 3.

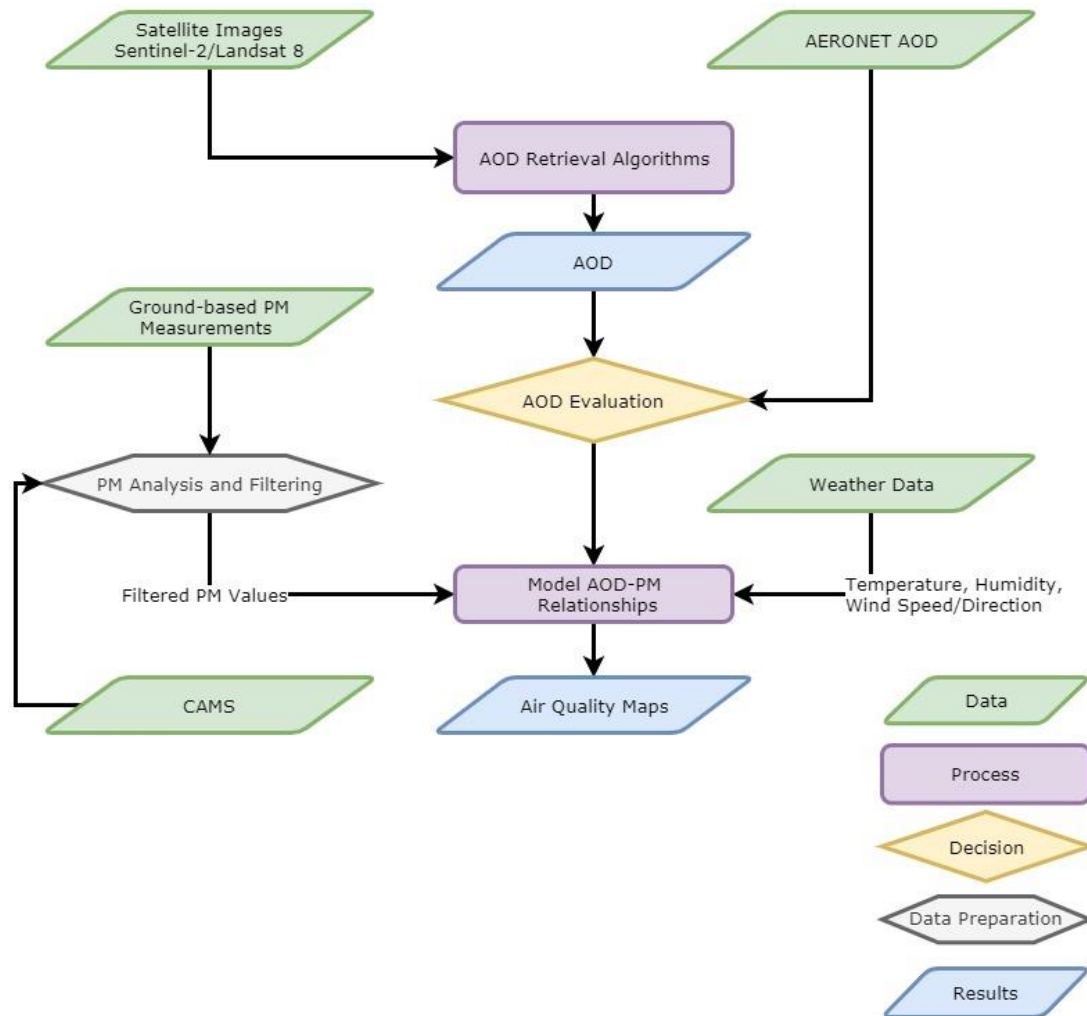


Figure 3: High-resolution aerosol mapping workflow.

5 Expected Achievements

The study project primarily aims at producing high spatial resolution air quality maps for the city of Stuttgart which will show spatial and temporal variations of aerosols in the city. City regions with high pollution concentrations such as high traffic regions and industrial regions are thus expected to be easily identifiable. The results will also be used to examine the temporal variations in days of a week, months and seasons in a year. We also expect to identify appropriate AOD retrieval algorithms suitable for the Sentinel-2 and Landsat images. By modelling the AOD-PM relationships, the suitability of satellite derived AOD to predict near surface air pollution will be determined.

6 Acknowledgement

The project „i_city: intelligent city“ is sponsored by the Federal Ministry of Education and Research (BMBF) under the promotion code 13FH9I01IA and supervised by the project executing organization VDI Technologiezentrum GmbH for the BMBF

7 References

- Bilal, M., Nichol, J.E., Bleiweiss, M.P. and Dubois, D. (2013), “A Simplified high resolution MODIS Aerosol Retrieval Algorithm (SARA) for use over mixed surfaces”, *Remote Sensing of Environment*, Vol. 136, pp. 135–145.
- CAMS (2018), “Copernicus Atmosphere Monitoring Service”, available at: <https://atmosphere.copernicus.eu/> (accessed 09/20/2018).
- Gillingham, S.S., Flood, N., Gill, T.K. and Mitchell, R.M. (2012), “Limitations of the dense dark vegetation method for aerosol retrieval under Australian conditions”, *Remote Sensing Letters*, Vol. 3 No. 1, pp. 67–76.
- Guanter, L., Alonso, L. and Moreno, J. (2005), “First results from the PROBA/CHRIS hyperspectral/multiangular satellite system over land and water targets”, *IEEE Geoscience and Remote Sensing Letters*, Vol. 2 No. 3, pp. 250–254.
- Guanter Palomar, L. (2007), *New algorithms for atmospheric correction and retrieval of biophysical parameters in Earth Observation. Application to ENVISAT/MERIS data*, Universitat de València.
- Hagolle, O., Huc, M., Villa Pascual, D. and Dedieu, G. (2015), “A Multi-Temporal and Multi-Spectral Method to Estimate Aerosol Optical Thickness over Land, for the Atmospheric Correction of FormoSat-2, LandSat, VEN μ S and Sentinel-2 Images”, *Remote Sensing*, Vol. 7 No. 3, pp. 2668–2691.
- Kaufman, Y.J. and Sendra, C. (1988), “Algorithm for automatic atmospheric corrections to visible and near-IR satellite imagery”, *International Journal of Remote Sensing*, Vol. 9 No. 8, pp. 1357–1381.
- Kaufman, Y.J., Wald, A.E., Remer, L.A., Gao, B.-C., Li, R.-R. and Flynn, L. (1997), “The MODIS 2.1- μ m Channel—Correlation with Visible Reflectance for Use in Remote Sensing of Aerosol”, *IEEE Transactions on Geoscience and Remote Sensing*, Vol. 35 No. 5, pp. 1286–1298.
- Keukelaere, L. de, Sterckx, S., Adriaensen, S., Knaeps, E., Reusen, I., Giardino, C., Bresciani, M., Hunter, P., Neil, C., van der Zande, D. and Vaiciute, D. (2018), “Atmospheric correction of Landsat-8/OLI and Sentinel-2/MSI data using iCOR algorithm. Validation for coastal and inland waters”, *European Journal of Remote Sensing*, Vol. 51 No. 1, pp. 525–542.
- Levy, R.C., Mattoo, S., Munchak, L.A., Remer, L.A., Sayer, A.M., Patadia, F. and Hsu, N.C. (2013), “The Collection 6 MODIS aerosol products over land and ocean”, *Atmospheric Measurement Techniques*, Vol. 6 No. 11, pp. 2989–3034.
- Louis, J., Debaecker, V., Pflug, B., Main-Korn, M., Bieniarz, J., Mueller-Wilm, U., Cadau, E. and Gascon, F. (2016), “Sentinel-2 Sen2Cor. L2A Processor for Users”.
- LUBW (2018), “Landesanstalt für Umwelt Baden-Württemberg. Stationsvergleich”, available at: <http://udo.lubw.baden-wuerttemberg.de/public/pages/selector/index.xhtml> (accessed 09/24/2018).
- Main-Korn, M., Pflug, B., Louis, J., Debaecker, V., Müller-Wilm, U. and Gascon, F. (2017), “Sen2Cor for Sentinel-2”.
- Nair, P. (2017), “Stuttgart residents sue mayor for 'bodily harm' caused by air pollution”, *The Guardian*, 3 February, available at: <https://www.theguardian.com/cities/2017/mar/02/stuttgart-residents-sue-mayor-bodily-harm-air-pollution> (accessed 09/18/2018).
- North, P. and Heckel, A. (2010), *Sentinel-3 Optical Products and Algorithm Definition: SYN Algorithm Theoretical Basis Document*.
- OK Lab Stuttgart (2018), “Feinstaub selber messen - Open Data und Citizen Science aus Stuttgart”, available at: <https://luftdaten.info/> (accessed 09/24/2018).
- Osterath, B. (2016), “Stuttgart: Germany's 'Beijing' for air pollution?”, *DW*, 20 January, available at: <https://www.dw.com/en/stuttgart-germanys-beijing-for-air-pollution/a-18991064> (accessed 09/18/2018).
- Richter, R., Louis, J. and Berthelot, B. (2011), *Sentinel-2 MSI – Level 2A Products Algorithm Theoretical Basis Document, S2PAD-ATBD-0001*.
- United Nations (2019), *World Urbanization Prospects: The 2018 Revision*, New York.
- WHO (2006), *Air quality guidelines: Global update 2005 particulate matter, ozone, nitrogen dioxide, and sulfur dioxide*, World Health Organization, Copenhagen.

Food insecurity, Fortunate Index and Refuse Removal as Indicators for Resilience to Disasters

PMU Schmitz ^{a, b}

^aDepartment of Geography, University of South Africa, Florida 1709, South Africa – schimpmu@unisa.ac.za

^bDepartment of Geomatics, Computer Science and Mathematics, University of Applied Sciences, Stuttgart

KEY WORDS: *Disasters, fires, floods, open source GIS, publicly available data.*

ABSTRACT:

This chapter looks at the use of open source GIS (QGIS), imagery from Google Earth and publicly available data. The object was to use these sources to determine areas in a municipality that are vulnerable to disasters. Three datasets using public data from Statistics (South Africa), namely food security, the Fortunate Index and data on refuse removal were used to determine areas of vulnerability and resilience. These three datasets were based on Mayunge's capital to reduce vulnerability and improve resilience. Once these vulnerable and resilient areas had been identified, supplementary data from Google Earth and flood line data was used to determine the risks in vulnerable areas for the purposes of disaster response and mitigatory actions.

1 Introduction

1.1 Background

Baker (2012) indicates that the urban poor are much more vulnerable to disasters than their more affluent counterparts. The urban poor generally reside in areas which are unsuitable for safe habitation. Thus, they are exposed to disasters such as flooding, landslides, and fires. These areas in most instances lack proper basic services, which makes it difficult for residents to, for instance, access to safe potable water (Baker 2012).

This chapter discusses the use of the Fortunate Index, food security and refuse removal data to indicate, on the basis of a Geographical Information System, resilience or the lack thereof to disasters. The aim is to use either the Fortunate Index or food security, or both, to determine sites within a city that could present with limited or no resilience to disasters in order for a city to accordingly plan for its disaster response and post-disaster support.

For the purposes of this chapter, three types of disasters, namely floods, fire, and drought, are discussed since they are the most common in South Africa (Napier & Rubin 2002, Olorunfemi 2011, Ziervogel et al. 2016, du Plessis 2019, Walls et al. 2019). Flood and fire are fast-onset disasters, while droughts are slow-onset disasters.

The next section discusses the Fortunate Index and is followed by a discussion on food security since these two are used as indicators for resilience.

1.2 Fortunate Index

The Fortunate Index was originally developed by de Bruin to determine people's perceptions of being fortunate. It uses Census 2011 data from South Africa (de Bruin 2013) and was refined by Moulton (2016). The Fortunate Index looks at what the person wants, and the expected services received (Schmitz et al. 2015). The object behind this index, which is based on the use of publicly available data, such as data from a census, is to determine the level of fortunateness of a people/community. The aim is to cut out expensive survey costs, but still to gain an accurate impression of how fortunate, or unfortunate, a community is, or perceives itself to be (de Bruin 2013, Schmitz et al. 2015, Moulton 2016).

The Fortunate Index is loosely based on the Gross National Happiness (GNH) Index from Bhutan which rather than using the standard GDP measure of development, tracks a people's wellbeing, which in its turn is affected by the level of economic development of the society in question (Adler 2009, Brooks 2013). The Fortunate Index is based on 11 indicators selected by a sample population from the Census 2011 data, and if these

indicators apply to them, the subjects should feel that they are fortunate. The 11 indicators and their weights are shown in Table 1 (Schmitz et al. 2018).

Indicator	Weight
Being employed	9.25
A degree/diploma/certificate from a tertiary institution such as a university	8.00
A permanent house that you own yourself	7.63
Access to a reliable piped water supply	7.09
Electricity for lighting	6.31
Electricity for cooking	6.27
Flush toilet	6.05
Household appliances (refrigerator, stove, washing machine)	4.41
Own a car	4.21
Cell phone/Telephone in the house	3.48
Access to internet	3.28

Table 1. Fortunate Index indicators (Schmitz et al. 2018).

Based on the availability and access to the services, and using the Census 2011 data, five classes of fortunateness were developed, namely Completely Fortunate, which indicates that almost all of the above-listed expectations have been favourably met; Fortunate indicates that most of the above have been met; Content means that a large set of the above-listed indicators have been realized; Unfortunate indicates that some of the above have been met; and Completely Unfortunate indicates that most of the above expectations have not been met (Schmitz et al. 2018).

Figure 1 shows the Fortunate Index for the City of Tshwane at the Small Area Layer level. The Small Area Layer level is a level developed by Statistics South Africa. It consists of a cluster of enumerator areas and is the smallest mappable area unit that is made publicly available by Statistics South Africa (Verhoef & Grobbelaar 2005).

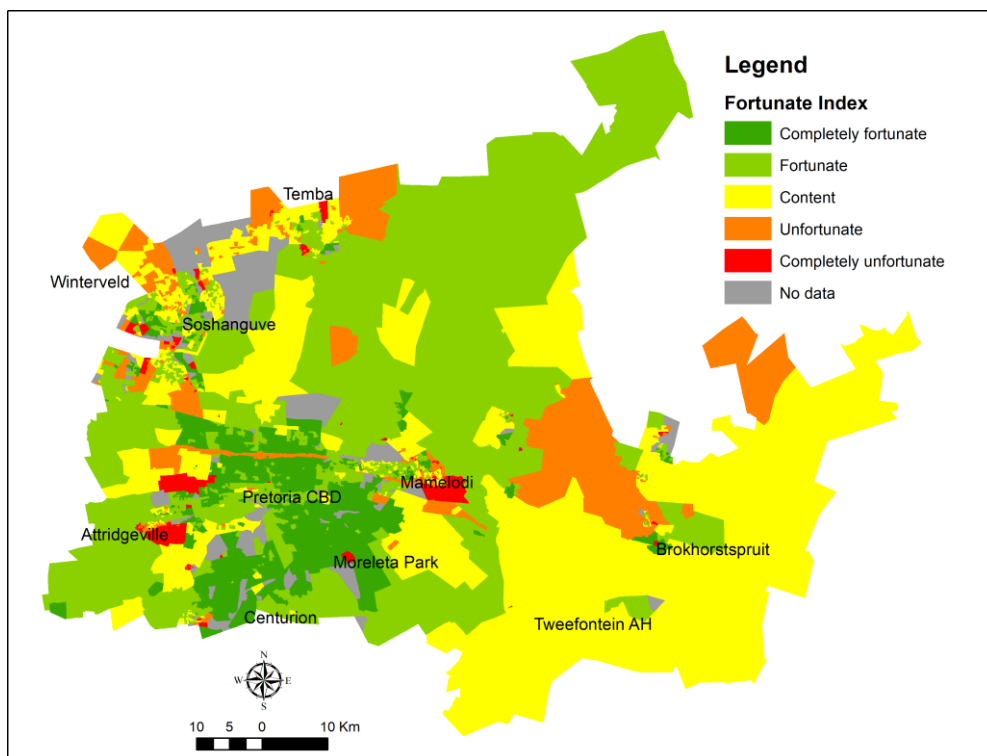


Figure 1. Fortunate Index for the City of Tshwane (Figure 5, Schmitz et al. 2018)

1.3 Food security

In September 2015, the United Nations accepted 17 Sustainable Development Goals (SDGs) with the aim to transform the world in the next 15 years into a better place. These 17 SDGs comprise of 169 targets with their respective indicators to achieve these goals. SDG 2: Zero Hunger deals specifically with food security with the aim to end hunger, achieve food security and improved nutrition and promote sustainable agriculture (United Nations 2018).

This chapter looks at food security as one of the options for fostering resilience in the event of disasters, this meaning that food security combined with level of fortunateness could indicate that there are enough resources available for the community to be sufficiently resilient in a disaster. The opposite could indicate to the authorities that a specific area may not be disaster-resilient, in which case the authority would then plan to put mitigatory measures in place to serve these vulnerable areas.

Statistics South Africa has based its food security parameters on those of the Food and Agriculture Organisation’s Food Insecurity Experience Scale (FIES) (Stats SA 2016). These are (Stats SA 2016):

1. Have run out of money to buy food in the past 12 months (noMon12Mnths)
2. Have run out of money to buy food for five or more days in the past 30 days (no Mon5Days)
3. Skipped a meal in the past 12 months (skipMeal12Mnths)
4. Skipped a meal for five more days in the past 30 days (skipMeal5Days)

These values (numbers) were released by Statistics South Africa only at the local municipal level. A dasymetric methodology using absolute poverty data from the 2011 Census was applied to disaggregate the food security data to the level of the Small Area Layer (SAL) in the City of Tshwane (Schmitz et al. 2018). Table 2 shows the number of people experiencing food insecurity in the City of Tshwane (Stats SA 2016) and Figure 2 shows the disaggregated distribution of food insecurity, expressed as a percentage number of people per SAL, at the SAL level in the metro (Schmitz et al. 2018).

	noMon12Mnths	noMon5Days	skipMeal12Mnths	skipMeal5Days
Yes	505742	288807	329092	186247
No	2749905	213587	2928695	141970
Do not know	16959	2678	16135	635
Not applicable	0	2766863	0	2944829
Unspecified	2547	3216	1230	1470
Total	3275152	3275152	3275152	3275152

Table 2. Food insecurity in the City of Tshwane

1.4 Resilience

The two sections above discussed the Fortunate Index and food security. To place these two parameters in the context of disaster resilience, it is necessary to discuss resilience briefly and how these two parameters interact in terms of the attribute of being resilient.

Natural and man-made disasters and their impact on humans are on the increase globally (de Haen & Hemrich 2007, Cutter 2013). The impact of disaster on humans is in most instances greater than that on the economy (Cutter 2013). Owing to their geographical locations in cities and towns, the poor are in most instances the hardest hit (de Haen & Hemrich 2007, Cutter 2013). De Haen & Hemrich (2007) and Cutter (2013) indicate the importance of resilience in communities if they are to survive disasters. De Haen & Hemrich (2007) looks at resilience from a food security viewpoint, which is one of the parameters used in this chapter. On the other hand, Cutter (2013) looks at it from a sustainability viewpoint. The next few paragraphs look at resilience as a concept for surviving disasters.

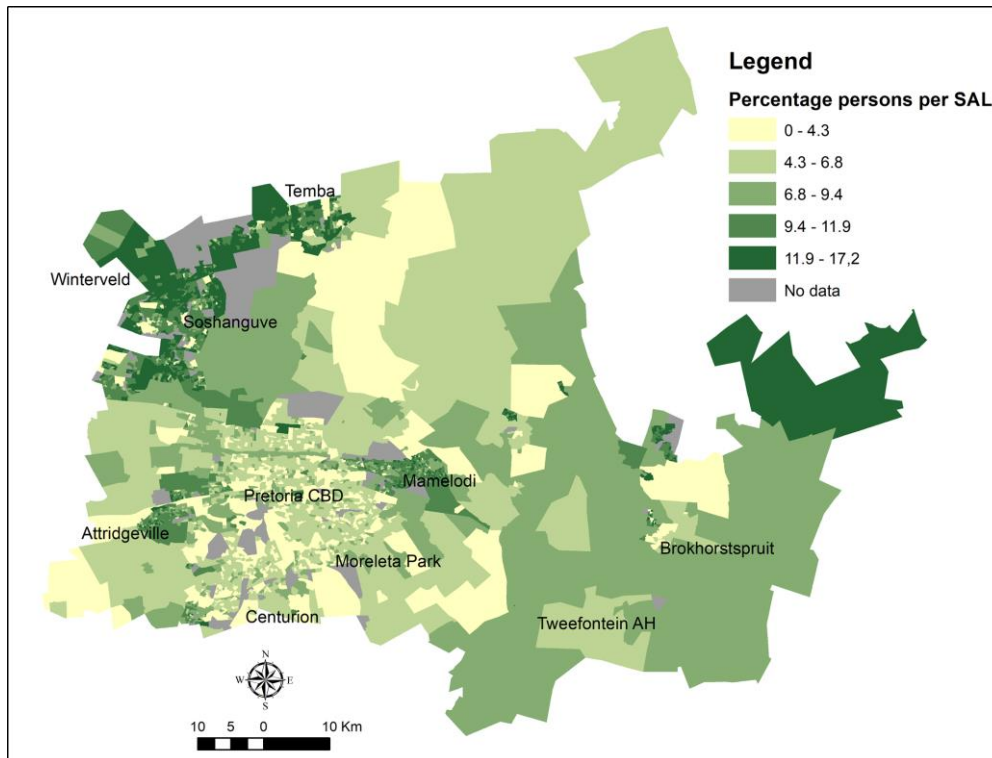


Figure 2. Variable: no money to buy food for five or more days in the past 30 days (Figure 1, Schmitz et al. 2018).

Mayunga (2007:4) refers to community disaster resilience “as the capacity or ability of a community to anticipate, prepare for, respond to, and recover quickly from impacts of disaster”. Mayunga (2007) indicates that communities should learn and adapt in order to mitigate the impact of disasters and recover more quickly in the future. Mayunga (2007:5) proposes that “community capital”, which comprises of economic resources, skills, assets, services, etc. determines a community’s disaster-resilience capacity.

The aim of this study is to compare the Fortunate Index (FI) and food security with Mayunga’s (2007) community capital as a proxy to determine a community’s capacity to survive a disaster and to provide a mechanism to allow local municipalities to prepare appropriate disaster responses for different communities.

This comparison is presented in Table 3. The first two columns are based on the context given by Mayunga (2007:6, Figure 2), and the other two columns are based on the Fortunate Index and food security.

Form of capital	Indicator of resilience	FI indicator	Food security	Refuse removal
Social capital	Trust, norms, networks Income, savings, investment. Education, health, skills, knowledge/information. Housing, public facilities, business/industry.	None	Food security	
Economic capital		Being employed		
Human capital		Post-matric qualification, access to the internet,		
Physical capital		Services (water, sanitation, electricity, telecoms), own house		
Natural capital	Resources stocks, land and water, ecosystems.	None		Refuse removal

Table 3. Comparison between Mayunga’s (2007) capital, refuse removal, Fortunate Index and food security

From Table 3, it can be ascertained that the Fortunate Index does not include social capital and natural capital. Social capital, as defined by Mayunga (2007), includes community cooperation, voluntary organisations, churches and other religious entities, etc. The assumption by this author is that social capital is difficult to determine at various locations in the City of Tshwane and is not defined as a category in the Census 2011 data. The assumption can thus be made that in most instances, social capital for the purpose of this chapter exists in some form or the other and should thus be excluded from the analysis.

With regard to natural capital, Mayunga (2007) lists various variables such as air quality, water quality, soil quality and the presence of nature reserves, wetlands and forests. A proxy that could be used from the Census 2011 is refuse removal as an indicator of the physical pollution of the natural environment. This means that if the refuse is not removed, it will end up in streams and the environment. This is especially typical of informal settlements in South Africa, as illustrated in Figure 3. Refuse removal was not regarded as part of being fortunate by the sample population when the Fortunate Index was compiled.

Figure 4 shows the percentage of no refuse removal in the City of Tshwane. It is evident from Figure 4 that large parts of the metro have access to adequate refuse-removal services; however, there are also areas with no refuse-removal services. In such cases, there is the option of burning refuse. However, this could lead to fire outbreaks under dry conditions, high temperatures and strong winds, these the conditions for fuelling fires.

This section discussed resilience using the Mayunga (2007) approach to determine a community's resilience to disasters with the proxies listed in Table 3. There are various other methodologies available to determine and build resilience such as those striving for the eradication of poverty and hunger, universal primary education, a reduction in child mortality, improved health, partnerships for development and environmental sustainability, as promulgated by Cutter (2013) or the PEOPLES Resilience Framework of Renschler et al (2010).



Figure 3. Dumping and burning of refuse at an informal settlement (Source: Author)

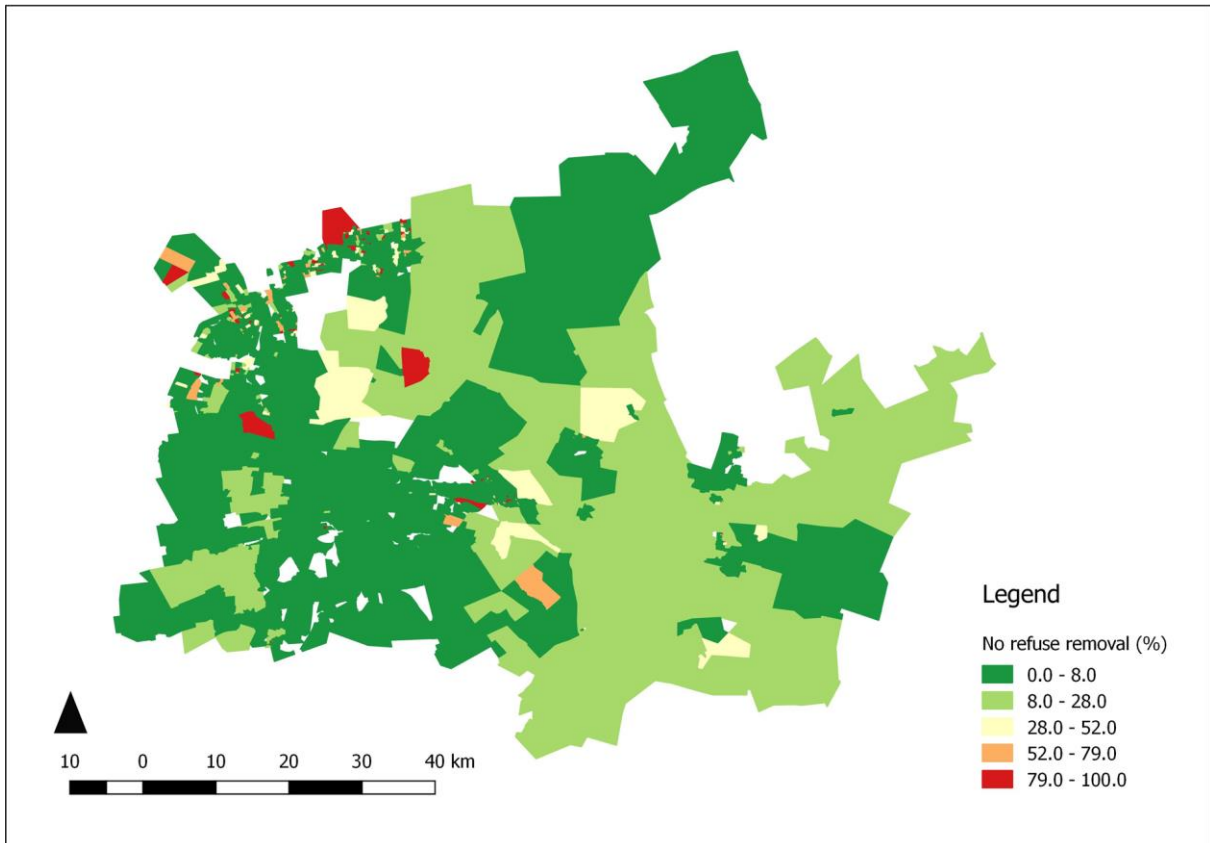


Figure 4. Percentage of areas of no refuse removal in the City of Tshwane

PEOPLES is the acronym for Population and Demographics, Environmental/Ecosystem, Organised Governmental Services, Physical Infrastructure, Lifestyle and Social-Cultural Capital (Renschler et al. 2010:1). These have a similar approach to Mayunga's (2007) five types of capital for developing resilience in communities. For the purpose of this chapter, Mayunga's (2007) approach is used to identify areas of limited resilience in terms of disasters.

The next section gives an overview of the three common disaster areas, namely fire, flood, and drought, that have a significant impact on the resilience of communities.

1.5 Disasters

The three most common disasters in urban areas are discussed. Two of these are fast-onset disasters, namely fires and floods. The third is drought which is a slow-onset disaster.

1.5.1 Fire

Walls et al. (2017) indicate that world-wide over a billion people live in informal settlements, which in most instances accommodate a high density of buildings built from various types of materials. The residents in most instances use paraffin or gas for energy and lighting (Napier & Rubin 2002). These circumstances are conducive to a high incidence of fires. When these fires break out, they ravish large parts of the community, as explained by Walls et al. (2017), in their description of a recent fire in Cape Town, South Africa, which left approximately 4 500 people homeless and destitute. These fires occur worldwide and Twigg et al. (2017) indicate that annually over 300 000 people die in fires and that 95 percent of these occur in developing countries with a high incidence in informal settlements.

According to Napier & Rubin (2002), there are two types of fire in South African informal settlements. The first type is the large fire, which obliterates a large number of dwellings in a flash, and which is regarded as a disaster by the various authorities. The second type is the small fire that burns continuously, and which affects only a few people and by which a single or a few dwellings are burnt down. These occur more regularly at the same location and erode the victims' resilience to this type of disaster over time (Napier & Rubin 2002).

1.5.2 Floods

Mitigation of the impact of flooding in an urban context is achieved through structural solutions, such as stormwater reticulation, pondages and canals, as well as by educating residents and other land users, through land-use planning and the promulgation of regulations, such as building restrictions below the 1 in 50-year flood line (Andjelkovic 2001, Ziervogel et al. 2016). However, people living in informal settlements in urban areas are in most instances located in or near marginalized areas such as wetlands, below the 1 in 50-year flood line and adjacent to flood detention ponds which are prone to flooding and/or other hazards (Napier & Rubin 2002, Olorunfemi, 2011, Rodina & Harris 2016, Ziervogel et al. 2016).

The focus for the purpose of this paper was on areas below the 1 in 50-year flood line, which are considered to be the most vulnerable. There are events that are more extreme than the 1 in 50-year flood event, but these may also affect the formal and less vulnerable areas as well. The advantage of using the 1 in 50-year flood line is that this line is required for regulating development in a city or town (CSIR 2000) and is thus available for analysis.

1.5.3 Drought

Drought or famine is a slow-onset disaster which could have an impact on the resilience of a community. Droughts have far-reaching economic impacts, as demonstrated by Napier & Rubin (2002:6) who reported on the drought of 1991 and 1992 which led to the loss of 49 000 direct agricultural jobs and 20 000 non-agricultural jobs in KwaZulu-Natal, South Africa. Napier and Rudin (2002) further indicated that these people had no choice but to move to vulnerable urban areas in order to survive.

The impact of a drought on a city was highlighted by reports on the recent drought in Cape Town which nearly caused a “Day Zero” scenario, where approximately 3.7 million residents’ taps would have been switched off (Wolski 2018). This “Day Zero” drought was not restricted to Cape Town, but also affected both the Western Cape and Eastern Cape provinces.

Droughts, including the “Day Zero” drought, cause severe impacts on communities and test their resilience to the extreme. They are subjected to even further impacts since droughts are followed in most instances by severe flooding, as in the case of KwaZulu-Natal between 1994 and 1996 that occurred after the aforementioned drought (Napier & Rudin, 2002).

For the purpose of this chapter, droughts are seen as driving forces behind people, motivating them to escape to vulnerable areas with limited or even non-existent economic means to face the challenge of the next flood or fire event.

2 Methodology

For the purpose of this chapter, the following data sets, based on Table 3, were used to determine vulnerability and resilience to disasters. The main aim of this chapter was to illustrate the use of publicly available data, data obtained through open source GIS software (QGIS) and the Google Earth search engine, to identify vulnerable areas in order to ultimately improve the resilience of the residents in question.

The relevant data sets are listed as follow:

- The Fortunate Index, which looks at Mayunga’s (2007) economic capital, human capital and physical capital;
- Food security, which looks at Mayunga’s (2007) economic capital. Food security is considered in this chapter to be a strong indicator of resilience;
- Refuse removal or the lack thereof which is regarded as a proxy for Mayunga’s (2007) natural capital.

Since Mayunga’s (2007) social capital is difficult to determine on the basis of the publicly available data, for the purpose of this chapter it was assumed that it was a given and excluded from the analysis.

The data used to determine the Fortunate Index were sourced from the 2011 Census in South Africa, while the methodology used to determine the Fortunate Index was sourced from de Bruin (2013), Schmitz et al. (2015), Moulton (2016) and Schmitz et al. (2018).

The data used to determine food security in the City of Tshwane were based on data from Statistics South Africa’s 2016 Community Survey and the 2011 Census data for determining the poverty line.

The food security category in the 2016 Community Survey was at the municipal level and the poverty line was determined at the Small Area Layer (SAL) level. Using the poverty line data, the dasymetric process, discussed in Schmitz et al. (2018), was followed to disaggregate the food security data from the municipal level to the SAL level. The variable, “Skipped a meal for five or more days in the past 30 days (skipMeal5Days)” was used as the food security indicator.

Refuse removal data at the SAL level were sourced from Statistics South Africa and the variable “No disposal” was used to indicate whether a place had a form of refuse removal or not.

These three variables were heuristically weighted to indicate vulnerability or resilience. The reason for using heuristics is that it is an accepted form of weighting, even though each person may weight each variable differently, depending on his or her experience of it. Furthermore, it is a method to determine a first-cut vulnerability that is able to accommodate municipalities with low budgets.

The heuristic approach cannot be regarded as perfect, however, but, based on the discussion by Neth & Gigerenzer (2015:6) that “heuristics are seen as adaptive tools that allow people to make accurate, efficient, and robust decisions under uncertainty” it has value Their list of examples of cases where heuristics have been used in the absence of concrete facts to convey a concept or an idea in order to find an acceptable solution or answer to a problem validates this approach (Neth & Gigerenzer 2015).

Table 4 shows the classifications and weighting to determine vulnerability and resilience for the prioritization of areas for disaster management and mitigation.

Variable	Weight	Class	Vulnerability and resilience calculator
Food security - FS (%skipMeal5Days)	0.3	0% to 3% (5) 3% to 6% (4) 6% to 10% (3) 10% to 19% (2) 19% to 42% (1)	Vulnerability/Resilience = $(FS * 0.3) + (FI * 0.6) + (RR * 0.1)$ Five classes: Very vulnerable Vulnerable Could be vulnerable Resilient Very resilient
Fortunate Index – FI	0.6	Very unfortunate (1) Unfortunate (2) Content (3) Fortunate (4) Very fortunate (5)	
Refuse removal – RR (%No Disposal)	0.1	0% to 8% (5) 8% to 28% (4) 28% to 52% (3) 52% to 79% (2) 79% to 100% (1)	

Table 4. Variables used to determine vulnerability and resilience

Once the vulnerable areas had been identified, other data such as flood lines and Google Earth imagery were used to determine the type of structures, access, etc. in order to react to a flood or fire disaster, and also to suggest possible methods for mitigating the disaster. The data were exported as .KMZ or .KML files which could then be imported into Google Earth. A visual inspection of the area could then be conducted with plans based on all the information available being made to deal with the responses, and mitigatory measures could then be planned.

3 Analysis and discussion

The previous section discussed the methodology in determining vulnerable and resilient areas in the City of Tshwane. This section looks at the applications of these results. Figure 1 shows the Fortunate Index for the City

of Tshwane, while Table 4 shows the classification to calculate vulnerability and resilience. Figure 4 shows the percentage of no disposal or no refuse removal for the City of Tshwane, and Table 4 shows the classification of vulnerability and resilience in this respect. All of the class boundaries were determined using the natural breaks (Jenks) method in QGIS.

Figure 5 shows the food security's variable, "Skipped a meal for five or more days in the past 30 days (skipMeal5Days)". Table 4 shows the classification to calculate vulnerability and resilience.

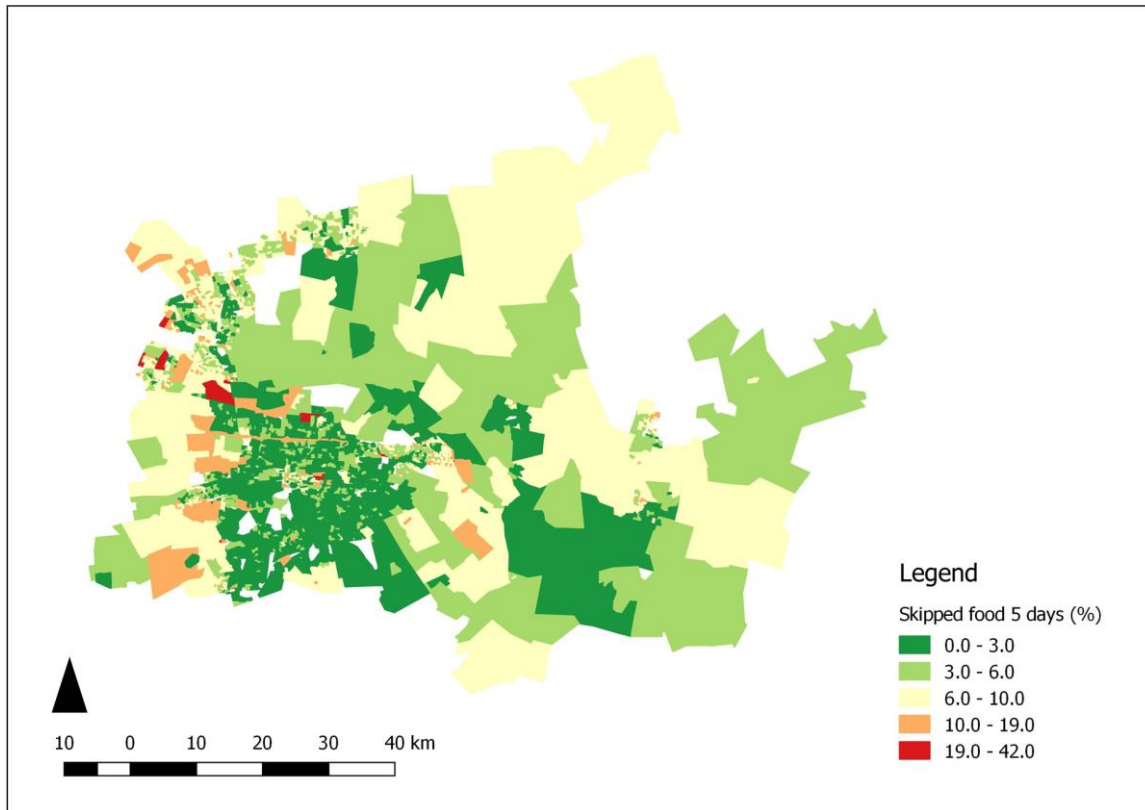


Figure 5. Variable: Skipped a meal for five or more days in past 30 days

The results of the calculations to determine vulnerability and resilience as presented in Table 4 were used in QGIS and the resultant map is shown in Figure 6. From Figure 6, it can be seen that large parts of the City of Tshwane are either very vulnerable or vulnerable. In most instances, these areas are spatially associated (coincide) with rural informal settlement areas and portions of townships.

Other data such as the 1 in 100-year flood lines and data from Google Earth could then be used to determine the impacts of flood and fire in these vulnerable areas, as shown in Figure 7 and Figure 8. Figure 8 is an enlargement of the same area in Figure 7 that is enclosed in a black ellipse. Figure 8 could be used to visually inspect possible impacts such as flooding and fires and potential responses to the disaster as in access to the disaster area and possible triage locations that are annotated as in Figure 8.

The long-term mitigatory measures to deal with the effects of the disaster could be to move persons out of the flood-endangered areas close to the river and to upgrade the area by replacing the informal structures with formal structures and by reblocking the area. The creation of open spaces for recreation and triage would be an option that the municipality could look into.

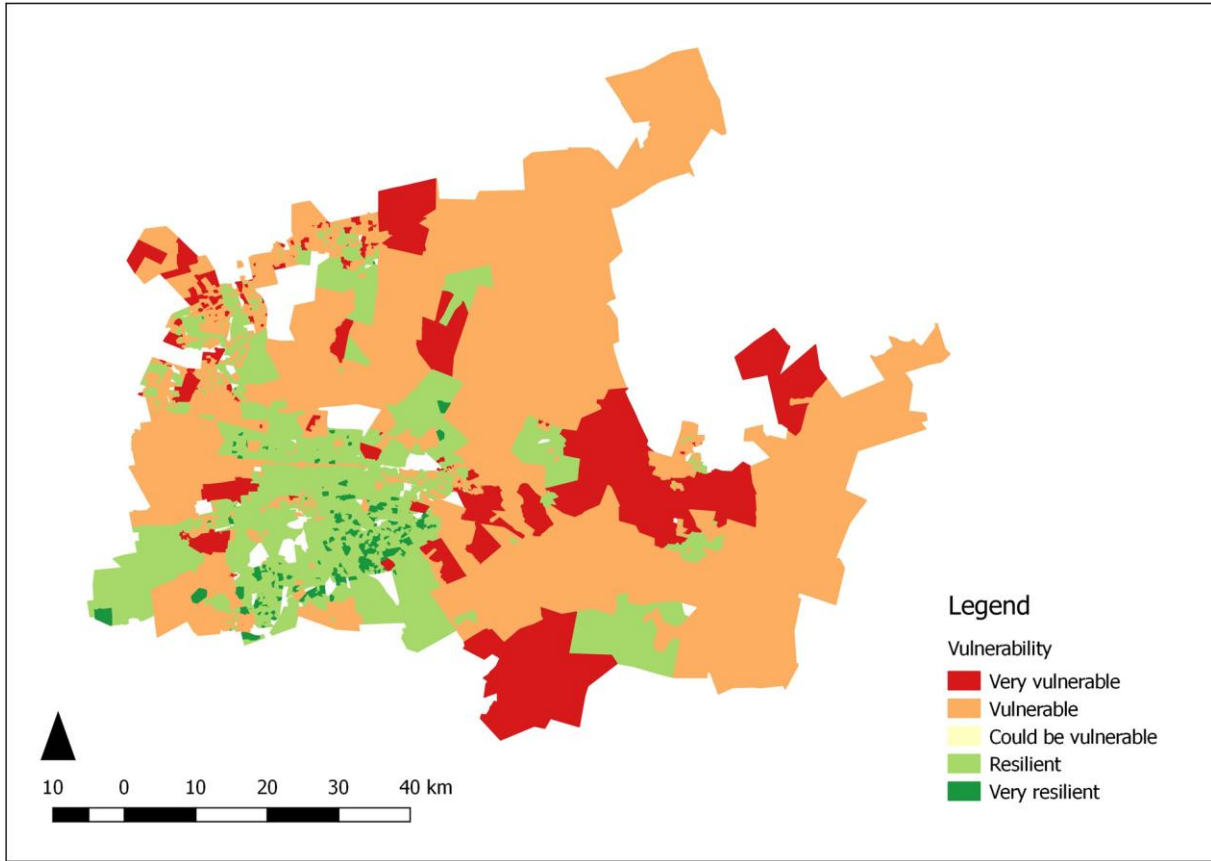


Figure 7. Vulnerable and resilient areas in the City of Tshwane

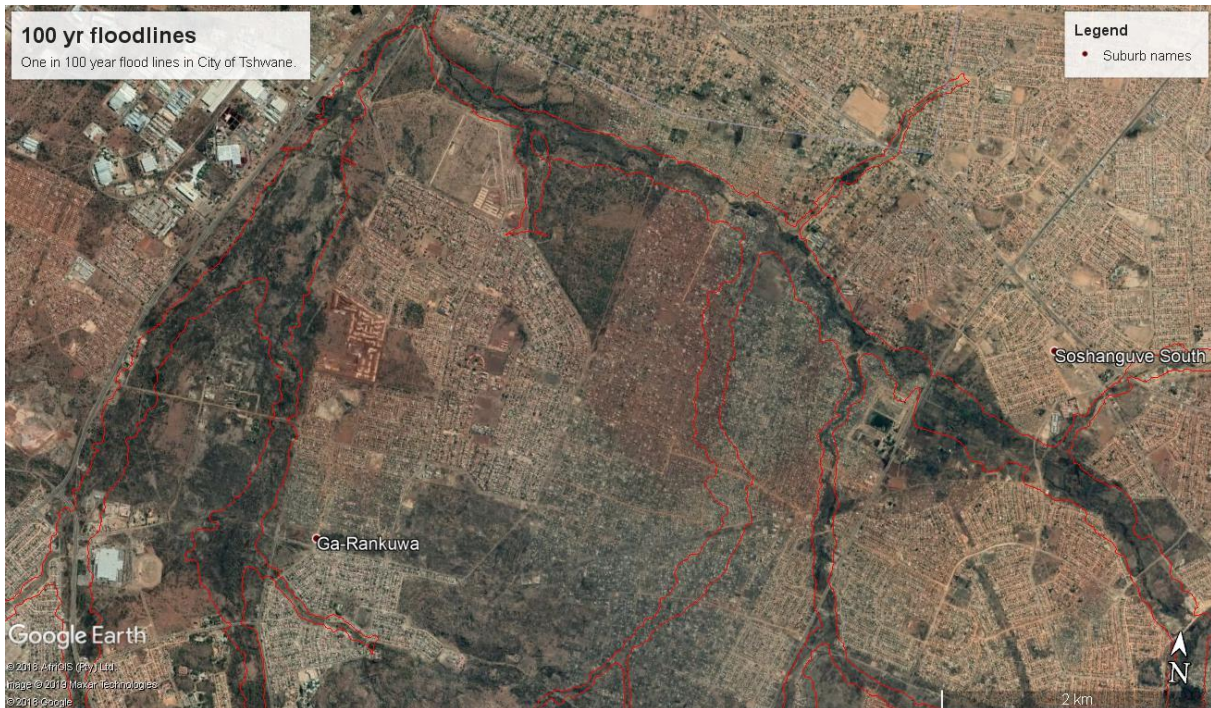


Figure 8. Google Earth image and the 1 in 100-year flood line in a vulnerable area

4 Conclusion

This chapter discussed the use of publicly available data and open source GIS (QGIS) to determine vulnerable and resilient areas in a municipal area, as presented in Figure 7. The next step was to use this information, data from Google Earth and supplementary data such as that concerning the 1 in 100-year flood line. Through visual inspection of the area, experience and local knowledge, a disaster-response and -mitigation model was designed, as presented in Figure 8.

It is hoped that this information, which can be generated at little or no cost to a municipality, could be used to improve the resilience of disaster victims, and as an aid in disaster management planning. This information could also be used in the prioritization of areas for upliftment and to assist in alleviating poverty, improving food security and sustainability as per the various Sustainable Development Goals of the United Nations.

5 Acknowledgements

The author would like to acknowledge Applied Geoinformatics for Society and Environment (AGSE) for their invitation for him to participate in AGSE 2018 and the subsequent invitation to submit this chapter. The author would like to acknowledge the support received by the University of South Africa for the opportunity to attend AGSE 2018 and to write this chapter.

6 References

- Alejandro, A., 2009. Gross National Happiness in Bhutan: A Living Example of an Alternative Approach to Progress (2009). Social Impact Research Experience (SIRE). 1. <http://repository.upenn.edu/sire/1>
- Andjelkovic, I., 2001. Guidelines on non-structural measures in urban flood management. IHP-V | Technical Documents in Hydrology | No. 50 UNESCO, Paris, 2001.
- Baker, J.L., 2012. Climate change, disaster risk, and the urban poor: cities building resilience for a changing world. The World Bank, Washington, D.C., United States of America.
- Brooks, J.S., 2013. Avoiding the Limits to Growth: Gross National Happiness in Bhutan as a Model for Sustainable Development. *Sustainability* 5(2013), pp. 3640 – 3664.
- CSIR, 2000. Guidelines for Human Settlement Planning and Design, Volume 2. CSIR Building and Construction Technology. Pretoria, South Africa. Boutek Report No. BOU/E2001. ISBN 0-7988-5498-7.
- Cutter, S.L., 2013. Building Disaster Resilience: Steps Toward Sustainability. *Challenges in Sustainability* 1(2), pp. 72 – 79.
- de Bruin, S., 2013. Developing a Fortunate Index. Honours Project Report, Department of Geography, Geoinformatics and Meteorology, University of Pretoria, Pretoria, South Africa.
- de Haen, H. & Hemrich, G., 2007. The economics of natural disasters: implications and challenges for food security. *Agricultural Economics* 37(1), pp. 31 – 45.
- du Plessis, A., 2019. Water as an inescapable risk: current global water availability, quality and risks, with a specific focus on South Africa. Springer.
- Mayunga, J.S., 2007. Understanding and Applying the Concept of Community Disaster Resilience: A capital-based approach. Available from: https://www.u-cursos.cl/usuario/3b514b53bcb4025aaf9a6781047e4a66/mi_blog/r/11._Joseph_S._Mayunga.pdf Accessed on 13 November 2019.
- Moult, D., 2016. A Refinement of the Fortunate Index: a Means of Measuring People's Perception of Service Delivery. Honours Project Report, Department of Geography, Geoinformatics and Meteorology, University of Pretoria, Pretoria, South Africa.
- Napier, M. & Rubin, M., 2002. Managing environmental and disaster risks affecting informal settlements: lessons in innovative practice from South African local authorities. Sustainable livelihoods in the integration of informal settlements in Asia, Latin America and Africa, 10-13 October 2002, Surabaya, Indonesia.

- Olorunfemi, F.B., 2011. Managing flood disasters under a changing climate: Lessons for Nigeria and South Africa. NISER Discussion Paper No. 1, 2011. Social and Governance Policy Research Department, Nigerian Institute of Social and Economic Research (NISER), P. M. B. 5, U. I. Post Office, Ibadan, Nigeria.
- Renschler, C.S., Frazier, A.E., Arendt, L.A., Cimellaro, G.P., Reinhorn, A.M. & Bruneau, M., 2010. Developing the 'PEOPLE'S Resilience Framework for defining and measuring disaster resilience at the community scale. In the Proceedings of the Ninth U.S. National and 10th Canadian Conference on Earthquake Engineering. July 25-29, 2010, Toronto, Ontario, Canada • Paper No 1827.
- Rodina, L. & Harris, L.M., 2016. Resilience in South Africa's urban water landscape. Opinion Piece, published in The Conversation Africa (2016, June 14).
- Schmitz, P., Eksteen, S. & de Bruin, S., 2015. Towards a new way of measuring service delivery in Gauteng: calculating a Fortunate Index. South African Journal of Geomatics, 4(3) Geomatics Indaba Special Edition pp 317-325.
- Schmitz, P., Pillay, L., Moul, D., 2018. Fortunate Index and Food Security: City of Tshwane Case Study using GIS. Paper presented at the AfricaGEO 2018 Conference, 17 to 19 September 2018, Emperor's Palace Convention Centre, Ekurhuleni, South Africa. Proceedings of the Academic Track of Africa GEO 2018. ISBN 978-0-620-80873-6
- Statistics SA, 2016. Community Survey 2016: Statistical Release. Statistics South Africa, Pretoria, South Africa.
- Twigg, J., Christie, N., Haworth, J., Osuteye, E. & Skarlatidou, A., 2017. Improved Methods for Fire Risk Assessment in Low-income and Informal Settlements. International Journal of Environmental Research. Public Health 2017, 14, 139 pp 1 – 12.
- Verhoef, H. & Grobbelaar, N., 2005. The development of a Small Area Layer for South Africa for census data dissemination. Available from: <http://www.cartesia.org/geodoc/icc2005/pdf/poster/TEMA26/HELENE%20VERHOEF.pdf> Accessed on 12 November 2019
- United Nations, 2018. Transforming our world: the 2030 Agenda for Sustainable Development. Viewed 12 November 2019 < <https://www.un.org/sustainabledevelopment/sustainable-development-goals/#>>
- Walls, R., Olivier, G. & Eksteen, R., 2017. Informal settlement fires in South Africa: fire engineering overview and full-scale tests on "shacks". Fire Safety Journal, 91(2017), pp. 997 – 1006.
- Wolski, P., 2018. How severe is Cape Town's "Day Zero" drought? Significance, April 2018, significancemagazine.com
- Ziervogel, G., Waddell, J., Smit, W. & Taylor, A., 2016. Flooding in Cape Town's informal settlements: barriers to collaborative urban risk governance, South African Geographical Journal, 98(1), pp. 1-20.

Digital Elevation Model Generation From CARTOSAT-1 Using LEICA Photogrammetry Suite

Karuppasamy S ^{a*}

^a Department of Civil Engineering, SRM Institute of Science and Technology,
Kattankulathur – 603203, Tamilnadu (India), - karuppasamy.s@ktr.srmuniv.ac.in

KEY WORDS: *Cartosat-1, Digital Elevation Model, Leica Photogrammetry Suite, Demo*

ABSTRACT:

The term Digital Elevation Model (DEM) is generally referred to a digital representation of the topographic surface in three dimensions with elevation described above the sea level. The elevation is the basic source of information for generating the DEM. The elevation can be derived using various methods such as digitizing the contour lines from the Toposheet, Terrestrial survey using Electronic Distance Measurement (EDM), Totalstation and Global Positioning System (GPS). The elevation measurements can also be measured from Aerial, Satellite, Drone survey and Airborne LIDAR Terrain Mapping (ALTM) techniques. The accuracy of elevation measurements using the terrestrial survey is high, but it is costly and time consuming. The accuracy of the elevation measurements from the aerial survey such as aerial photographs, low altitude drone photographs and ALTM based 3D point clouds are high, but it is also time consuming, costly and in addition, this method requires permission from the government in country like India. The accuracy of the elevation measurements from the satellite survey is lower than the terrestrial and aerial survey but it is economical and easily available. The idea of the software demo is to utilize the Indian Remote sensing produced Cartosat-1 (IRS-P5) launched on Cartosat-1 in May 2005, is used as source data for the generation of Digital Elevation Model using Leica Photogrammetry Suite. A Cartosat-1 satellite data is provided with the fore and aft scenes, both fore and aft carries the Rational Polynomial Coefficients (RPC). RPC coefficients were used to specify the geometric model, which defines the internal characteristics and external parameters. The information's are required for DEM generation is Cartosat-1 aft, fore scenes, RPC Geometric model and GCPs (Ground Control Point). The process includes the project setup, GCP, Tiepoint measurement, Triangulation, identify and correct weak Tie Point connection and eventually accuracy assessment based on the GCPs.

Flood Vulnerable Zone Identification In Tamirabarani River Using CARTOSAT-1, Tirunelveli, Tamilnadu, India

Karuppasamy S ^{a*}

^a Department of Civil Engineering, SRM Institute of Science and Technology,
Kattankulathur – 603203, Tamilnadu (India), - karuppasamy.s@ktr.srmuniv.ac.in

KEY WORDS: *Flood, Vulnerable Zone, Tamirabarani River*

ABSTRACT:

Thamirabarani River is a perennial river that originates from the Podhigai hills located in Western Ghats and drain in the Bay of Bengal. The Thamirabarani river basin has several dams located near the Western Ghats. The basin has experienced flood during heavy rainfall in some years. The idea of the study is to identify the low lying areas nearby the Thamirabarani River using Cartosat-1 Satellite based DEM and the regions that are vulnerable to flood are studied through the geospatial technology. In this study, Cartosat-1 is used as source data for the generation of DEM. The study extracted the low lying areas close to the River basin from Cartosat-1 and the help of GIS technology, the study identified the flood vulnerable zone in the study area. The study categorize the flood vulnerable zones into three categories such as highly vulnerable, medium and low vulnerable areas based on the impact of flood inundation in the study area. It was revealed from the study that there are regions highly vulnerable to flood are Sriviakuntam, Ambasamudram and Vickramasingapuram. The area are medium vulnerable to the flood are Tharuvai, Thenpathu, Vilagam, Melapalayam and Keelanatham and the low vulnerable regions are found distributed throughout the basin. The identification flood vulnerable zone is essential requirement for both city planner and government official for the decision making during and before the flood in the study area.

Geo-statistical Analysis and Modelling of Malaria Distribution in Namibia

Heita Anditanga M. M.

Namibia University of Science and Technology

KEY WORDS: *Geo-statistics, Spatial phenomena, Malaria, Namibia*

ABSTRACT:

In Namibia malaria is one of the most life threatening disease caused by parasites that transmits the disease through the bites of an infected Anopheles female mosquito.

Geo-statistics is a class of spatial statistics that analyzes and predicts the values associated with spatial and spatiotemporal phenomena.

Geographical patterns and indicators allows us to use Geo-statistical methods and tools to effectively identify malaria hotspots and cold spots in Namibia. Advances in model-based geo-statistics (Spatial Statistics) and geographical information systems (GIS) have enabled researchers including students to better understand factors affecting malaria risks and transmissions, more accurately determining the limits of malaria risks at a national level.

My approach and findings from this study may be used by various national malaria programs to identify health facilities in high malaria risk areas to target health and environmental services to take serious deliveries to reduce the risk of Malaria within our country. The study will also demonstrate the use of existing data resource platforms such as Digital Namibia (www.digitalnamibia.na) and our very own readily available platform PolyDB (Database) that helped me visualize and produce a geographic analysis to evaluate health system performances that identifies within and across the countrys malaria spatial patterns and distribution.

The dataset used to carry out the Geo-statistical analysis represents the outbreak of Malaria cases each year between 1995 and 1999.

Open Source as inner Habit and the Impact of the OSGeo Foundation

F.-J. Behr

Stuttgart University of Applied Sciences, Germany –franz-josef.behr@hft-stuttgart.de

KEY WORDS: Open Source, OSGeo, Commons

ABSTRACT:

Development, maintenance and usage of free and open source software solutions, standards and data can be observed in the geospatial information technology. More and more individuals and companies have committed themselves to the idea of Open Source and completed their portfolio with freely available components.

The public lecture will present the fundamental principles of this movement, its motivating factors and basic business models of the Open Source realm.

Early stage detection of Bark Beetle infestation using UAV (Unmanned Air Vehicle) based Hyperspectral and Thermal image

Rajan Paudyal^{1,*}, Peter Hofmann¹, Martin Hais², Marco Heurich³, Rainer Pöschl¹, Stefan Kunze¹, Milan Novák², Petr Doležal², Stanislav Grill², Markéta Davidková², Miloš Prokýšek², Martin Stary⁴, and Wolfgang Dorner¹

¹Technische Hochschule Deggendorf, Technology Campus Freyung

²Department of Ecosystem Biology, Faculty of Science, University of South Bohemia

³Bavarian Forest National Park, Department of Conservation and Research

⁴National Park of Šumava

*Correspondence: rajan.paudyal@th-deg.de; Tel.: +49-8551-91764-41

KEY WORDS: *Disturbance, Bark Beetle, UAV, Hyperspectral, Thermal IR*

ABSTRACT:

Disturbances caused by bark beetles infestation are a massive problem for forestry in Europe. Current remote sensing methods, due to its limited spatial resolution, fall short to detect the infested trees as no discoloration of the tree needle occurs during the early attack stage of the beetles. Terrestrial inspection can be used but is not practicable in large forest areas. Thus, effective methods allowing an early stage detection of bark beetle infestation of larger areas is needed for conducting prompt forest management practices. This research aims at investigating this method using UAV based imaging with hyperspectral and thermal IR sensors. The high temporal and spatial resolution data of these sensors are used for monitoring and analyzing behavioral changes occurred in the infested tree. The paper present outlines the preliminary result of image analysis and concludes the potential of this method for an effective early stage detection of bark beetle infestation.

Risk Sensitive Land Use Planning (RSLUP)

Umesh Kunwar

Remedy Engineering Pvt. Ltd (Nepal)

KEY WORDS: *Disaster risks, participatory approach, risk-sensitive landuse planning*

ABSTRACT:

The presentation is about incorporating the Disaster Risk in our planning process so that we plan safe settlement. Via this presentation presenter will share the experience of GIS Professional in Risk Sensitive Land Use Planning in Nepal, RSLUP

Cities in the developing world are facing increasing risks of disasters. Nepal on the other hand is ravaged by the multiple natural hazard annually resulting of significant loss of lives and properties. Nepal's location is highly and active tectonic region of the Himalayan belt with increased risk of earthquake disaster. In terms of vulnerability to natural disaster, UNDP/BCPR has ranked Nepal as the eleventh in terms of risks from Earthquake and thirteenth in terms of risk from flood.

Risk Sensitive Land Use Planning is a participatory approach that includes disaster risk reduction efforts in the conventional land use planning. In reaction to multiple and economic forces that interplay with in the society where the components of risk and hazard are generally overlooked or given less priority, this approach utilizes information related to potential hazard risks and resource constraints with in the area to develop a more risk resilient settlement that has right mix of both development and planning process. This also helps to reduce disaster damage before they happen.

Due to diverse geographical coverage, Nepal is prone to various geological and hydro-meteorological hazards. Recent civil unrest, recurring floods, landslides, epidemics has led to severe economic direct and economic losses. The impact has been further aggravated due to catalytic factors like climate change, depletion of glacier, global warming and rapid unsafe urbanization. Risk assessment provides information for decision makers and planners to identify counter measures to reduce the exposure to risks. Risk mapping is the first step for forming the national, local and sectoral disaster mitigation planning.

Increasing urbanization resulting to poorly planned settlements is becoming a major driver of disaster risks. Rapid and uncontrolled urbanization is increasing the exposure of populations and infrastructure to potential hazards. There is a need to better plan growth in terms of infrastructure and construction by taking into account hazard and risk parameters that can protect these investments from major damages. There is also a need to improve the delivery of core services such as health, education, social welfare, transportation, power, water, sanitation, and others so that these services will continue to function even after major catastrophic events such as earthquakes. These are important considerations especially for cities where there are high concentrations of businesses, industries, and populations and where the negative impact of disasters is very high. Building a city's resiliency to disasters should be on top of government's agenda since the loss of life, destruction of property, and disruption of essential services have huge socio- economic, and even political, implications.

The following are the different type of risk

- Flood hazard Risk
- Landslide Hazard Risk
- Seismic Hazard Risk
- Fire Hazard Risk
- Industrial Hazards Risk

The use of Map-server and Geo-server in the Geographic Information Technology world

Kevin A.J Geingob

Namibia University of Science and Technology

KEY WORDS: *Map-server, Geo-server, Spatial Data Infrastructure, Namibia*

ABSTRACT:

Map-server and Geo-server are types of Map servers

What they are, their purpose and functionalities would be explained in depth. Other related aspects such as why they are very vital in the industry and how they come about to produce these functionalities, why they are used more often in modern times would be explained as well.

These Servers would be explained more in detail in terms of their contribution within the Spatial Data Infrastructure. Emphasizing on the NSDI compiled by NSA, there will also be a short explanation on its software infrastructure and also the infrastructure the servers use to make it possible for data sharing.

Other components such as webservers with examples would also be involved because of the fact that Map servers cannot run on their own. Although they have spatial capabilities, they are not able to serve as webservers. We need to introduce webservers such as apache to serve as an intermediary between the user and the map-server. We will also highlight some differences between Map-servers and Geo-server. Which one is more convenient and why!

Food insecurity, Fortunate Index and income as possible indicators for vulnerability (Workshop)

Peter Schmitz^{a, b}

^aDepartment of Geography, University of South Africa, Florida 1709, South Africa – schimpmu@unisa.ac.za

^bDepartment of Geomatics, Computer Science and Mathematics, University of Applied Sciences, Stuttgart

KEY WORDS: *Disasters, fires, floods, open source GIS, publicly available data.*

ABSTRACT:

The aim of this workshop is to introduce the participants to use publicly available data to determine areas of vulnerability using food insecurity, fortunate index and income as proxies.

- Food security: According the World Food Program (WFP) is the availability and adequate access to sufficient, safe and nutritious food to maintain an active and healthy life. The opposite is food insecurity.
- Fortunate index (FI): The FI consists of 11 indicators selected by interviewees that gives a feeling of being fortunate. The 11 indicators range from owning a permanent house, employment to accessing the Internet and having a post-matric qualification.
- Poverty: In this workshop we will use the Food Poverty Line of R335 per person per month in 2011 as given by Stats SA in South Africa.

The data used in the workshop will be of the City of Tshwane (Pretoria) in South Africa.

The outcome of the workshop is to identify areas vulnerability with regards to food security (SDG 2: Zero Hunger). These areas of vulnerability could also indicate vulnerability and low resilience to disasters such as flash floods and fire.

Requirements:

GIS Lab or participants' own laptop (QGIS will then be installed on the laptops) if there is no lab available.
WiFi/Internet access (nice to have but not required)

All data will be made available to the participants.

Workshop – hands-on activity: 90 minutes

Interoperability issues in disaster contexts - with an Internally Displaced People worked example

Christine Broenner

Geoinformation Management and Interoperability Expert, Germany, broenner@whenmapsmatter.com

KEY WORDS: *Interoperability, Internally Displaced People (IDP), natural disasters, displacement*

ABSTRACT:

Millions of people are displaced worldwide every year through natural disasters such as floods, earthquakes, landslides, storms and wildfires. Countries concerned aim to support displaced people by responding to their immediate needs, restoring their sustainable livelihoods and reducing the risk of new displacement. GIS, with its integrating analysis capabilities, is eminently suitable to support these complex multi-stakeholder contexts in which internal displacement is set. Effective collaboration and decision-making in such contexts requires various degrees of interoperability. Participants will reflect on these issues in a case study involving internally displaced people.

